A Methodology for the Optimization of Rolling Process

by

Mohammed Abdul Samad

A Thesis Presented to the

FACULTY OF THE COLLEGE OF GRADUATE STUDIES

KING FAHD UNIVERSITY OF PETROLEUM & MINERALS

DHAHRAN, SAUDI ARABIA

In Partial Fulfillment of the
Requirements for the Degree of

MASTER OF SCIENCE

In

MECHANICAL ENGINEERING

June, 1997

INFORMATION TO USERS

This manuscript has been reproduced from the microfilm master. UMI films the text directly from the original or copy submitted. Thus, some thesis and dissertation copies are in typewriter face, while others may be from any type of computer printer.

The quality of this reproduction is dependent upon the quality of the copy submitted. Broken or indistinct print, colored or poor quality illustrations and photographs, print bleedthrough, substandard margins, and improper alignment can adversely affect reproduction.

In the unlikely event that the author did not send UMI a complete manuscript and there are missing pages, these will be noted. Also, if unauthorized copyright material had to be removed, a note will indicate the deletion.

Oversize materials (e.g., maps, drawings, charts) are reproduced by sectioning the original, beginning at the upper left-hand corner and continuing from left to right in equal sections with small overlaps. Each original is also photographed in one exposure and is included in reduced form at the back of the book.

Photographs included in the original manuscript have been reproduced xerographically in this copy. Higher quality 6" x 9" black and white photographic prints are available for any photographs or illustrations appearing in this copy for an additional charge. Contact UMI directly to order.

UMI

A Bell & Howell Information Company
300 North Zeeb Road, Ann Arbor MI 48106-1346 USA
313/761-4700 800/521-0600

A METHODOLOGY FOR THE OPTIMIZATION OF ROLLING PROCESS

BY

MOHAMMED ABDUL SAMAD

A Thesis Presented to the

FACULTY OF THE COLLEGE OF GRADUATE STUDIES

KING FAHD UNIVERSITY OF PETROLEUM & MINERALS

DHAHRAN, SAUDI ARABIA

In Partial Fulfillment of the
Requirements for the Degree of

MASTER OF SCIENCE
In

MECHANICAL ENGINEERING

JUNE 1997

KING FAHD UNIVERSITY OF PETROLEUM AND MINERALS
DHAHRAN, SAUDI ARABIA

COLLEGE OF GRADUATE STUDIES

This thesis, written by

Mohammed Abdul Samad

under the direction of his Thesis Advisor, and approved by his Thesis committee, has been presented to and accepted by the Dean, College of Graduate Studies, in partial fulfillment of the requirements for the degree of

MASTER OF SCIENCE IN MECHANICAL ENGINEERING

Thesis Committee:

Ravi S. Rao

Dr. Ravi S. Rao (Chairman)

Dr. Abdel Rahman N. Shuaib (Member)

Dr. M. Ouerfelli (Member)

Dr. Mohammed O. Budair
(Department Chairman)

Dr. Abdallah M. Al-Shehri
(Dean, College of Graduate Studies)

Date: 23-6-97

COLLEGE OF GRADUATE STUDIES

Dedicated to

My

Parents and Sisters

whose patience and perseverance

led to this accomplishment.

Acknowledgements

In the name of Allah, Most Gracious, Most Merciful

"Read in the name of thy Lord and Cherisher, who created. Created man from a [leech-like] clot. Read and thy Lord is Most Bountiful. He Who taught [the use] of the pen. Taught man that which he knew not. Nay, but man doth transgress all bounds. In that he looketh upon himself as self-sufficient. Verily, to thy Lord is the return [of all]" (The Holy Quran, Surah 96)

All praise and glory be to Almighty Allah who gave me courage and patience to carry out this work, and peace and blessings of Allah be upon Prophet Muhammad. Acknowledge is due to King Fahd University of Petroleum and Minerals for providing support for this research.

My deep appreciation goes to my major thesis advisor **Dr. Ravi S. Rao**, for his constant help, guidance and the countless hours of attention he devoted throughout the course of this work. He was always kind, understanding and sympathetic to me.

Thanks to my thesis committee members Dr. Shuaib and Dr. Ouerefelli for their interest, cooperation, advice and constructive criticism.

Special thanks are due to my colleagues and friends for their help and encouragement. They have made my stay at KFUPM a very pleasant and unforgettable experience.

I am also indebted to the Department Chairman Dr. M. O. Budair and other faculty members for their support.

Finally, my heartfelt thanks and gratefulness to my parents and other family members for their encouragement and moral support.

Contents

List of Figures

List of Tables

Abstract

Name: Mohammed Abdul Samad

Title: A Methodology for the Optimization of Rolling Process

Major Field: Mechanical Engineering

Date of Degree: June, 1997.

This research focuses on the optimization of sheet rolling process. In order to optimize the process effectively, the existing process model has been enhanced especially the neutral zone where the friction changes sign over a region rather than at a point. Pressure and frictional stress distributions as well as total load and torque are thereby estimated as functions of the various rolling parameters. In this analysis, roll flattening has also been taken into account.

The main problem of determining the optimum design parameters of sheet rolling is considered. The problem is formulated and solved as a constrained nonlinear programming problem by considering the radius of rolls, front and back tensions as design variables. Minimization of the deflection of rolls is considered as the objective function for single pass rolling and minimization of the total energy consumption for multipass rolling. Constraints are placed on the induced stresses, neutral angle and the angle of bite for both cold and hot rolling.

It has been found that the deflections in the rolls increase with increasing reduction in thickness. In the case of multipass rolling, the optimum number of passes have been found. For example, in the case of reducing a sheet of steel by 40%, the optimum number of passes have been found to be three, for the total energy consumption to be minimum.

Keywords: *Rolling, Friction, Optimization.*

Master of Science Degree
King Fahd University of Petroleum and Minerals
Dhahran, Saudi Arabia

خلاصة الرسالة

الإسم	:	محمد عبد الصمد
العنوان	:	منهجية الحصول على أمثل عملية دلفنة
الدرجة	:	الماجستير في العلوم
التخصص	:	الهندسة الميكانيكية
تاريخ الدرجة	:	جون ١٩٩٧ م

ينصب البحث على ايجاد العملية المثلى لدلفنة الألواح · ولإيجاد هذه العملية المثلى بشكل مؤثر تم تحسين نموذج العملية الموجودة وخاصة من المنطقة المحايدة حيث يؤثر تغيير الإحتكاك في منطقة ليس في مجرد نقطة · وقد تم التنبؤ بتوزيع الضغط واجهاد الاحتكاك وكذلك الحمل الكلي والعزم الكلي كدوال تعتمد على مختلف متغيرات عملية الدلفنة وقد تم أيضا اعتبار استواء الدرفيل ·

وقد تم أخذ المشكلة الأساسية لتحديد التصميم الأ مثل لدلفنة النزع في الاعتبار · وقد تم تحليل المشكلة وحدها كمشكلة مع الأخذ في الإعتبار نصف قطر الدلفين و الشد الأمامي والخلفي كمتغيرات للتصميم وقد اعتبر تقليل انحراف الدرفيل كدالة موضوعية لدرفيل أحادي الممر وكذلك تقليل استهلاك الطاقة الكلية لدرفيل متعدد الممرات · وقد تم وضع القيود على الإجهادات المتولدة ، وزاوية الحياد وكذلك زاوية العض لكل من الدلفنة على البارد والدلفنة على الساخن · وقد وجد أن الإنحراف في الدلفين يزيد بنقصان سمك اللوح وفي حالة الدلفنة متعددة الممرات فقد وجد أمثل عدد للممرات وعلى سبيل المثال ، في حالة تقليل لوح الصلب بمقدار ٤٠٪ فإن العدد الأمثل للمحرك هو ٣ حتى يكون استهلاك الطاقة الكلي في أقل قيمة له ·

مصلحات البحث : دلفنة - احتكاك - تصميم - أمثل

درجة الماجستير في العلوم

جامعة الملك فهد للبترول والمعادن

الظهران - المملكة العربية السعودية

جون ١٩٩٧

Nomenclature

c Strength constant

d Diameter of the bearing housing

E Youngs modulus

f Friction factor

G Roll torque

h_0 Initial sheet thickness

h_1 Final sheet thickness

k Yield stress in pure shear

L Length of contact arc

L_{adh} Length of the adhesion zone

m Strain-rate sensitivity

n Strain hardening exponent

P Roll load

q Normal pressure

q' Normal pressure at limit of proportionality

R Roll radius

R' Deformed roll radius

S_0 Yield stress in plane strain

V Peripheral velocity of the roll

w Width of the strip

$\bar{\epsilon}$ Effective strain

μ Coefficient of friction

σ_0 Effective stress

σ_1 Back tension

σ_2 Front tension

σ_c Induced stresses in the rolls

σ_b Bending stress

σ_s Torsional stresses

τ Frictional stress

τ' Frictional stress at limit of proportionality

ϕ Roll gap angle

ϕ_N Angle of neutral angle

ϕ_x Angle coordinate of the beginning of the length of neutral zone

ϕ_y Angle coordinate of the end of the length of neutral zone

ν Poison's ratio

α Bite angle

Chapter 1

Introduction

Rolling is one of the oldest metal-working processes in industry. It is the process of reducing the thickness or changing the cross-section of a workpiece by compressive forces exerted by a pair of rotating rolls. The basic operation in this category is flat rolling, where the rolled products are in the form of flat plates and sheets. Plates are used for structural applications such as bridges, ships, boilers, and nuclear vessels. Sheets are used for a great variety of applications such as sheet metals for automotive and other transportation equipment, appliances, beverage cans, containers, welded tubing, and office and kitchen equipment. In view of the tremendous amount and variety of rolled products manufactured every year, a thorough understanding of the basic principles and the updating of the technology of the process is essential for the production of better quality rolled products.

1.1 Mechanics of the Process

In flat rolling the desired shape of the metal is obtained by plastic deformation taking place between two rolls with parallel axes revolving in opposite directions. A schematic illustration of the flat rolling is shown in Figure 1.1 . The crystals are elongated in the direction of rolling, and the material emerges at a faster rate than it enters as the thickness reduction takes place in the roll gap. In hot rolling the crystals start to reform after leaving the zone of deformation, but in cold rolling they retain substantially the shape given to them by the action of the rolls.

The rolls make contact with the metal over a length of contact depicted by arc AB in Figure 1.1. At a certain point of contact the surfaces of the material and the roll move with the same speed. This point is called as the no-slip point or the neutral point C, in Figure 1.1. From C to the exit at A, the metal is in effect being extruded and moves faster than the roll surface. In this zone, friction between workpiece and rolls opposes the motion. Normal and friction forces at a point are depicted in Figure 1.1. The metal moves slower than the rolls between the points C and B, and the friction between the workpiece and the roll acts in the direction of the rolling, aiding the process, and the resultant friction force over arc CB draws the metal into the roll gap. The position of the no-slip point C in arc AB depends upon the amount of reduction, the diameters of the rolls, and the coefficient of friction. The neutral point C tends to move to A as the amount of reduction and the angle

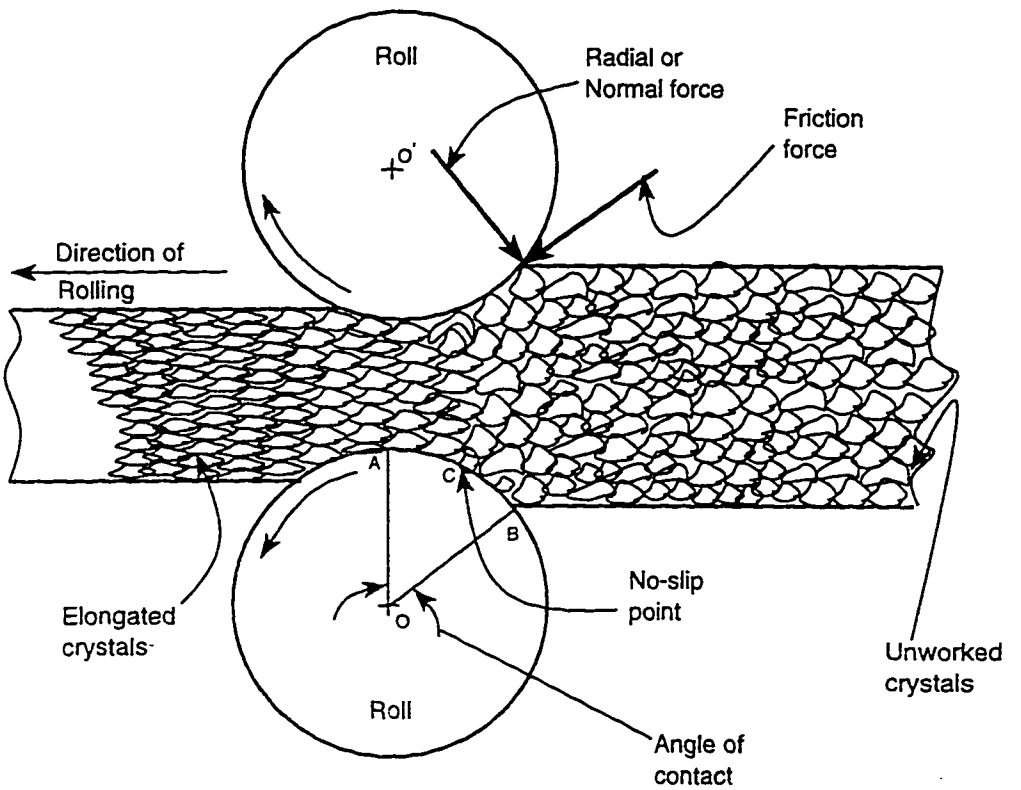

Figure 1.1: Schematic illustration of flat rolling.

of contact increase [1]. When the angle of contact called the bite angle exceeds the angle of friction, the rolls cannot draw the metal spontaneously into the space between them. When the angle of contact is more than twice the angle of friction between roll and work, point C coincides with A, and the metal cannot be drawn through by the rolls even if placed between them, i.e., the rolls begin to slip. That is because the horizontal component of the normal pressure of the rolls against the metal equals and nullifies the horizontal component of friction tending to draw the metal along.

The frictional force between roll and the workpiece in the driving direction approaches the normal force times the coefficient of friction. This friction force multiplied by the surface speed of the rolls gives the power. The forces and power increase with increasing reduction in thickness. Thus, the strength and power capacity of the equipment and the workability of the metal determine how much a workpiece may be reduced at any one time.

If plastic deformation is carried out above the recrystallization temperature of the metal it is called as hot working. This process has the advantages of requiring lower forces because of lower strength and utilizing the greater ductility of the material. Furthermore, defects in the material like porosity can be eliminated by hot rolling. On the other hand, hot rolling has the disadvantages of poor dimensional control, poor strength and the presence of oxide layers on the workpiece due to heating in air.

Bars of all shapes, rods, sheets and strips are commonly finished in all common metals by cold rolling. Metals are cold rolled for improved physical properties, good surface finish, textured surfaces, dimensional control and machinability. Cold rolling is a practical means of producing the degree of hardness wanted in material. Cold rolling produces uniform thicknesses and close tolerances in sheets and bars. Machinability of most steels is improved by cold rolling and for that reason, cold-rolled stock is widely used in fast automatic machining operations. The problem of designing hot and cold rolling mills has been of interest to engineers for a long time. This is evident from the fact that many theories and empirical relations have been developed for calculating the quantities such as roll forces, pressure distribution and power requirements for the deformation process, which are very important in the design of rolling mills. The recent trend towards high speed rolling of thin strips has demonstrated the increasing need of the design of rolling mills for controlling interstand tensions, thickness and shape. Although the procedures for the design of cold rolling mills are well established, not much research has been done in the area of finding optimal conditions and parameters for the rolling process. The advent of fast computers and the development of new mathematical programming techniques have opened up a new phase in the field of optimization.

The demand for good quality rolled products , and the awareness of conservation of energy is increasing every year. It has become essential to find the optimal operational conditions and process parameters for the rolling process. The availability of

fast computers and new mathematical programming techniques in the present age have made it possible to find them more efficiently. Hence the proposed work will focus on a comprehensive methodology to apply non linear programming techniques to optimize the rolling process effectively.

1.2 Objectives

Many approximate numerical solutions for rolling have been developed by several previous researchers, notably Orowan [2], Bland and Ford [3], Bland and Sims [4], Alexander and Ford [5]. Apart from Orowan, all other researchers had used trigonometric approximations and mean flow stress through the contact arc.

In order to optimize the process effectively, the physical model describing the process should be efficient. Christensen et al. [6] showed how the frictional stress can be considered to vary with pressure and friction factor, by introducing an approximate analytical expressions for the friction curves. Alexander et al. [7] had used the Amonton's law of friction in their model. However, their friction model was more akin to that proposed by Tselikov, as described by Javoronkov and Chaturvedi [8], wherein the frictional stress changes sign over a zone rather than a single point.

In this study, efforts will be made to incorporate the following features in the existing process model to make it more realistic:-

1. Friction model based on Wanheim and Bay's [9] as proposed by Christensen

et. al. [6] .

2. Treatment for the neutral zone, based on Chen and Kobayashi's [10] arc tangent function, to deal with neutral point.

This enhanced process model will be used to optimize the flat rolling process and find the optimal operational conditions and the process parameters. The objective functions considered are,

1. The minimization of the deflections of the rolls in the case of single pass rolling.

2. The minimization of the total energy consumed, in the case of multi pass rolling.

Friction plays a very important role in the rolling process. Thus the effect of changing the coefficient of friction on the optimal conditions will also be studied. A parametric study will also be done in the case of single pass rolling to find the effect of changing the rolling parameters like the radius of the rolls, front and back tensions on the objective function which is the minimization of the deflections of the rolls.The optimization technique to be used in our study is the Sequential Quadratic Programming (SQP). The radius of the rolls, front and back tensions are taken as the design variables and constraints are placed on the induced stresses, the neutral angle and the bite angle.

Chapter 2

Literature Review

Rolling has been the subject of study for many researchers. Many theories and methods for analysing the rolling process have been developed during the past decades. The various analytical methods developed are, the slab analysis methods, the slip line field methods, the upper bound methods and the finite element methods. Slab analysis, based on a simplified equilibrium of forces, was suggested by Von-Karman [11] and Siebel and Fangmeier [12]. The well known friction hill type pressure distribution resulted and their theory was based on the assumption that plane sections remain plane during rolling. In addition, the yield strength of the material during rolling and the coefficient of friction along the interface were assumed to be constants. However, in reality the friction varies along the interface in the roll gap and the material as it moves through the roll gap gets workhardened. Trinks [13] developed a graphical technique to solve Von Karman's equation, and Tselikov's

[14] assumptions of the pressure form and angle of the neutral point made Von Karman's equation possible to integrate. These two theories were based on the common assumptions that a plane of vertical section remains plane during rolling, and that the rolls slip on the material except at the neutral plane.

Orowan [2] abandoned the assumption of plane sections remaining plane in the slab analysis, and the inhomogeneous deformation model developed by him is generally regarded as a notable contribution to the exact theory of rolling. The pressure distribution between the rolls and material was obtained by a graphical method of integration of the equation. The complexity of his methods encouraged later researchers, notably Bland and Ford [15, 16] and Sims [17, 18], to develop solutions based on a simplifying assumption that allowed analytical expressions to be developed, thus avoiding most of the numerical integration involved at several points in Orowan's theory. Unfortunately, this led to a sacrifice in accuracy, not serious in estimating the roll force, but much more so in determining the roll torque. In an attempt to produce greater precision in the prediction of these parameters, Ford et al. [3, 19], and Bland and Sims [4] made considerable modifications to the simplified theory of cold rolling developed by Bland and Ford [16]; in particular they accounted for the contributions of the entry and exit elastic arcs of contact and endeavored to allow in some degree for the variation of the yield stress in the plastic arc of contact, which had been previously assigned a constant mean value. The number of different models relating to rolling theories were summarized by Underwood [20]. Tarnovskii

et al.[21], and Roberts [22]. Murty and Lenard [23] evaluated the predictive ability of some of those models by comparing them with the laboratory experiments. They found out that the Orowan model [2] as computerized by Alexander [24] yielded adequate predictions of roll forces and not quite so good, but on occasion acceptable, calculations of roll torques.

With the widespread availability of the modern digital computer, the complexity of the differential equation is no longer a barrier for obtaining an exact numerical solution; Alexander [24] assumed homogeneous deformation in the roll gap and solved von Karman's basic differential equation using the fourth-order Runge-Kutta method with the mixed boundary condition, which is either the Coulomb condition or the extreme limiting condition at sticking. Venter and Abd-Rabbo [25]included the influence of inhomogeneous deformation, and the governing differential equation given by Orowan was solved by taking into account the mixed boundary conditions of sticking and slipping at the roll/strip interface. Later Alexander and et.al. [26] proposed slip line field solutions for a range of geometrical configurations, and found that a critical reduction exists for any given ratio of roll radius to strip thickness at which deformation pattern changes significantly. Wanheim [27], investigated the friction at high normal pressures based on the slip line field analysis and compared them with the experimental results, showing the dependence of frictional stress on the sliding length.

Christensen et al. [6] showed how the frictional stress can be considered to vary

from $\tau = \mu q$ to $\tau = fk$, by introducing an approximate analytical expressions for the friction curves. Alexander et al. [7] had used the Amonton's law of friction in their model but they incorporated the neutral zone in it. Their friction model was more akin to that proposed by Tselikov, as described by Javoronkov and Chaturvedi [8], wherein the frictional stress changes sign over a zone rather than a single point. In this research work, the pressure distribution over a neutral zone has been taken into account and discussed in the process model.

2.1 Optimization

The above mentioned theories and approaches were developed for the designing of the rolling mills, but as it is evident from the literature that not much work has been done in the area of process optimization.

The work by Avitzur [28] is one of the few attempts made in applying some theoretical considerations to the problem of tandem mill optimization. In his work, the rate of production is maximized by considering the interstand tensions, the thickness of the material in between any two adjacent mills and the speed of the mills as the design variables. A method of successive approximation is used to find the optimal conditions.

In his work, Avitzur used the process model based on the upper bound analysis. The upper bound analysis is more practical and closer to the reality in terms of the

force and power calculations as it takes into consideration even the redundant energy. However, the major disadvantage of the upper bound method is the assumption of rigid-perfectly plastic material behaviour, i.e. the workhardening of the materials is neglected [29]. In our work we will be considering the process model based on the slab analysis method. This is justified because the redundant energy in the rolling of thin strips is very small and thus its effect on the final results can be negligible.

Shivpuri et.al [30], presented a methodology for roll pass optimization. They used a three dimensional finite element simulation to arrive at an iterative scheme for reducing the number of passes and improving metal flow in the passes, in the shape rolling. Turley [31], presents a methodology to select the optimum work roll size for cold rolling applications.

Rao and Kumar [32] applied the non-linear programming techniques to the problem of the optimization of single pass and multipass rolling process. In their work, two objectives, namely, the minimization of the deflection of rolls and the minimization of the power required for rolling, are considered in the case of the single pass rolling, and the minimization of the sum of deflections of all the rolls lying in series is considered as the objective in the case of tandem mill rolling. Radius of rolls, and front and back tensions were considered as design variables. Constraints were placed on the induced stresses, the neutral angle and angle of bite. A parametric study was also conducted in the case of single pass rolling to find the effect of changing the rolling parameters like initial strip thickness, percentage reduction on the optimum

results. They implemented the Sequential Unconstrained Minimization technique to solve the optimization problem. In their analysis, they considered a simple model developed by Ford et al. [16] based on the slab analysis method. However, in their model too the frictional stress changes its sign at a single point rather than a zone. In our study, the existing process model will be enhanced by incorporating the neutral zone which is more realistic. This is supported by the experimental results of Christensen [6]. The optimization technique implemented in our study is Sequential Quadratic Programming.

This modified model will be used to obtain the optimal conditions in the case of single and multipass rolling processes by taking different objective functions as will be discussed in the chapter of optimization (chapter 4).

Chapter 3

Process Model

The basis for any optimization model of a process is an efficient physical model which describes the process effectively and realistically in terms of the various related process parameters. This chapter describes how the existing rolling process model has been modified to make it more realistic and efficient, by incorporating the following features:

1. Friction model based on Wanheim and Bay's [9] as proposed by Christensen et. al. [6] .

2. Treatment for the neutral zone, based on Chen and Kobayashi's [10] arc tangent function, to deal with neutral point.

To date, researchers have been using the Amonton's law of friction, which is $\tau = \mu q$ or $\tau = fk$ whichever is smaller in the roll gap, where τ is the frictional

stress, μ is the coefficient of friction, f is the friction factor and k is the stress in shear. However in our study, efforts will be made to incorporate the friction model of Wanheim and Bay [9] where the frictional stress (τ) is a function of pressure which seems to be more realistic. It has also been assumed till now that the frictional stress changes its sign over a point called the neutral point. However, it is evident from the experimental results of Christensen et al. [6] that the frictional stress changes its sign over a zone which is termed as a neutral zone rather than a single point. Thus, the above two features will be incorporated in the process model which will make it more realistic and efficient when compared to the existing ones.

3.1 Friction Model

The conventional friction model adopted is the Amonton's law $\tau = \mu q$, full sticking $\tau = k$ or a combination of these two, i.e. whichever is smaller, where τ is the frictional stress, μ is the coefficient of friction, q is the normal pressure and k is the yield stress in shear. But, Wanheim and Bay [9, 33] have given an improved model for the frictional shear stress, assuming it to be a certain function of the roll pressure (q) and friction factor (f).

The model presented by them is as follows: At low pressures $0 \leq q/\sigma_0 \leq 1.5$, the frictional stress is proportional to the normal stress as shown in Figure 3.1, where σ_0 is the equivalent yield stress. At high normal pressures $3 \leq q/\sigma_0 \leq \infty$, the frictional

stress is almost constant. They proposed that the intermediate range $1.5 \leq q/\sigma_0 \leq 3$ is a transition region over which τ/k increases smoothly with q/σ_0. Christensen et al [6] presented the approximated analytical expression for the friction curves which are as follows:

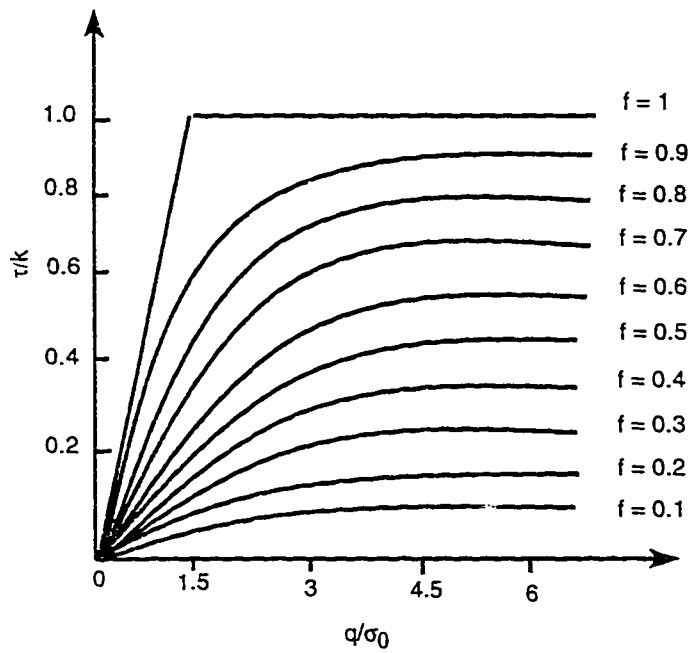

Figure 3.1: Frictional stress as a function of normal stress and friction factor

$$\frac{\tau}{k} = (1 - \sqrt{(1-f)})\frac{q/\sigma_0}{q'/\sigma_0} for \frac{q}{\sigma_0} \leq \frac{q'}{\sigma_0} \tag{3.1}$$

$$\frac{\tau}{k} = \frac{\tau'}{k} + (f - \frac{\tau'}{k})[1 - exp(\frac{(q'/\sigma_0 - q/\sigma_0)\tau'/k}{(f - \tau'/k)q'/\sigma_0})] for \frac{q}{\sigma_0} > \frac{q'}{\sigma_0} \tag{3.2}$$

where τ' and q' express the limit of proportionality between friction and normal stress:

$$\frac{\tau'}{k} = 1 - \sqrt{(1-f)} \tag{3.3}$$

$$\frac{q'}{k} = \frac{1 + \frac{\pi}{2} + Arccosf + \sqrt{(1-f^2)}}{\sqrt{3}(1 + \sqrt{(1-f)}} \approx 1.5 \tag{3.4}$$

The derivation of the above equations is explained in detail in the Appendix A.

The relationship between coefficient of friction and friction factor for $q \leq q'$ is estimated by combining Equations 3.1 and 3.4

$$\mu = \frac{f}{1 + \frac{\pi}{2} + Arccosf + \sqrt{(1-f^2)}} \tag{3.5}$$

Thus, Christensen [6] incorporated the above mentioned friction model in a general analysis of normal and frictional stress distribution using the slab method. Unfortunately, in this model, just as most previous models, the frictional stress changes sign abruptly at the neutral point. This sudden change gives rise to a normalized pressure distribution with a sharp peak at the neutral point. This is clearly unrealistic, as can be seen from the experimental data which shows that the frictional stress changes sign over a zone rather that at a single point [6]. This concept is adopted

in our physical model to make the pressure distribution more realistic which will be explained later in the chapter.

3.2 The Theoretical Analysis

3.2.1 Development of the basic equations

From the equilibrium of forces on any element in the deformation zone as shown in Figure 3.2 during flat rolling and using the various geometrical relationships of the rolling process we obtain the following basic differential equation [1]:

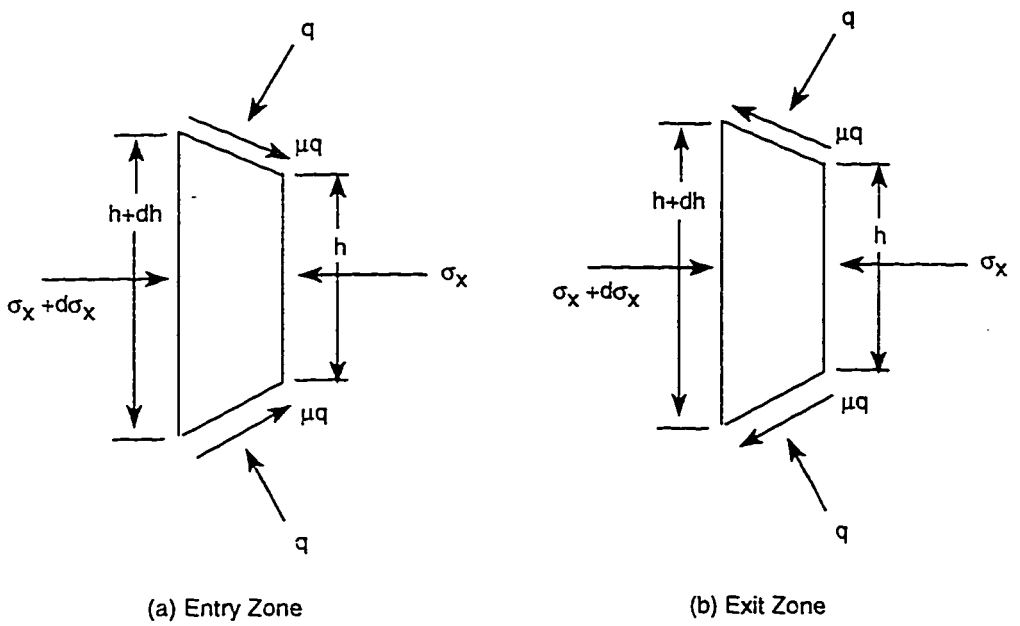

Figure 3.2: Stresses on an element in flat rolling: (a) Entry zone, (b) Exit zone.

$$\pm\frac{d\tau}{d\phi}tan\phi(h_1+2R(1-cos\phi))\pm\tau(h_1+2R)(1+tan^2\phi)$$
$$-\frac{dq}{d\phi}(h_1+2R(1-cos\phi))+2S_0Rsin\phi$$
$$+\frac{dS_0}{d\phi}(h_1+2R(1-cos\phi))=0 \tag{3.6}$$

where the lower sign corresponds to the inlet zone and the upper sign to the outlet zone. In this equation the expressions for the frictional stress, Equations 3.1 and 3.2, are to be inserted based on the range of normal pressure namely; from now on the analysis is performed with respect to the magnitude of the normal pressure:

- Low Pressure ($q \leq q'$)
- High Pressure ($q > q'$).

Low normal pressure

Inserting Equation 3.1 in Equation 3.6 leads to the following first order, linear differential equation.

$$\frac{dq}{d\phi}+M_1(\phi)q'=M_2(\phi) \tag{3.7}$$

where

$$M_1(\phi)=\frac{\mu(h_1+2R)(1+tan^2\phi)}{(\mu tan\phi-1)(h_1+2R(1-cos\phi))}$$
$$M_2(\phi)=-\frac{2S_0Rsin\phi+\frac{dS_0}{d\phi}(h_1+2R(1-cos\phi))}{(\mu tan\phi-1)(h_1+2R(1-cos\phi))}$$

The initial boundary conditions are calculated with the help of the Mohr's circle [6].

High normal pressure

The normal pressure will exceed the limit of proportionality q' if the contact length and friction increases and thus the simple friction model, Equation 3.1, will no longer be valid. Thus, the expression in Equation 3.2 should be inserted in the basic differential equation 3.6 instead. This leads to the following nonlinear differential equation which can be solved numerically:

$$\frac{dq}{d\phi} = \frac{\mp[C_1 - C_2 exp((q' - q)C_3)]C_4(1 + tan^2\phi)}{\pm C_2 C_3 exp((q' - q)C_3)tan\phi(C_4 - 2Rcos\phi) - (C_4 - 2Rcos\phi)} - \frac{2S_0 Rsin\phi\frac{dS_0}{d\phi}(C_4 - 2Rcos\phi)}{\pm C_2 C_3 exp((q' - q)C_3)tan\phi(C_4 - 2Rcos\phi) - (C_4 - 2Rcos\phi)} \tag{3.8}$$

where

$k = k(\phi)$

$S_0 = S_0(\phi)$

$C_1 = \tau' + k(f - \tau'/k)$

$C_2 = k(f - \tau'/k)$

$C_3 = \frac{\tau'/k}{q'(f - \tau'/k)}$

$C_4 = h_1 + 2R$

3.2.2 The constitutive equations

The material properties during the cold and hot rolling processes depend on the strain and the strain rate, respectively. Therefore, constitutive equations for these

processes will differ as shown below.

Cold rolling process

The strain hardening of the plate material is assumed to be in accordance with the following equation for the cold rolling process:

$$\sigma_0 = K(\bar{\epsilon})^n$$

$$S_0 = \frac{2}{\sqrt{3}} K(\bar{\epsilon})^n \tag{3.9}$$

where K is the strength constant that depends on strain and the type of material and n is the strain hardening exponent.

The assumption of plane strain deformation results in an effective strain through the roll gap of :

$$\bar{\epsilon} = \frac{2}{\sqrt{3}} ln \frac{h_0}{h} = \frac{2}{\sqrt{3}} ln \frac{h_0}{h_1 + 2R(1 - cos\phi)} \tag{3.10}$$

where h is expressed as a function of ϕ by Equation 3.11.

$$h = h_1 + 2R(1 - cos\phi) \tag{3.11}$$

Hot rolling process

In hot rolling, the material properties are dependent on the strain rate rather than on the strain. The estimation of the strain rate sensitivity of metals at high temperatures is one of the major problems in the calculation of the forces during hot

rolling. The average strain rate in flat rolling can be obtained by dividing the strain by the time that it takes for an element to undergo this strain in the roll gap. The time can be approximated as L/V. Thus, the strain rate is given by:

$$\dot{\bar{\epsilon}} = \frac{V}{L} ln \left(\frac{h_0}{h_f} \right) \tag{3.12}$$

The equivalent flow stress in the material is calculated as follows:

$$\sigma_0 = c\dot{\bar{\epsilon}}^m \tag{3.13}$$

where c ia the strength constant that depends upon strain, temperature and material, and m is the strain rate sensitivity of the flow stress.

The flow stress in the plane strain is given by:

$$\sigma_0 = \frac{2}{\sqrt{3}} c\dot{\bar{\epsilon}}^m \tag{3.14}$$

where m is the strain rate sensitivity. The flow stress of the material corresponding to the above strain rate is calculated and then substituted in the proper equations and the pressure distributions, incorporating the neutral zone, is obtained.

3.3 Modified Model

It is known that in the above model and most previous models the frictional stress changes sign abruptly at the neutral point. This sudden change gives rise to a

normalized pressure distribution with a sharp peak at the neutral point as shown in the Figure 3.5. This distribution has been found to be clearly unrealistic as is evident from the experimental results presented by Christensen et al. [6]. Thus, we try to incorporate the concept of the neutral zone in our model where the frictional stresses change sign over a zone rather than a point. Our model is more akin to that proposed by Chen and Kobayashi [10].

3.3.1 Length of the neutral / adhesion zone

The length of the adhesion zone (L_{adh}) depends upon the (length of contact arc)/(mean thickness) ratio, which is L/h_{ave} in the present notation. The length of the adhesion zone is determined using an equation developed by Tarnovskii et al. [21] which is as follows;

$$m = (0.79 - 0.27\theta)\frac{L_{adh}}{L} + \frac{1}{2}\left(1 - \frac{\alpha}{2\mu}\right)\left(1 - \frac{L_{adh}}{L}\right) \tag{3.15}$$

where

$m = \phi_N/\alpha$

On the basis of experimental graphs of $L_{adh}/L = F(L/h_{ave})$ are derived the following relationships. These are valid for $0 < L/h_{ave} < 3.0$:

for Aluminum

$$\frac{L_{adh}}{L} = \frac{9 - \left(\frac{L}{h_{ave}}\right)^2}{12} \tag{3.16}$$

for Copper

$$\frac{L_{adh}}{L} = \frac{9 - \left(\frac{L}{h_{ave}}\right)^2}{15} \tag{3.17}$$

3.3.2 Frictional stress in the neutral zone

Once the length of the neutral zone is determined, a velocity dependent frictional stress proposed by Chen and Kobayashi [10] is used to calculate the new pressure distribution. The proposed frictional stress is given by :

$$\tau_N = fk\left(\left(\frac{2}{\pi}\right)tan^{-1}\left(\frac{V_R}{a}\right)\right) \tag{3.18}$$

where

$V_R = V_{Strip} - V_{Roll}$

$V_{Roll} = V cos\phi_N$

$V_{Strip} = V cos\phi$

$a = 10^{-1.5}$

The above equation (Equation 3.18) when substituted in the basic differential equation (Equation 3.6) results in :

$$\frac{dq}{d\phi} = \frac{2S_0 R sin\phi}{h_1 + 2R(1 - cos\phi)} + \frac{dS_0}{d\phi} \pm \frac{\tau_N(h_1 + 2R)(1 + tan^2\phi)}{h_1 + 2R(1 - cos\phi)} \pm \frac{d\tau_N}{d\phi} tan\phi \tag{3.19}$$

3.3.3 Numerical calculations

The linear first order differential equation (Equation 3.7) is integrated over the whole arc of contact, working inwards from both the ends using a fourth order Runge-Kutta process. The increments taken for the computational calculations are in the range of 0.001. The calculations with the Equation 3.7 are performed till the pressure does not exceed the limiting value given by Equation 3.4. When it does, the calculation following the low pressure equation (Equation 3.7) is stopped and the high pressure equation (Equation 3.8) is used instead. The pressure distribution obtained from these calculations is shown in Figure 3.5.

Once the position of the neutral point is found by the intersection of the entry and exit curves, the length of the adhesion zone is approximately calculated by using Equations 3.15 to 3.17 depending upon the L/h_{ave} ratio. In this adhesion zone, a new pressure distribution is obtained by integrating Equation 3.19. The various steps involved are given in the Figure 3.3.

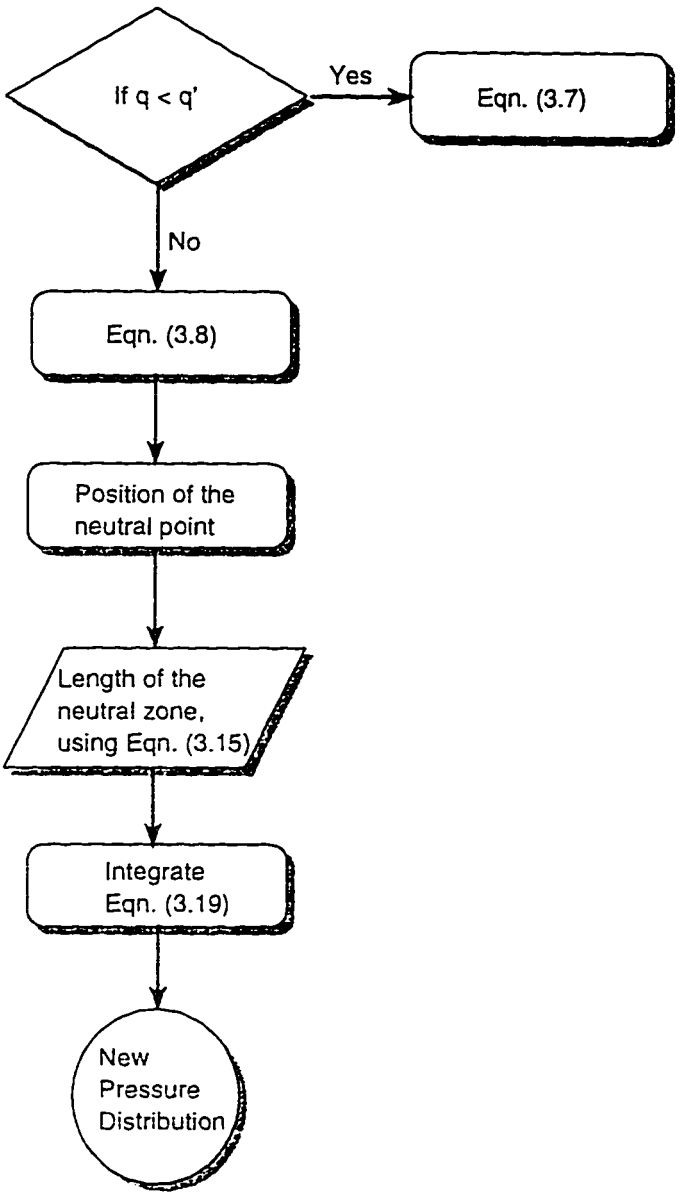

Figure 3.3: Numerical calculations

3.4 Pressure Distribution Incorporating the Neutral Zone

From the experimental data [6], as shown in Figure 3.4, it can be seen clearly that the frictional stress changes its sign over a zone rather than a point. This concept has been incorporated in developing the present physical model. Figure 3.5 shows the comparison of the original Christensen's [6] pressure distribution and the pressure distribution obtained from our enhanced model. The pressure distributions have been normalized by dividing it with the mean yield stress. It can be observed that the pressure distribution obtained from the enhanced physical model with the neutral zone is in accordance with the experimental data. The material used in our study is steel whose pressure distribution is as shown in the Figure 3.6.

The above mentioned enhanced physical model, incorporating the neutral zone is used in:

(a) The optimization of the single pass rolling process with the minimization of the deflection of the rolls as the objective function.

(b) The optimization of the multipass rolling process with the minimization of the energy consumption as the objective function.

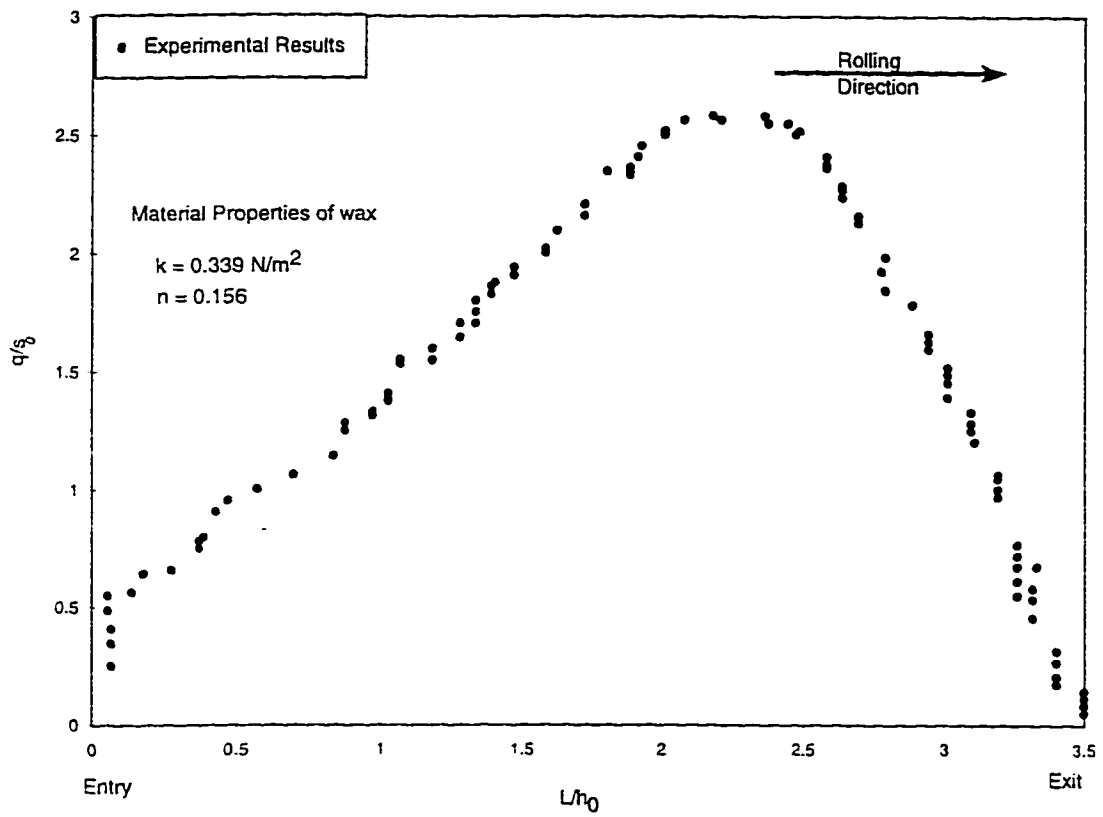

Figure 3.4: The experimental results of Christensen et al.

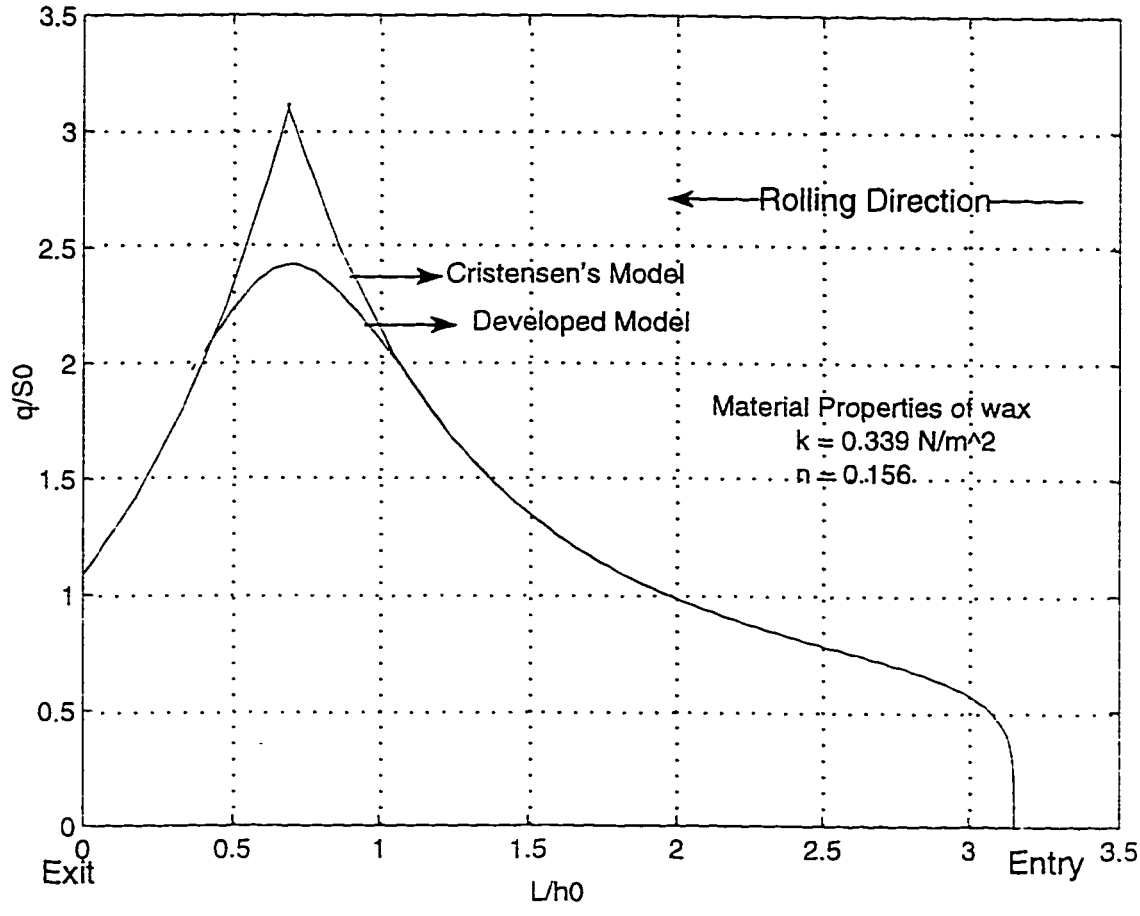

Figure 3.5: Comparison of Christensen's model and the developed model

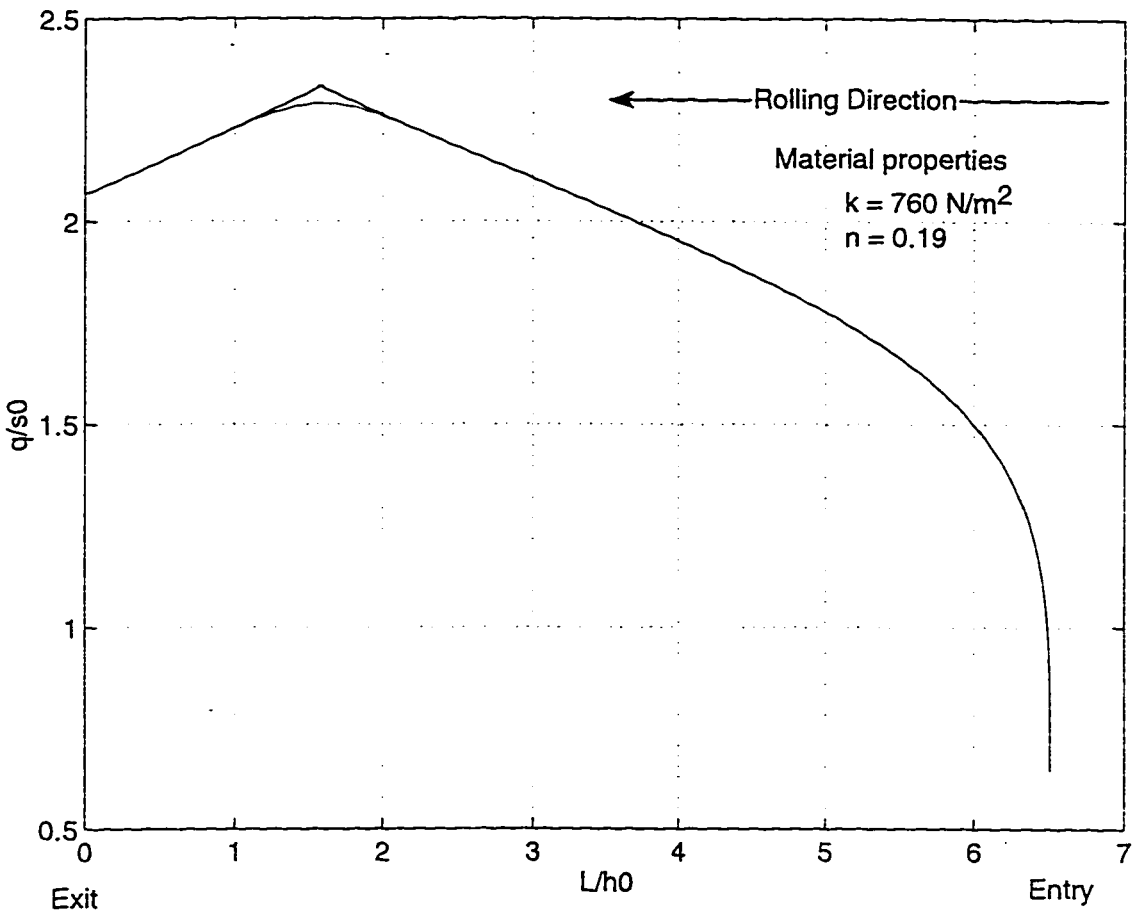

Figure 3.6: Comparison of Christensen's model and the developed model for steel

Chapter 4

Optimization of the Rolling Process

4.1 Formulation of The Problem

The optimization problem of the rolling process can be formulated as a mathematical programming problem, which can be stated in standard form as follows:

Find $\overline{X}$ which minimizes/maximizes the objective function $f(\overline{X})$

subject to the constraints $g_i(\overline{X}) \leq 0, i = 1, 2, ..., m$

where $\overline{X}$ is called the design vector consisting of the design variables $x_1, x_2, ...$

In the present study, the minimization of the deflection of the rolls for single pass rolling and the minimization of the energy consumed for the multipass rolling are considered as the objective functions respectively for two different cases with

the constraint set as follows.

Constraint Set:

1. Bounds on the design variables: All design variables are considered positive, i.e. the lower bound on the variables is set to zero.

$$x_i \geq 0, i = 1, 2, 3 \tag{4.1}$$

2. Bounds on the neutral angle: If the neutral angle,ϕ_N, is less than zero, the rolls will skid over the material and if it is greater than the bite angle (α), the rolls jam and will not move. Hence, the neutral angle is restricted as,

$$0 \leq \phi_N \leq \alpha \tag{4.2}$$

3. Bounds on the angle of bite: The maximum angle of bite is dictated by the friction between the rolls and the material. If the angle of bite, α, is more than twice the angle of friction , the rolls begin to slip because the friction is not high enough to pull the material through the roll gap. Further the bite angle is restricted to be positive so that

$$0 \leq \alpha \leq 2tan^{-1}\mu \tag{4.3}$$

4. Bounds on the induced stresses: The stress induced in the rolls (σ_c) due to combined bending and torsion should not exceed a certain permissible value, σ_{max}, dictated by the strength of the roll material:

$$\sigma_c \leq \sigma_{max} \tag{4.4}$$

5. Bounds on the power or deflection : When minimization of deflections is taken as the objective function, the energy (power) required for the rolling process, e_r, is restricted as:

$$e_r \leq e_{max} \tag{4.5}$$

where e_{max} is the maximum energy available. On the other hand when the energy (power) required for rolling is taken as the objective for minimization, the deflections of the rolls (δ_r), is restricted as

$$\delta_r \leq \delta_{max} \tag{4.6}$$

where δ_{max} is the maximum permissible deflection.

6. Bound on the maximum strain induced in the material to be rolled: An upper bound is being placed on the strain induced in the material to be rolled, such that the strain at any point of reduction does not exceed the strain at fracture obtained from a standard tensile test.

$$\bar{\epsilon} < \bar{\epsilon}_f \tag{4.7}$$

where $\bar{\epsilon}$ is the true strain at any point and $\bar{\epsilon}_f$ is the true strain at fracture.

In the following sections the optimization of the cold and the hot rolling processes will be dealt with, and the results will be presented.

4.2 CASE 1: Minimization of the Roll Deflections

In this section we will deal with the optimization of the single pass rolling, taking deflection of the rolls as the objective function for both cold rolling and hot rolling processes.

The reason for considering the minimization of the deflection of the rolls, as the objective function in the case of single pass rolling is given below.

During the cold and hot rolling of sheet and strip, it can be observed that cross-sections of the product are not exactly rectangular but are most often convex as shown in Figure 4.1a, while rectangular shapes as shown in Figure 4.1b are difficult to find within certain tolerance limits. Deflections in the rolls play a very important role while rolling thin strips, such as rolling of aluminum foil, since it may cause a large variation in the thickness of the rolled product.

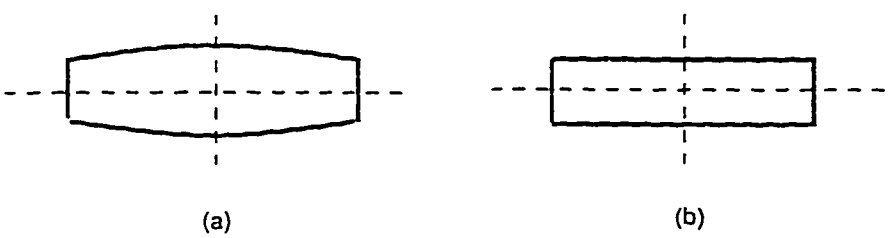

Figure 4.1: Cross-sections of rolled sheet and strip: (a) Convex. (b) Rectangular.

It is the responsibility of the roll designer to choose a roll which ensures that these variations from the true rectangular shape do not exceed permissible tolerances and

also that the surface of the final product is flat and free from twisting and rippling at the center and edges.

The quality of the final product depends mainly on the deflections of the rolls. The more is the deflection the more the sheet or strip will be bulged in the center. Thus to reduce the bulging and to ensure that the rolled sheet is flat, the designer has to see to it, that the deflections in the rolls is minimum and does not exceed a certain specified limit. Of course, this effect is normally taken into account in the design of rolls by putting a camber. Roll camber can be defined as the allowance provided in the roll for any deflections so that the roll after loading is almost flat in shape. But inspite of this it is always desirable to have minimum deflections in the rolls. The roll deflections also have an effect on the roll life. For this purpose a roll with a specific roll radius, has to be designed to ensure that the product will be of good quality.

In this present study, efforts are being made to obtain the optimum values of the design variables namely, roll radius, front and back tensions, so that the deflection in the rolls is minimum.

4.2.1 Governing equations

During optimization, the numerical values of the objective functions and the constraints, as well as their rates of change with respect to the design variables have to be found several times. In order to evaluate the functions f and g_i, where $i = 1, 2, ...j$

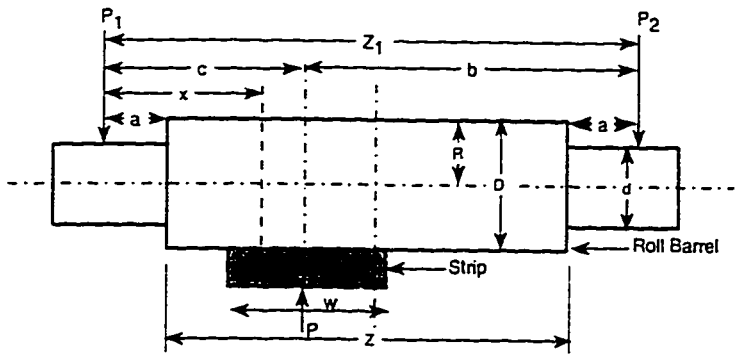

Figure 4.2: Forces acting on the roll barrel

for any specified values of R, σ_{bt} and σ_{ft} where R is the roll radius and σ_{bt} and σ_{ft} are the back and front tensions respectively, a complete analysis of the rolling process has to be made. The expressions of δ_r, σ_N, α, σ_c and e_r in terms of the design variables R, σ_{bt} and σ_{ft} are given in the following section.

1. Deflection of the rolls (δ_r): From Figure 4.2 the deflection at any point of the roll can be expressed as the sum of the deflection due to bending (δ_B) and shear (δ_S), which in turn can be expressed as follows [32, 34]:

$$\delta_B = \frac{P(x-a)}{24EI}\left[\frac{(x-a)^3}{Z} + Z^2 + 2Za - 2x(x+a)\right] \tag{4.8}$$

and

$$\delta_S = \frac{16P}{3\pi ED^2}\left[\frac{x(Z-x) - a(Z-a)}{Z}\right] \tag{4.9}$$

where

$$a = b - Z/2 \tag{4.10}$$

where E is the young's modulus of the roll material, I is the moment of inertia and P is the force on the rolls. In this study, we have taken the length of the roll barrel Z =4.4R, the diameter of the bearing housing d = 1.1R, and the length of the bearing a=1.01R, where R is the radius of the rolls [34].

Thus the deflection at the ends of the roll barrel (at $x = a$ and $x = 2b - a$), as shown in Figure 4.2 can be seen to be maximum (δ_r) with

$$\delta_r = (\delta_B)_{max} + (\delta_S)_{max} = \frac{PZ^2}{6ED^2}(5Z + 24a) + \frac{4PZ}{3\pi ED^2} \tag{4.11}$$

2. Neutral angle (ϕ_N): The rolled stock enters the gap with a speed less than the peripheral roll velocity. There is a point where the strip velocity is equal to the roll velocity, and this point is called the neutral point and is denoted by an angle called the neutral angle. Ford, Ellis and Bland [3] derived an approximate expression for the neutral angle as

$$\phi_N = (\frac{h_1}{R'})^{1/2}.tan\left[(\frac{h_1}{R'})^{1/2}.\frac{H_N}{2}\right] \tag{4.12}$$

where

$$H_N = \frac{H_1}{2} - \frac{1}{2\mu}log\frac{h_0}{h_1}\left[\frac{1-(\sigma_{ft}/k_1)}{1-(\sigma_{bt}/k_0)}\right] \tag{4.13}$$

$$H_1 = 2(\frac{R'}{h_1})^{1/2}tan^{-1}\left[(\frac{R'}{h_1})^{1/2}\alpha\right] \tag{4.14}$$

3. Bite angle (α): The bite angle is given by the following [1]

$$\alpha = cos^{-1}\left[1 - \frac{(h_0 - h_1)}{2R}\right] \tag{4.15}$$

4. Stress induced in the rolls (σ_c): By using the forces acting on the rolls and the simple theory of bending of beams, the bending stress (σ_b) and the torsional stresses(σ_s) in the rolls assuming that the material is rolled at the center of the rolls, are given by [32, 34],

$$\sigma_b = \frac{w.P}{\pi R^3}\left(Z_1 - \frac{w}{2}\right) \tag{4.16}$$

and

$$\sigma_s = \frac{2Gw}{\pi R^3} \tag{4.17}$$

The expression for the compound stress under the simultaneous action of bending and torsion for steel rolls is given by

$$\sigma_c = (\sigma_b^2 + 3\sigma_s^2)^{1/2} \tag{4.18}$$

5. Energy required (e_r): In cold rolling, energy is required for the following purposes:

   - to deform the material as it passes through the rolls.
   - to overcome the frictional forces in the roll neck bearings.
   - to pull the strip through the rolls when significant amounts of front and back tensions are used.
   - to balance the frictional losses in pinions, reduction gear etc.
   - to compensate for the losses in the electric motors, generators and the electric circuit.

In this study, the energy required for rolling is computed by considering the requirements for the first three factors. The power required can be computed from the following equation [34]:

$$e_r = 2\pi \left[2G + P\mu d + R(\sigma_{bt} + \sigma_{ft}) \left[1 + 2\frac{R}{h_1}(1 - cos\phi_N)\right]\right] \tag{4.19}$$

6. Strain induced in the test material ($\bar{\epsilon}$): The strain induced in the material to be rolled is given by the following equation.

$$ln(h_0/h_1) \tag{4.20}$$

7. Roll force(P) and roll torque(G) and the deformed radius(R'): The roll force and the roll torque required for the calculation of e_r, δ_r and σ_c can be computed as follows:

The roll force is assumed to be acting in the middle of the deformed contact arc ($\phi = \alpha/2$) and in the direction of the center of the deformed roll. The friction stress (τ) on the roll is considered positive when acting against the rotation and negative when acting in the direction of rotation. These assumptions lead to the following equation for the load [24].

$$\begin{aligned} P = R' \int_0^{\alpha} q cos(\phi - \frac{\alpha}{2}) d\phi - R' \int_0^{\phi_x} \tau sin(\phi - \frac{\alpha}{2}) d\phi \\ - R' \int_{\phi_x}^{\phi_N} \tau_N sin(\phi - \frac{\alpha}{2}) d\phi \\ + R' \int_{\phi_N}^{\phi_y} \tau_N sin(\phi - \frac{\alpha}{2}) d\phi + R' \int_{\phi_y}^{\alpha} \tau sin(\phi - \frac{\alpha}{2}) d\phi \end{aligned} \tag{4.21}$$

The torque is estimated according to the following expression [24]:

$$G = R'(R' - R)\int_0^{\alpha} qsin(\phi - \frac{\alpha}{2})d\phi + R'\int_{\phi_N}^{\phi_y}[R'\tau_N$$
$$-(R' - R)\tau_N cos(\phi - \frac{\alpha}{2})]d\phi + R'\int_{\phi_y}^{\alpha}[R'\tau$$
$$-(R' - R)\tau cos(\phi - \frac{\alpha}{2})]d\phi - R'\int_0^{\phi_x}[R'\tau$$
$$-(R' - R)\tau cos(\phi - \frac{\alpha}{2})]d\phi$$
$$- R'\int_{\phi_x}^{\phi_N}[R'\tau_N - (R' - R)\tau_N cos(\phi - \frac{\alpha}{2})]d\phi \qquad (4.22)$$

where the frictional stress in the neutral zone (τ_N) is given by Eqn. 3.18. Hitchcock [1], gave the equation for the deformed radius, by assuming that the actual normal stress distribution could be replaced by an elliptical one.

$$R' = R\left[1 + \frac{16(1-\nu^2)}{\pi E}\frac{P}{h_0 - h_1}\right] \qquad (4.23)$$

It can be seen that an iterative procedure has to be used to calculate the exact values of roll force and torque. The equations for P and G involve the deformed radius, R'. To start with, R' is assumed to be equal to R. Once the roll force and torques are calculated, the new value of P is used to find R' using the Eqn.4.23. The new value of R' is used to calculate more accurate values of P and G. This procedure is continued until two successive iterations produce the same value of P. G and R'.

4.2.2 Solution technique

In the present study, the CONSTR function of the Optimization Toolbox of MATLAB [35] has been used to solve the above formulated nonlinear problem. The code used in this work is given in Appendix B. This function utilizes the technique of Sequential Quadratic Programming Technique (SQP) for optimization which is outlined here.

In constrained optimization, the general aim is to transform the problem into an easier sub-problem which can be solved and used as the basis of an iterative process. A characteristic of a large class of early methods is the translation of the constrained problem to a basic unconstrained problem by using a penalty function for constraints, which are near or beyond the constraint boundary. These methods are now considered relatively inefficient and have been replaced by methods which have focussed on the solution of the Khun-Tucker (KT) equations. The KT equations are necessary conditions for optimality for a constrained optimization problem. The Khun-Tucker equations can be stated as:

$$\nabla f(x) + \sum_{i=1}^{m} \lambda_i \nabla g_i(x) = 0 \tag{4.24}$$

$$\lambda_i g_i(x) = 0 \qquad i = 1, \ldots, m \tag{4.25}$$

$$\lambda_i \geq 0 \qquad i = m_e + 1, \ldots, m \tag{4.26}$$

The solution of the KT equations forms the basis to many nonlinear programming algorithms. These algorithms attempt to compute directly the Lagrangian multipliers. Constrained quasi-Newton methods guarantee superlinear convergence by accumulating second order information regarding the KT equations using quasi-Newton updating procedure. These methods are commonly referred to as Sequential Quadratic Programming (SQP) methods since a QP sub-problem is solved at each iteration.SQP methods represent state-of-the-art in nonlinear programming methods. At each major iteration an approximation is made of the Hessian of the Lagrangian function using a quasi-Newton updating method. This is then used to generate a QP sub-problem whose solution is used to form a search direction for a line search procedure. An overview of the SQP is found in Gill et al. [36] The general method however, is stated below.

Technique

Given the general problem for the optimization, the principal idea of SQP is the formulation of a QP sub-problem based on a quadratic approximation of the Lagrangian function [35].

$$L(\bar{x}, \lambda) = f(\bar{x}) + \sum_{i=1}^{m} \lambda_i g_i(\bar{x}) \tag{4.27}$$

where $\bar{x}$, is the vector of the design variables, and λ_i is an estimate of the Lagrangian multipliers.

Step 1: An approximation to the Hessian of the Lagrangian function at each major iteration k is made using a quasi-Newton (BFGS) updating method as follows:

$$H_{k+1} = H_k + \frac{q_k q_k^T}{q_k^T s_k} - \frac{H_k^T H_k}{s_k^T H_k s_k} \tag{4.28}$$

where:

$$s_k = x_{k+1} - x_k \tag{4.29}$$

$$q_k = \nabla f(x_{k+1}) + \sum_{i=1}^{m} \lambda_i \nabla g_i(x)_{k+1} - (\nabla f(x_k) + \sum_{i=1}^{m} \lambda_i \nabla g_i(x)_k) \tag{4.30}$$

The matrix H_k is to be a positive definite approximation of the Hessian matrix of the Lagrangian function.

Step 2: The approximation to the Hessian obtained at each iteration is then used to generate a QP sub-problem by linearizing the nonlinear constraints.

i.e. minimize $\frac{1}{2} d^T H_k d + \nabla f(x_k)^T d$

$\nabla g_i(x)^T d + g_i(x) = 0 \; i = 1, 2, \ldots\ldots m_e$

$\nabla g_i(x)^T d + g_i(x) \leq 0 \; i = m_{e+1}, \ldots\ldots m$

Step 3: The solution to the QP sub problem produces a vector d_k which is used to form a search direction for a line search procedure.

$$x_{k+1} = x_k + \alpha_k d_k \tag{4.31}$$

The step length parameter α_k is determined by an appropriate line search procedure so that a sufficient decrease in a merit function is obtained.

The solutions obtained from this technique were checked for the local or global minimum. This has been done by checking for the convexity of the objective functions and the constraints. Any nonlinear constrained optimization problem is called a convex programming problem if the objective function $f(X)$ and the constraints $g_i(X)$ are convex [37]. A function $f(X)$ is said to be convex if for any pair of points X_1 and X_2 (X_1 and X_2 being the vectors formed by the design variables) and any λ,

$$f(\lambda X_2 + (1-\lambda)X_1) \leq \lambda f(X_2) + (1-\lambda) f(X_1) \tag{4.32}$$

where $0 \leq \lambda \leq 1$.

In other words the segment joining the two points should lie entirely above or on the graph of $f(X)$ as shown in Figure 4.3 which illustrates a convex function in one variable. It can be seen that a convex function is always bending upwards and hence it is apparent that the local minimum of a convex function is also a global minimum [37]. In our study we checked the convexity of the objective functions used, namely, the deflections in the rolls and the energy consumption by applying the condition given by the Equation 4.32. It was found that the objective functions and the constraints were nonconvex. Hence the solution may not be a global minimum but it may well be a local minimum.

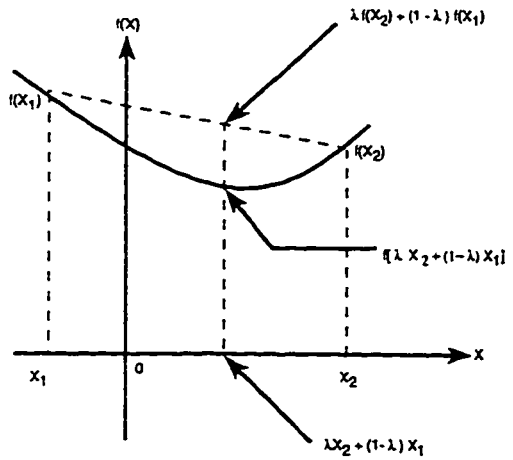

Figure 4.3: A convex function in one variable

The values of force (P) and torque (G), required to determine the various remaining parameters are calculated by the numerical integration of the Equations 4.21 & 4.22, respectively. These parameters are provided to the optimization routine at every iteration. The procedure of the calculations is shown clearly in the flow chart in Figure 4.4.

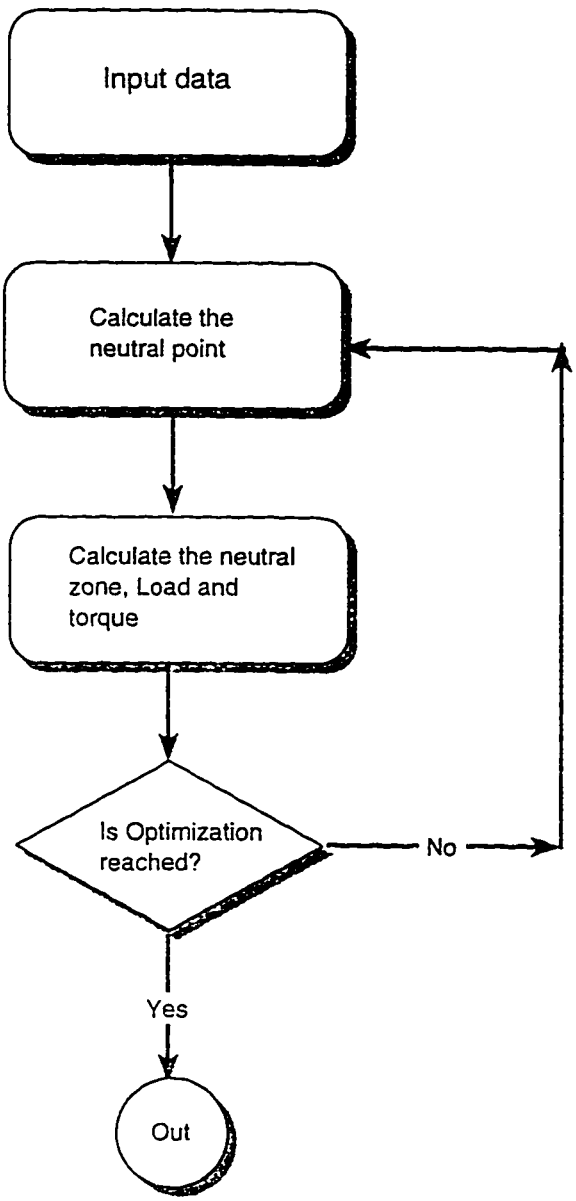

Figure 4.4: Flow chart describing the computational procedure

4.2.3 Results

The optimization results obtained for cold and hot rolling processes are presented, taking the minimization of the deflections of the rolls as the objective function.

Results for Cold Rolling Process

In the present work, cast steel is taken as the roll material, as it is the most commonly used material in the industry for the manufacturing of the rolls. The other data assumed for the numerical computations are as follows [1, 22], which are determined from the practical considerations of the rolling process:

- Maximum permissible stress in the rolls = $15X10^8 N/m^2$
- Modulus of elasticity of the roll material = $1758.00X10^3 N/m^2$
- Coefficient of friction = 0.055
- Poison's ratio for the material to be rolled = 0.3
- Upper bound on the power = $2X10^4 J/rev$
- Initial thickness of the material = $1.6X10^{-3} m$

For comparison purposes, the calculations were carried out for three commonly used materials in the industry, namely, annealed steel, copper and aluminum, whose material behavior is governed by the Equation 4.33:

$$\sigma_0 = K(\bar{\epsilon})^n \tag{4.33}$$

where K is the strength constant that depends on the strain and material, and n is the strain hardening exponent. The values of K and n for the above three materials are given in Table 4.1 [1]:

Table 4.1: Material properties at room temperature

Name of the Material	Strength Coefficient ($KinN/mm^2$)	Strain Hardening Exponent (n)
Steel	760	0.19
Copper	315	0.54
Aluminum	180	0.2

For the above three materials the values of the strain at fracture and the maximum permissible reduction in area that could be undertaken is given in the Table 4.2, [1].

Table 4.2: Values of ture strain at fracture for all the three materials

Name of the Material	Reduction in Area (%)	True Strain at fracture
Steel	66	1.07
Copper	76.54	1.45
Aluminum	84.74	1.88

The results of the optimization are shown in the Tables 4.3 to 4.5. The variation of the optimum values of roll deflection, roll radius and the back and front tensions with percentage reductions in thickness are shown in Figures 4.5 to 4.8.

Table 4.3: Optimum values of the design variables and the objective function for cold rolling of steel

Reduction %	Radius (m)	Back Tension (N/m^2)	Front Tension (N/m^2)	Deflection of the rolls (m)
10	0.5863	$6.11X10^7$	$7.26X10^7$	$8.0343X10^{-6}$
15	0.4121	$5.36X10^7$	$6.69X10^7$	$8.882X10^{-6}$
20	0.3011	$4.442X10^7$	$5.788X10^7$	$9.41X10^{-6}$
25	0.2383	$3.44X10^7$	$4.66X10^7$	$9.764X10^{-6}$
30	0.2089	$2.466X10^7$	$3.42X10^7$	$9.98X10^{-6}$
35	0.1979	$1.614X10^7$	$2.17X10^7$	$10.12X10^{-6}$
40	0.1905	$0.987X10^7$	$1.04X10^7$	$10.25X10^{-6}$

Table 4.4: Optimum values of the design variables and the objective function for cold rolling of copper

Reduction %	Radius (m)	Back Tension (N/m^2)	Front Tension (N/m^2)	Deflection of the rolls (m)
10	0.2142	$7.537X10^6$	$6.98X10^6$	$0.98X10^{-7}$
15	0.1865	$6.339X10^6$	$5.349X10^6$	$1.909X10^{-7}$
20	0.1661	$5.093X10^6$	$4.23X10^6$	$3.181X10^{-7}$
25	0.1507	$3.902X10^6$	$3.474X10^6$	$4.506X10^{-7}$
30	0.1384	$2.872X10^6$	$2.936X10^6$	$5.598X10^{-7}$
35	0.1269	$2.106X10^6$	$2.466X10^6$	$6.166X10^{-7}$
40	0.1143	$1.711X10^6$	$1.918X10^6$	$6.354X10^{-7}$

Table 4.5: Optimum values of the design variables and the objective function for cold rolling of aluminum

Reduction %	Radius (m)	Back Tension (N/m^2)	Front Tension (N/m^2)	Deflection of the rolls (m)
10	0.1896	$4.892X10^6$	$3.239X10^6$	$4.992X10^{-8}$
15	0.1681	$3.576X10^6$	$2.66X10^6$	$5.237X10^{-8}$
20	0.1504	$2.696X10^6$	$2.096X10^6$	$6.192X10^{-8}$
25	0.1355	$2.135X10^6$	$1.59X10^6$	$7.549X10^{-8}$
30	0.1229	$1.782X10^6$	$1.192X10^6$	$9.004X10^{-8}$
35	0.1115	$1.521X10^6$	$0.9462X10^6$	$1.024X10^{-7}$
40	0.1007	$1.241X10^6$	$0.9002X10^6$	$1.098X10^{-7}$

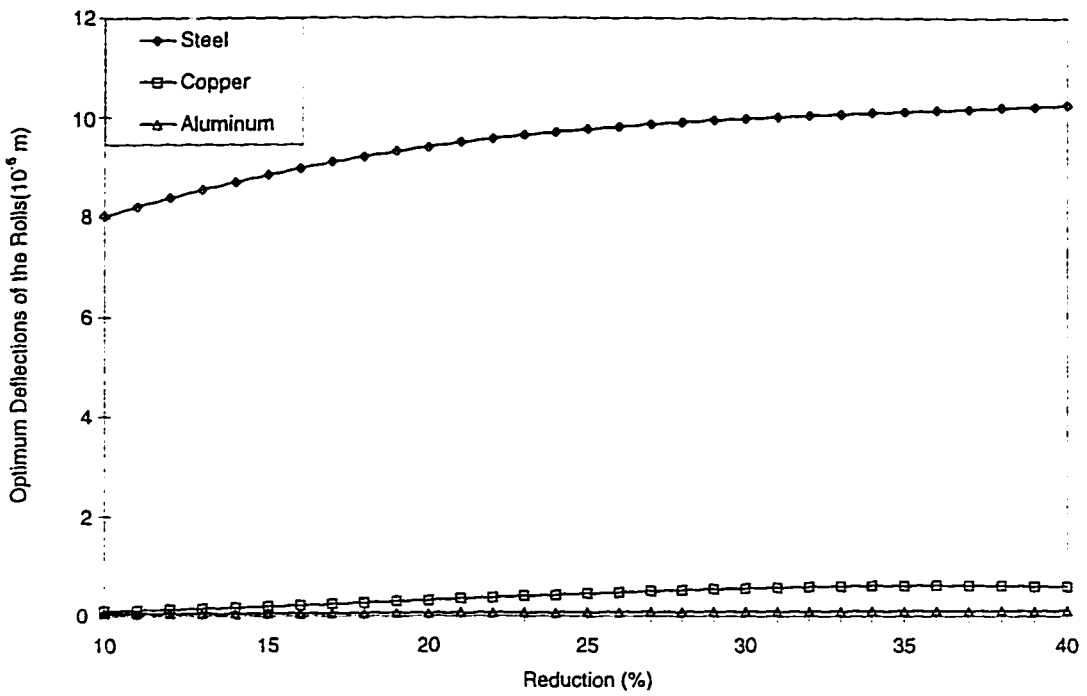

Figure 4.5: Variation of the optimum deflection of the rolls with percent reduction in thickness for cold rolling

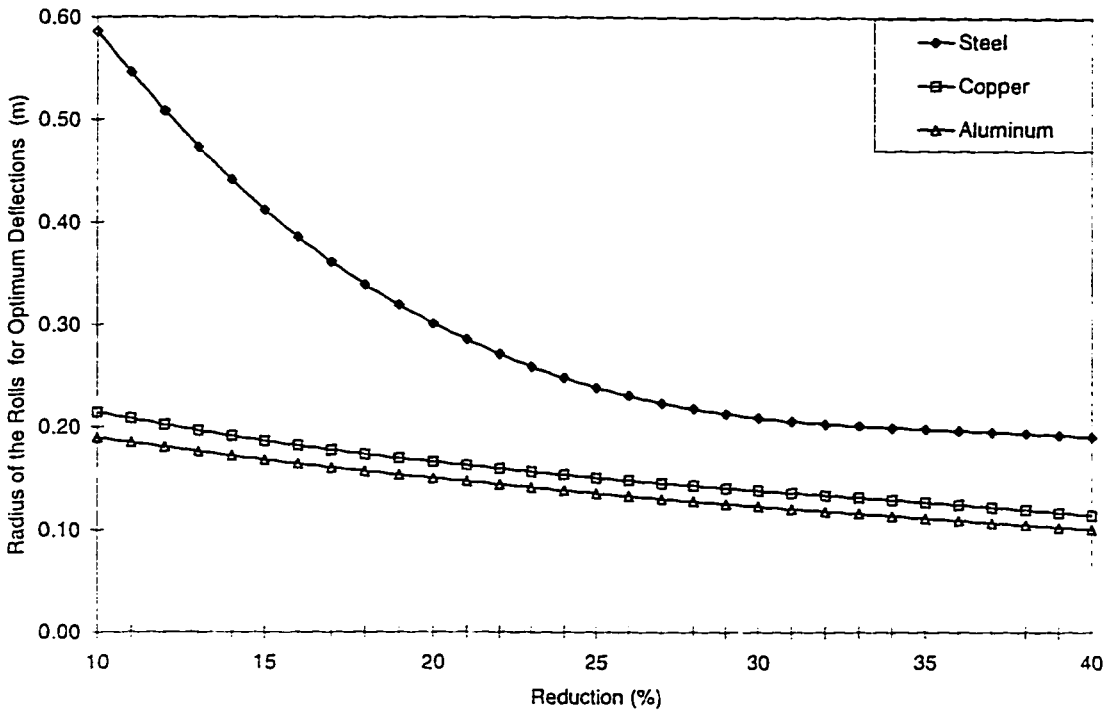

Figure 4.6: Variation of the optimum values of roll radius with percent reduction in thickness for cold rolling

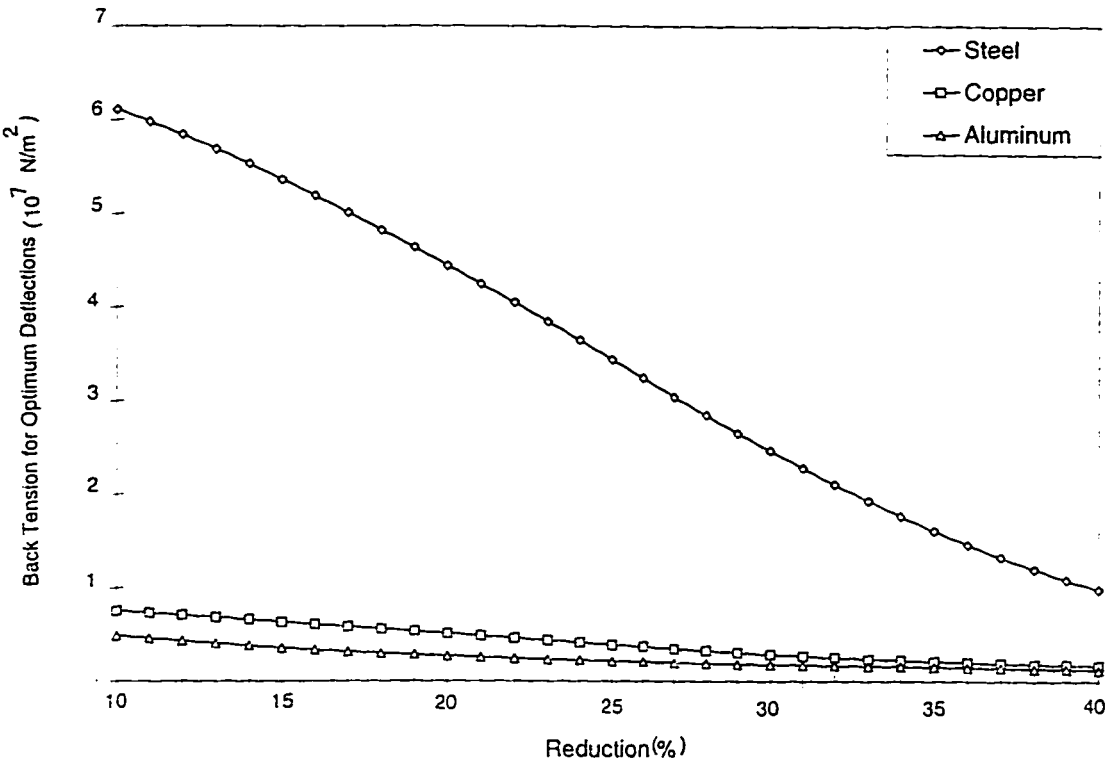

Figure 4.7: Variation of the optimum values of back tension with percent reduction in thickness for cold rolling

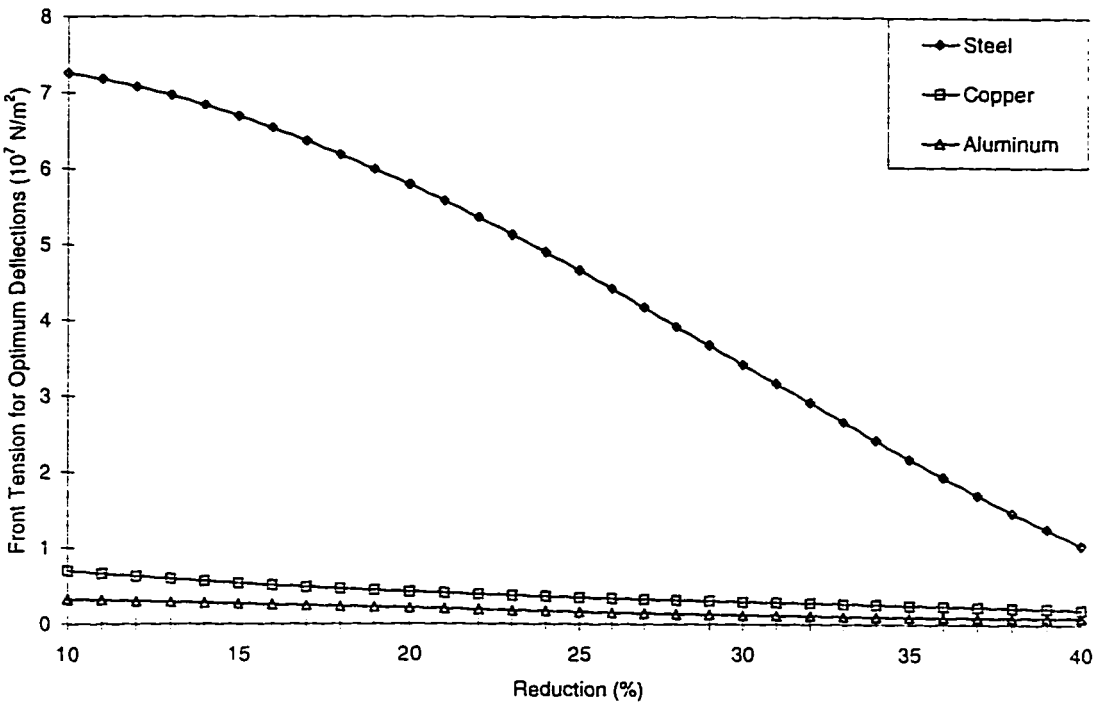

Figure 4.8: Variation of the optimum values of front tension with percent reduction in thickness for cold rolling

4.3 Sensitivity Analysis

A parametric study has been done to find the effect of various rolling parameters on the objective function which is the minimization of the deflection of the rolls. The various parameters taken into consideration are the coefficient of friction, roll radius, back tension and front tension.

Results of Optimization with different values of coefficient of friction, roll radius, back and front tensions

Results were also obtained for the optimization of the cold rolling of annealed steel, with different values of coefficient of frictions. The coefficient of friction has been varied from $\mu = 0.055$ to $\mu = 0.125$ [1, 22]. The results obtained are shown in the Figures from 4.9 to 4.12. The numerical values of the optimum design variables and the corresponding objective function results are given in Tables 4.6 to 4.9.

The roll radius has been varied from 0.4m to 0.6m with an increment of 0.1. The back tension has been also been varied accordingly and their effect on the objective function has been checked. The results are shown in Figures 4.13 to 4.15.

Table 4.6: Optimum values of the design variables and the objective function for cold rolling of steel with $\mu = 0.055$

Reduction %	Radius (m)	Back Tension (N/m^2)	Front Tension (N/m^2)	Deflection of the rolls (m)
10	0.5863	$6.11X10^7$	$7.26X10^7$	$8.0343X10^{-6}$
15	0.4683	$5.26X10^7$	$6.286X10^7$	$8.882X10^{-6}$
20	0.3711	$4.442X10^7$	$5.288X10^7$	$9.41X10^{-6}$
25	0.2946	$3.64X10^7$	$4.266X10^7$	$9.798X10^{-6}$
30	0.2389	$2.866X10^7$	$3.22X10^7$	$9.98X10^{-6}$
35	0.2039	$2.112X10^7$	$2.15X10^7$	$1.012X10^{-5}$
40	0.1897	$1.382X10^7$	$1.056X10^7$	$1.58X10^{-5}$

Table 4.7: Optimum values of the design variables and the objective function for cold rolling of steel with $\mu = 0.075$

Reduction %	Radius (m)	Back Tension (N/m^2)	Front Tension (N/m^2)	Deflection of the rolls (m)
10	0.6955	$9.935X10^7$	$9.286X10^7$	$2.078X10^{-5}$
15	0.6585	$8.976X10^7$	$8.923X10^7$	$3.196X10^{-5}$
20	0.6171	$8.125X10^7$	$8.435X10^7$	$4.214X10^{-5}$
25	0.5713	$7.383X10^7$	$7.821X10^7$	$5.131X10^{-5}$
30	0.5212	$6.75X10^7$	$7.083X10^7$	$5.948X10^{-5}$
35	0.4666	$6.225X10^7$	$6.219X10^7$	$6.664X10^{-5}$
40	0.4078	$5.81X10^7$	$5.23X10^7$	$7.28X10^{-5}$

Table 4.8: Optimum values of the design variables and the objective function for cold rolling of steel with $\mu = 0.1$

Reduction %	Radius (m)	Back Tension (N/m^2)	Front Tension (N/m^2)	Deflection of the rolls (m)
10	0.8129	$3.185X10^8$	$2.836X10^8$	$6.996X10^{-5}$
15	0.7967	$3.122X10^8$	$2.435X10^8$	$7.359X10^{-5}$
20	0.7724	$2.933X10^8$	$2.092X10^8$	$8.001X10^{-5}$
25	0.7399	$2.616X10^8$	$1.804X10^8$	$8.921X10^{-5}$
30	0.6992	$2.173X10^8$	$1.573X10^8$	$1.012X10^{-4}$
35	0.6503	$1.602X10^8$	$1.397X10^8$	$1.159X10^{-4}$
40	0.5933	$9.056X10^7$	$1.279X10^8$	$1.335X10^{-4}$

Table 4.9: Optimum values of the design variables and the objective function for cold rolling of steel with $\mu = 0.125$

Reduction %	Radius (m)	Back Tension (N/m^2)	Front Tension (N/m^2)	Deflection of the rolls (m)
10	0.9023	$6.872X10^8$	$6.933X10^8$	$9.994X10^{-5}$
15	0.8652	$6.282X10^8$	$6.065X10^8$	$8.79X10^{-5}$
20	0.8331	$5.761X10^8$	$5.293X10^8$	$1.002X10^{-4}$
25	0.8060	$5.307X10^8$	$4.614X10^8$	$1.368X10^{-4}$
30	0.7839	$4.922X10^8$	$4.031X10^8$	$1.978X10^{-4}$
35	0.7668	$4.604X10^8$	$3.541X10^8$	$2.831X10^{-4}$
40	0.7547	$4.355X10^8$	$3.147X10^8$	$3.927X10^{-4}$

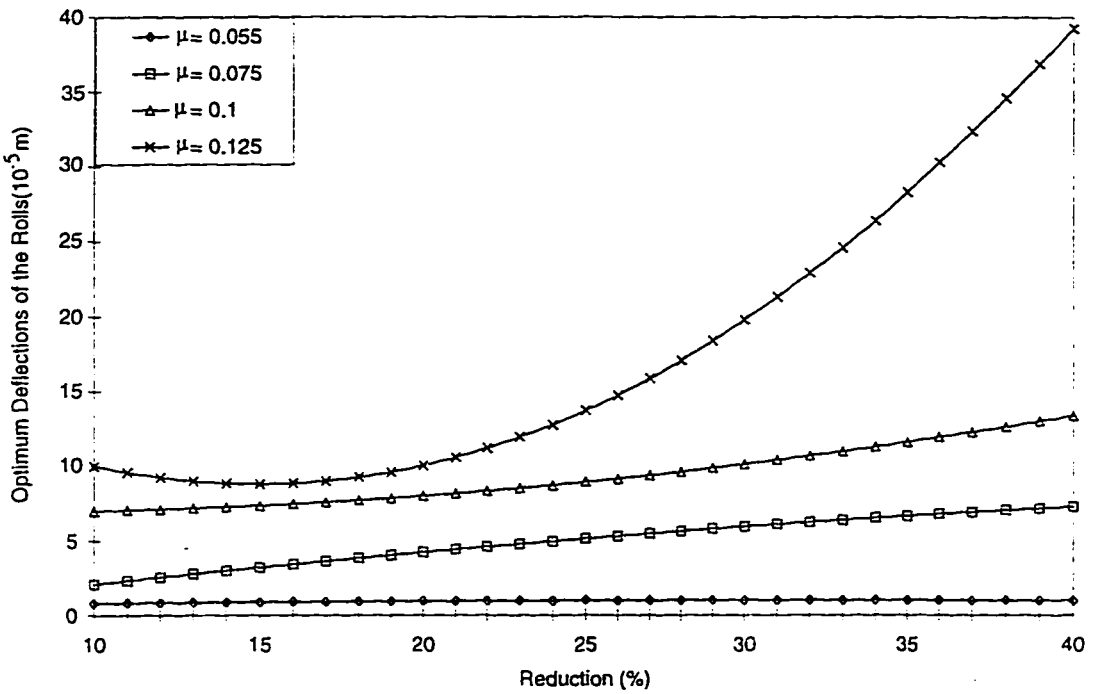

Figure 4.9: Variation of the optimum deflection of the rolls for cold rolling of steel as a function of coefficient of friction

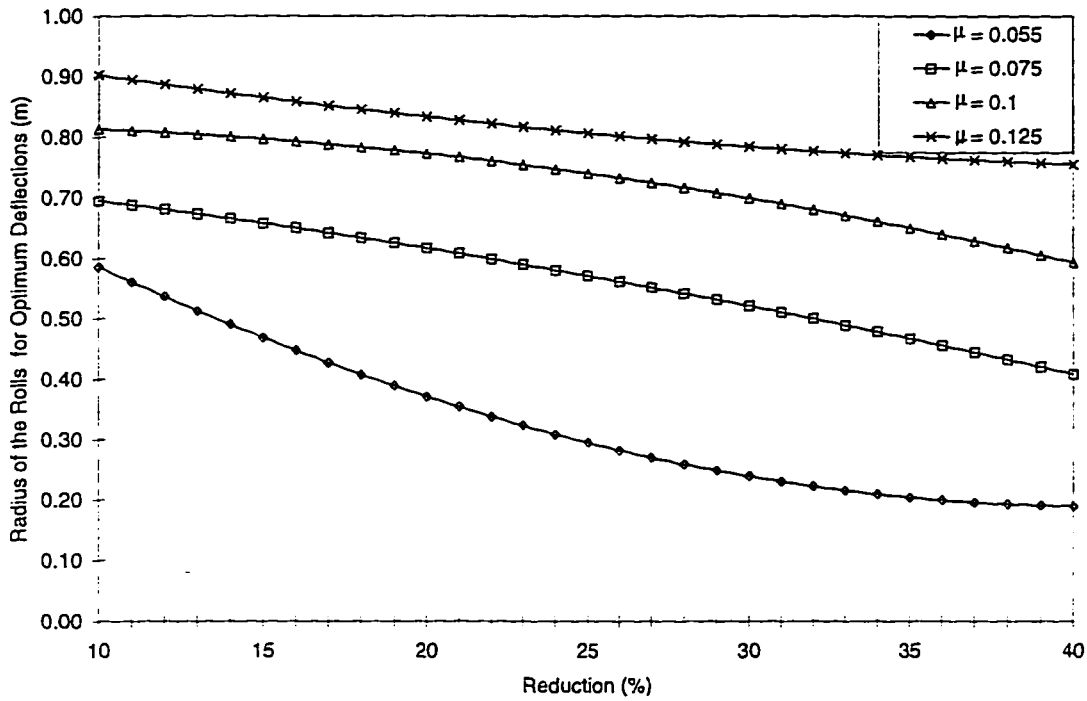

Figure 4.10: Variation of optimum values of roll radius for cold rolling of steel as a function of coefficient of friction

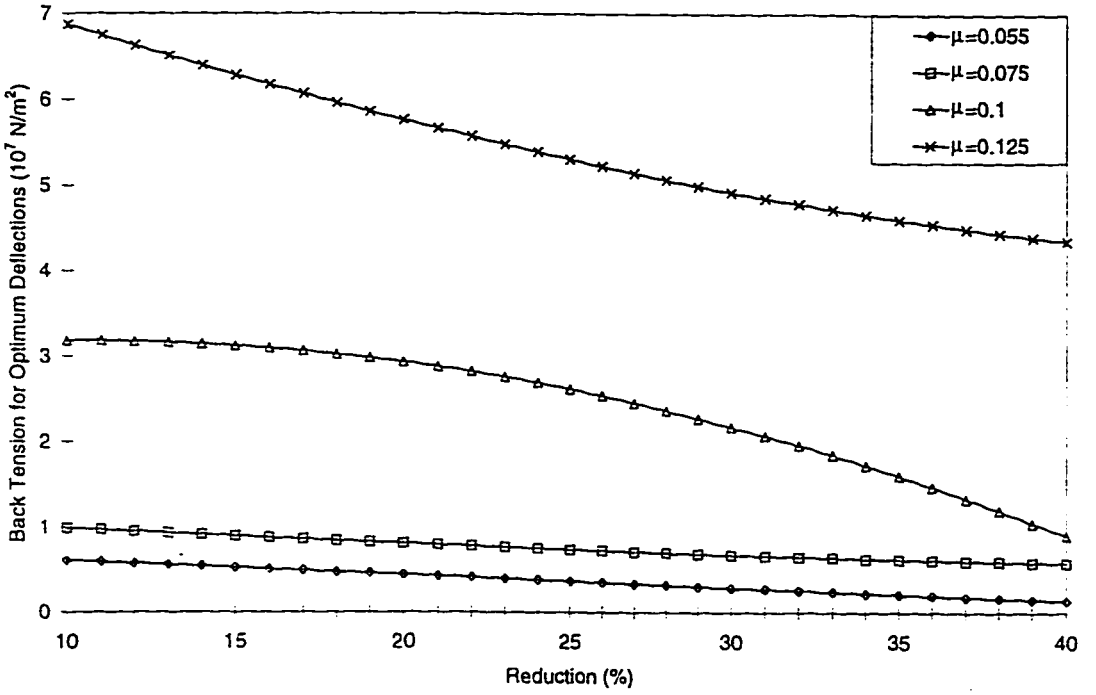

Figure 4.11: Variation of optimum values of back tension for cold rolling of steel as a function of coefficient of friction

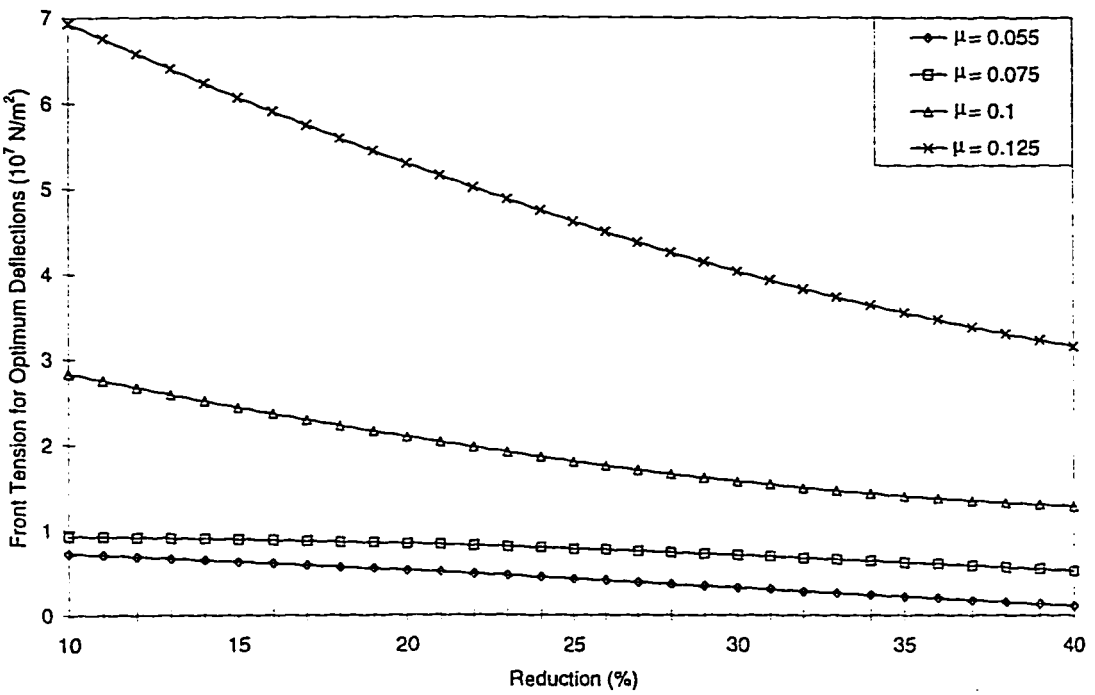

Figure 4.12: Variation of optimum values of front tension for cold rolling of steel as a function of coefficient of friction

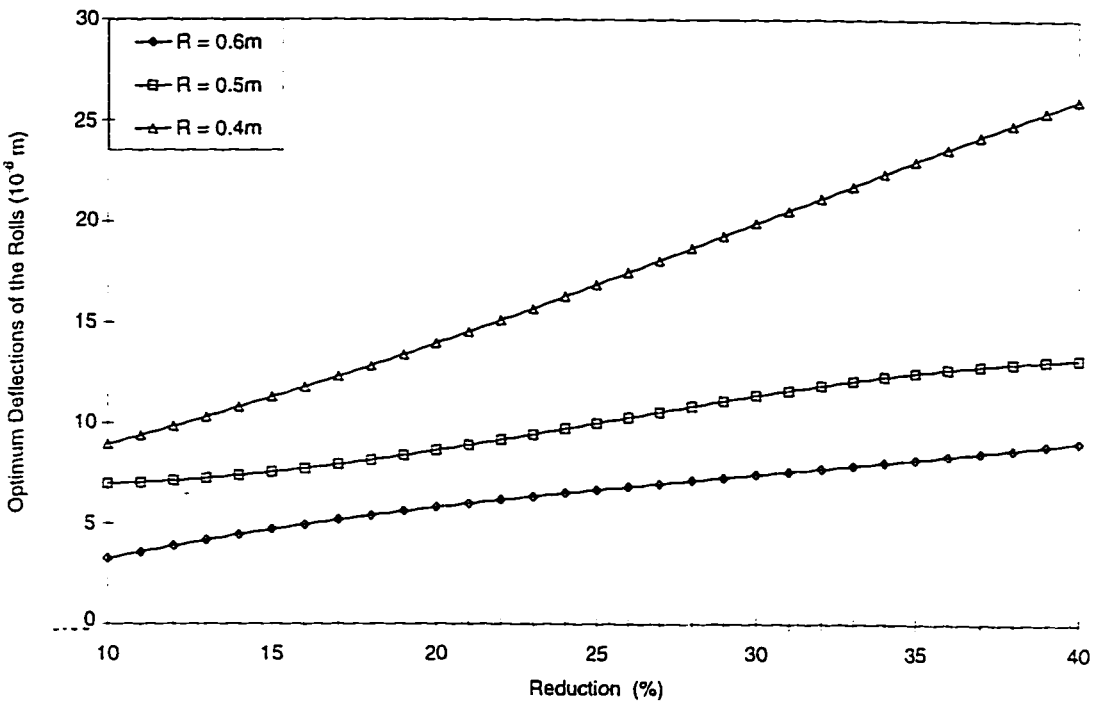

Figure 4.13: Variation of the optimum deflections of the rolls for cold rolling of steel as a function of roll radius

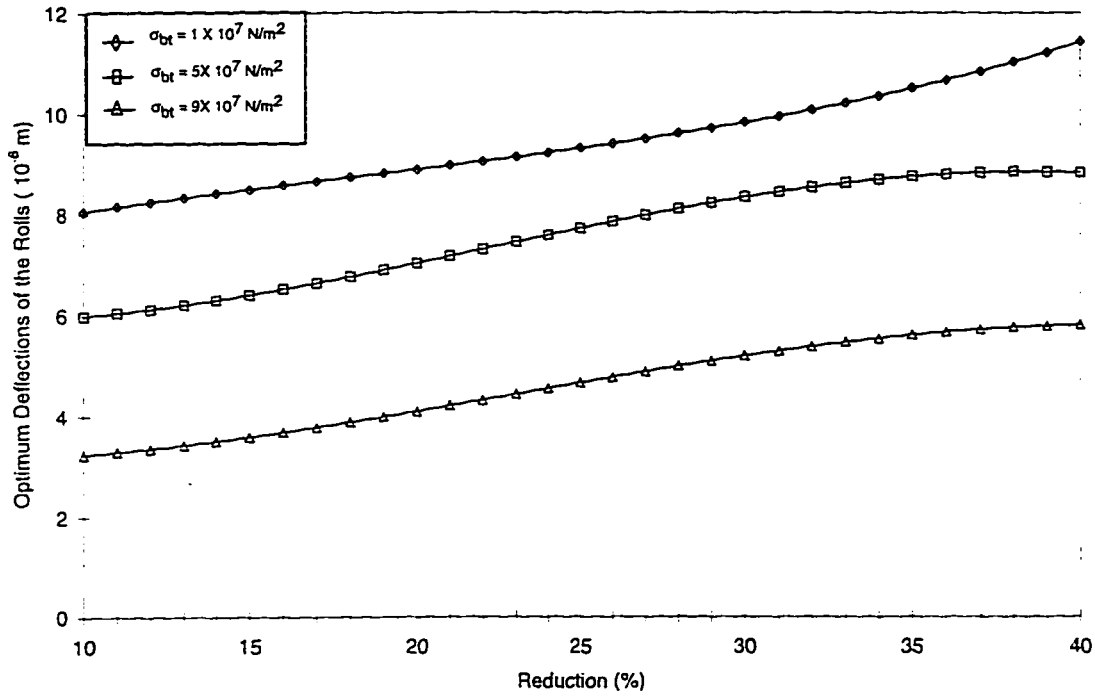

Figure 4.14: Variation of the optimum deflections of the rolls for cold rolling of steel as a function of back tension

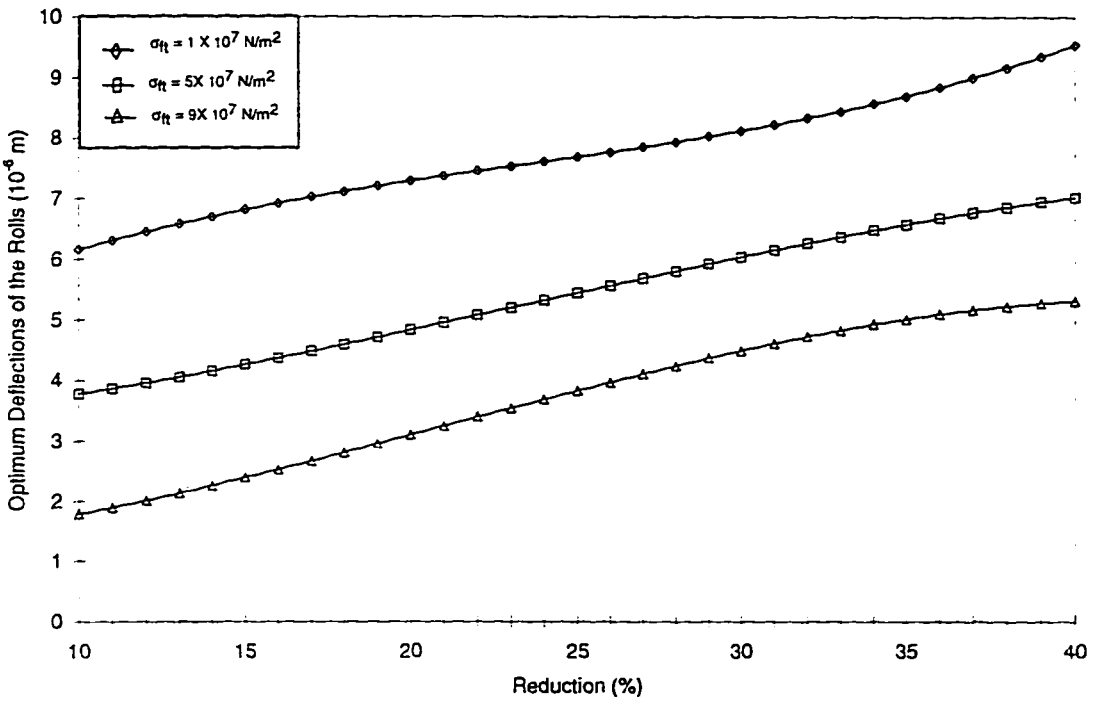

Figure 4.15: Variation of the optimum deflections of the rolls for cold rolling of steel as a function of front tension

Results for Hot Rolling Process

Cast steel is taken as the material for rolls as in cold rolling. The other data assumed for the numerical computations is as follows [1, 38] :

- Maximum permissible stress in the rolls = $15X10^5 N/m^2$
- Modulus of elasticity of the roll material = $1758.00X10^8 N/m^2$
- Coefficient of friction = 0.2
- Poison's ratio for the material to be rolled = 0.3
- Upper bound on the power = $2X10^3 J/rev$
- Initial thickness of the material = $25X10^{-3}m$

For comparison purposes, the calculations were carried out for three materials, namely, annealed steel, copper and aluminum, whose material behavior, at elevated temperatures is governed by the equations 4.34. For comparison purposes, the temperature considered is about 0.7 times the melting temperature of the materials.

$$\sigma_0 = c\dot{\bar{\epsilon}}^m \tag{4.34}$$

where c is the strength constant that depends upon temperature and material, and m is the strain rate sensitivity of the flow stress. The values of c and m for the above three materials are are given in Table 4.10, taken from references [1, 38]:

Table 4.10: Material properties at hot rolling temperature ($0.7T_m$)

Name of the Material	Strength Constant in ($c\ in N/mm^2$)	Strain rate Sensitivity (m)
Steel	138	0.11
Copper	72	0.14
Aluminum	23	0.2

The results of the optimization are shown in the Tables 4.11 to 4.13. The variations of the optimum values of roll deflection, roll radius and the back and front tensions with percentage reductions in thickness are shown in Figures 4.16 to 4.19.

Table 4.11: Optimum values of the design variables and the objective function for hot rolling of steel

Reduction %	Radius (m)	Back Tension (N/m^2)	Front Tension (N/m^2)	Deflection of the rolls (m)
20	0.2052	$6.779X10^5$	$8.801X10^5$	$7.221X10^{-9}$
30	0.1954	$5.316X10^5$	$7.293X10^5$	$7.755X10^{-9}$
40	0.1837	$4.176X10^5$	$6.032X10^5$	$9.854X10^{-9}$
50	0.1705	$3.311X10^5$	$4.947X10^5$	$13.79X10^{-9}$
60	0.1563	$2.676X10^5$	$3.972X10^5$	$19.84X10^{-9}$
70	0.1414	$2.223X10^5$	$3.036X10^5$	$28.27X10^{-9}$
80	0.1264	$1.907X10^5$	$2.073X10^5$	$39.37X10^{-9}$

Table 4.12: Optimum values of the design variables and the objective function for hot rolling of copper

Reduction %	Radius (m)	Back Tension (N/m^2)	Front Tension (N/m^2)	Deflection of the rolls (m)
20	0.1751	$2.006X10^5$	$2.798X10^5$	$7.286X10^{-10}$
30	0.1681	$1.426X10^5$	$2.151X10^5$	$7.579X10^{-10}$
40	0.1597	$1.105X10^5$	$1.615X10^5$	$9.072X10^{-10}$
50	0.1500	$0.9566X10^5$	$1.195X10^5$	$12.213X10^{-10}$
60	0.1397	$0.8971X10^5$	$0.9015X10^5$	$17.47X10^{-10}$
70	0.1289	$0.8418X10^5$	$0.7412X10^5$	$25.28X10^{-10}$
80	0.1183	$0.7065X10^5$	$0.7228X10^5$	$36.11X10^{-10}$

Table 4.13: Optimum values of the design variables and the objective function for hot rolling of aluminum

Reduction %	Radius (m)	Back Tension (N/m^2)	Front Tension (N/m^2)	Deflection of the rolls (m)
20	0.1492	$8.638X10^4$	$9.165X10^4$	$3.226X10^{-11}$
30	0.1455	$7.397X10^4$	$8.033X10^4$	$5.112X10^{-11}$
40	0.1385	$6.343X10^4$	$7.022X10^4$	$6.327X10^{-11}$
50	0.1292	$5.406X10^4$	$6.034X10^4$	$7.453X10^{-11}$
60	0.1189	$4.517X10^4$	$4.971X10^4$	$9.072X10^{-11}$
70	0.1088	$3.606X10^4$	$3.735X10^4$	$11.76X10^{-11}$
80	0.01002	$2.605X10^4$	$2.228X10^4$	$16.11X10^{-11}$

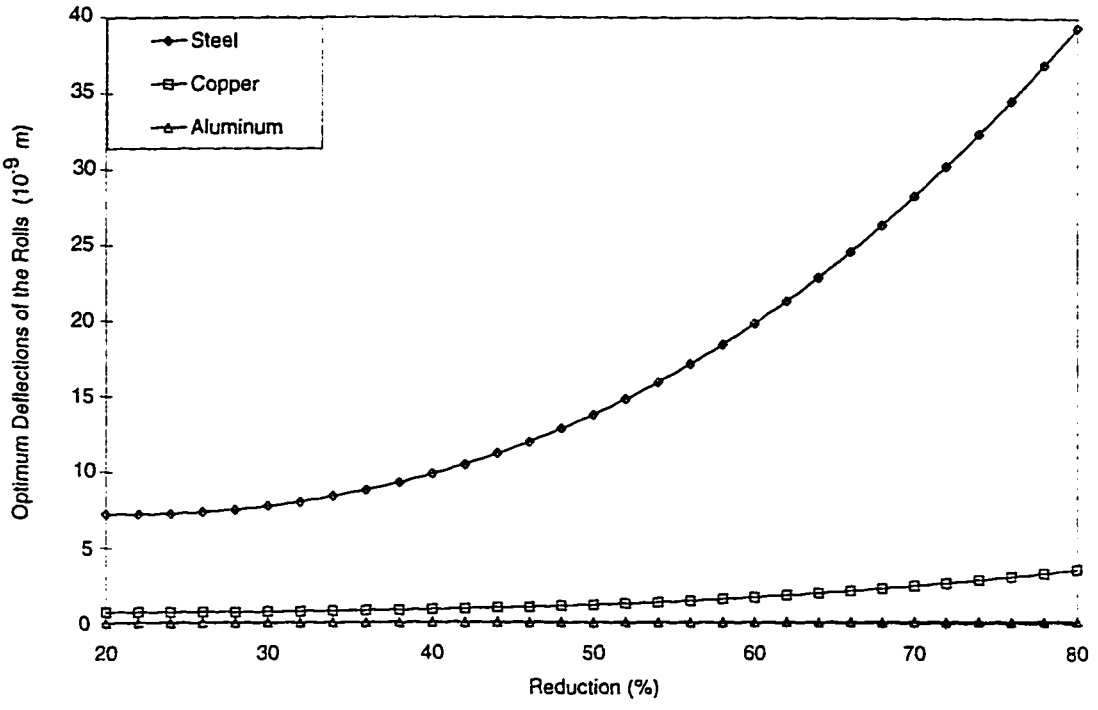

Figure 4.16: Variation of the optimum deflection of the rolls with percent reduction in thickness for hot rolling

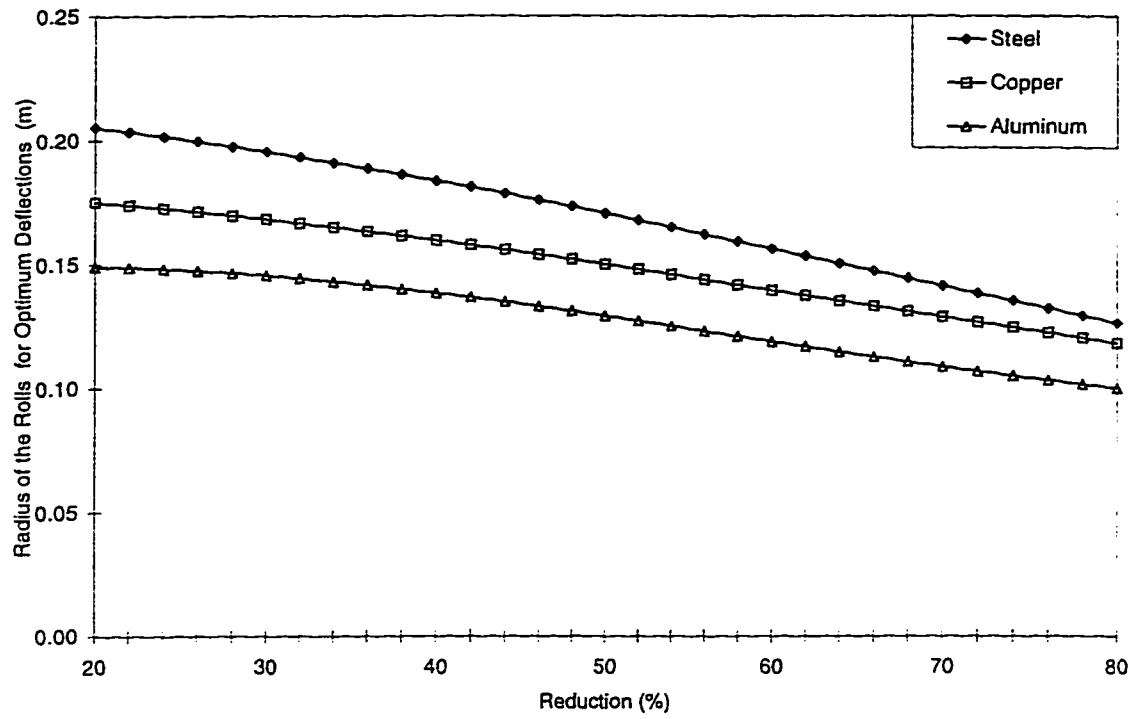

Figure 4.17: Variation of optimum values of roll radius with percent reduction in thickness for hot rolling

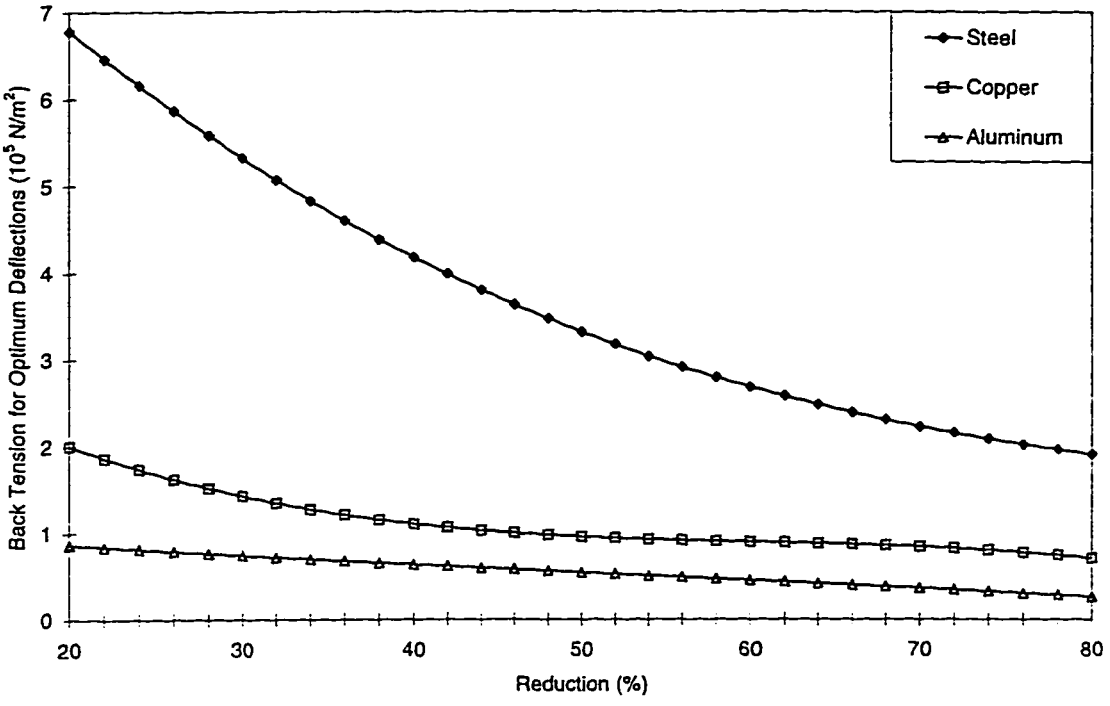

Figure 4.18: Variation of optimum values of back tension with percent reduction in thickness for hot rolling

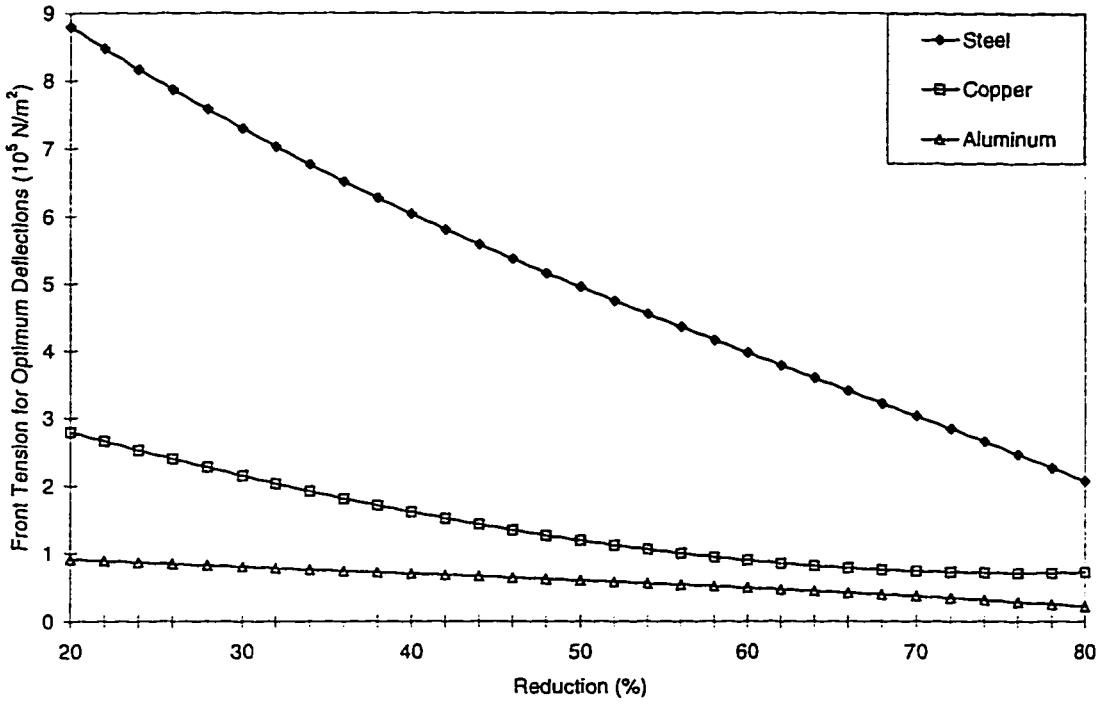

Figure 4.19: Variation of optimum values of front tension with percent reduction in thickness for hot rolling

Results of Optimization with different values of coefficient of Friction

Results were obtained for the optimization of the hot rolling of steel, with different values of coefficient of frictions. The coefficient of friction was varied from $\mu = 0.2$ to $\mu = 0.35$ [1, 38]. The results obtained are shown in the Figures from 4.20 to 4.23. The numerical values are given in Tables 4.14 to 4.17.

Table 4.14: Optimum values of the design variables and the objective function for hot rolling of steel for $\mu = 0.2$

Reduction %	Radius (m)	Back Tension (N/m^2)	Front Tension (N/m^2)	Deflection of the rolls (m)
20	0.2052	$6.779X10^5$	$8.801X10^5$	$7.221X10^{-9}$
30	0.1951	$5.339X10^5$	$7.327X10^5$	$7.618X10^{-9}$
40	0.1837	$4.176X10^5$	$6.032X10^5$	$9.854X10^{-9}$
50	0.1707	$3.228X10^5$	$4.913X10^5$	$13.92X10^{-9}$
60	0.1563	$2.676X10^5$	$3.972X10^5$	$19.84X10^{-9}$
70	0.1403	$2.339X10^5$	$3.207X10^5$	$27.59X10^{-9}$
80	0.1230	$2.279X10^5$	$2.621X10^5$	$37.17X10^{-9}$

Table 4.15: Optimum values of the design variables and the objective function for hot rolling of steel for $\mu = 0.25$

Reduction %	Radius (m)	Back Tension (N/m^2)	Front Tension (N/m^2)	Deflection of the rolls (m)
20	0.4253	$9.941X10^5$	$1.941X10^6$	$2.705X10^{-8}$
30	0.3646	$8.271X10^5$	$1.588X10^6$	$3.913X10^{-8}$
40	0.23097	$7.093X10^5$	$1.282X10^6$	$5.141X10^{-8}$
50	0.2604	$6.406X10^5$	$1.022X10^6$	$6.388X10^8$
60	0.2169	$6.212X10^5$	$0.8093X10^6$	$7.656X10^{-8}$
70	0.1790	$6.509X10^5$	$0.6428X10^6$	$8.943X10^{-8}$
80	0.1469	$7.298X10^5$	$0.5229X10^6$	$10.253X10^{-8}$

Table 4.16: Optimum values of the design variables and the objective function for hot rolling of steel for $\mu = 0.3$

Reduction %	Radius (m)	Back Tension (N/m^2)	Front Tension (N/m^2)	Deflection of the rolls (m)
20	0.5943	$4.317X10^6$	$5.222X10^6$	$8.317X10^{-8}$
30	0.5288	$3.618X10^6$	$4.533X10^6$	$9.196X10^{-8}$
40	0.4654	$3.019X10^6$	$3.892X10^6$	$11.98X10^{-8}$
50	0.4038	$2.523X10^6$	$3.298X10^6$	$16.66X10^{-8}$
60	0.3443	$2.121X10^6$	$2.753X10^6$	$23.26X10^{-8}$
70	0.2866	$1.822X10^6$	$2.225X10^6$	$31.75X10^{-8}$
80	0.2310	$1.623X10^6$	$1.805X10^6$	$42.15X10^{-8}$

Table 4.17: Optimum values of the design variables and the objective function for hot rolling of steel for $\mu = 0.35$

Reduction %	Radius (m)	Back Tension (N/m^2)	Front Tension (N/m^2)	Deflection of the rolls (m)
20	0.6542	$7.406X10^6$	$8.606X10^6$	$11.56X10^{-8}$
30	0.5832	$7.012X10^6$	$7.929X10^6$	$14.27X10^{-8}$
40	0.5226	$6.093X10^6$	$7.129X10^6$	$20.09X10^{-8}$
50	0.4723	$5.266X10^6$	$6.204X10^6$	$29.01X10^{-8}$
60	0.4325	$4.534X10^6$	$5.156X10^6$	$41.05X10^{-8}$
70	0.4030	$3.894X10^6$	$3.983X10^6$	$56.19X10^{-8}$
80	0.3839	$3.348X10^6$	$2.687X10^6$	$74.44X10^{-8}$

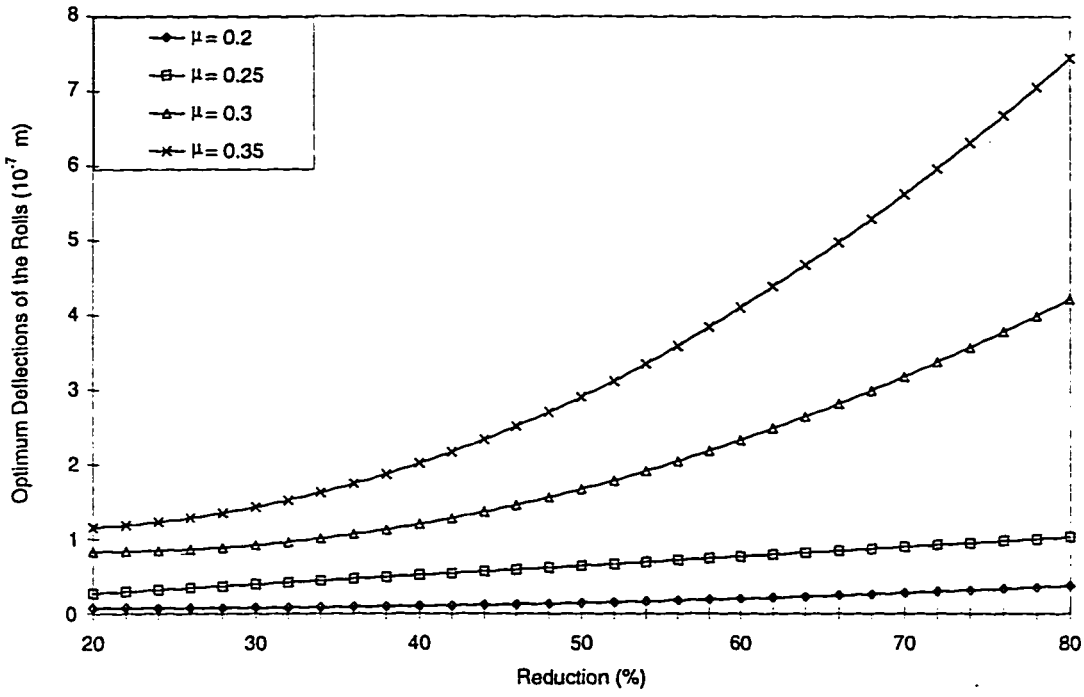

Figure 4.20: Variation of the optimum deflection of the rolls for hot rolling as a function of coefficient of friction

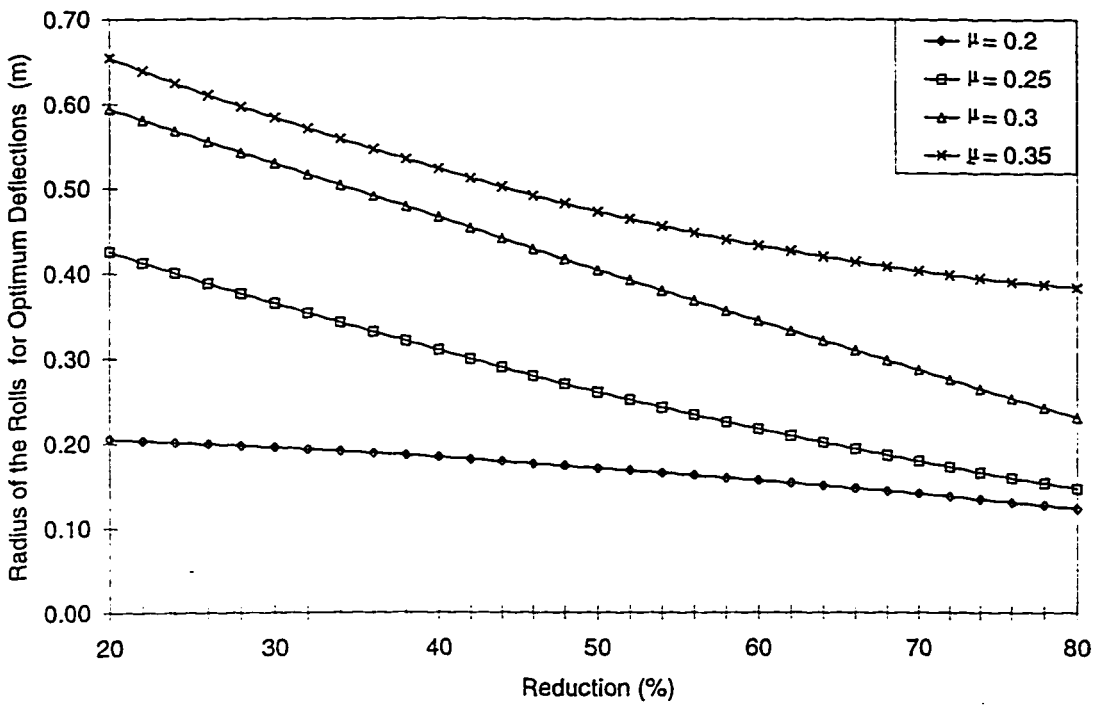

Figure 4.21: Variation of optimum values of roll radius for hot rolling as a function of coefficient of friction

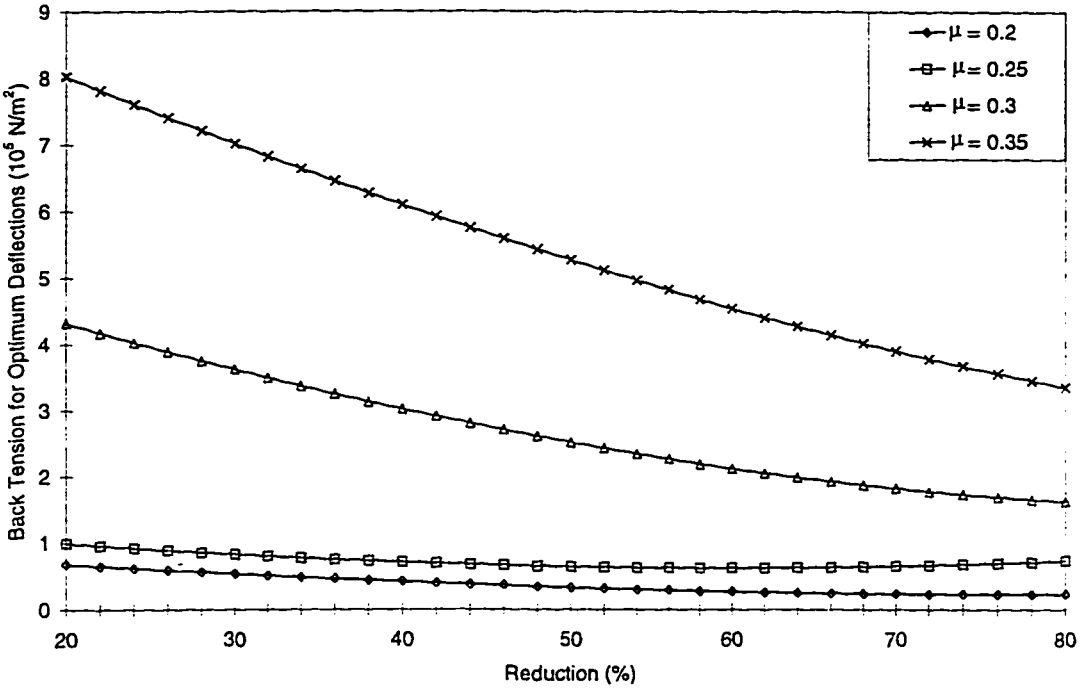

Figure 4.22: Variation of optimum values of back tension for hot rolling as a function of coefficient of friction

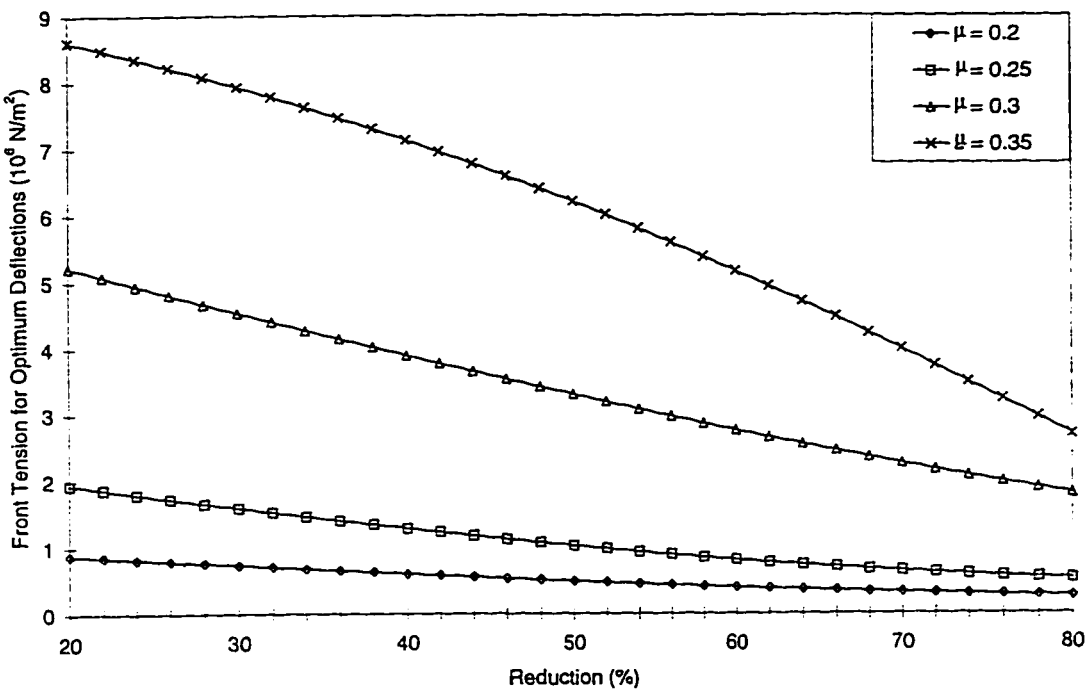

Figure 4.23: Variation of optimum values of front tension for hot rolling as a function of coefficient of friction

4.3.1 Discussions

The problem of determining the optimum design parameters of single pass strip rolling has been considered. The problem has been formulated and solved as a constrained nonlinear programming problem, considering the roll radius, and the front and back tensions as design variables. The minimization of the deflections of the rolls has been considered as the objective function. Constraints have been placed on the induced stresses, neutral angle and the angle of bite. An upper bound has also been placed on the energy required for rolling.

Cold Rolling with Constant Coefficient of friction

The design optimization problem has been solved for three materials, namely, steel, copper and aluminum, for an input thickness of $1.6X10^{-3}$ m. Different percentage reductions up to 40 percent have been considered in each case. The computer time taken for solving one optimization problem is approximately 6 minutes. The variation of the optimum values of roll deflections, roll radius and the front and back tensions with a variation in the percentage reductions have been shown in Figures 4.5 to 4.8. The optimum values of the objective function and the design parameters are given in Tables 4.3 to 4.5.

The following observations have been made from the optimization results obtained in the case of cold rolling of all the three materials, with a coefficient of friction of 0.05:

1. The roll deflections increase with an increase in the percentage reduction for all the three materials. However the magnitude of deflections are the greatest in the case of steel and lowest for aluminum. This is because of the high strength of steel when compared to copper and aluminum.

2. The radius of the rolls decreases with increasing reduction in thickness.

3. The front and back tensions also decrease with increasing reduction in thickness.

These trends may be explained from the fact that the deflections of the rolls is dependent upon the roll force and the roll radius. From Equation. 4.11, it can be seen that the deflections of the rolls is directly proportional to the roll force (P) and is inversely proportional to the roll radius (R). Seeing the problem of minimizing the deflections, in view of the different factors affecting it, we observe that the same can be achieved either by reducing the roll force or by increasing the roll radius.

However as heavy reductions are undertaken, the force (P) on the rolls increase, which in turn increases the deflections (δ_r) in them. The objective of this study being the minimization of the deflections, the roll force has to be reduced to achieve the same. This could be done by decreasing the roll radius and increasing the front and back tensions. However, the roll force being more sensitive to the change in roll radius than the change in the magnitude of tensions, the radius is reduced with heavy reductions. The results obtained, as shown in Table 4.3 and Figure 4.6, seem

to agree with the above explanation.

However, as the roll radius decreases, the deflection of the rolls tends to increase, which again can be controlled by increasing the tensions. But, the magnitude of the tensions and the radius of the rolls is governed by the various bounds such as on the energy available for rolling and the maximum permissible stresses induced in the rolls, etc. given in the optimization model. Thus, the magnitude of the tensions cannot exceed a certain value for a given reduction. Due to the interdependency of all these factors on one another, a compromise is reached between the values of the roll radius and the tensions, during optimization, so that the value of the objective function, i.e. the deflection of the rolls is minimum. Thus the trend of the back and front tensions, with increasing reductions as shown in Table 4.3, Figure 4.7 and Figure 4.8, respectively, can be explained.

Effect of Changing the Various Rolling Parameters

Friction in rolling plays a very important role because the rolls cannot pull the strip into the roll gap without it. Moreover, the forces and power requirements depend considerably on friction. In cold rolling, the coefficient of friction μ usually ranges between 0.02 and 0.3, depending on the materials and lubricants used. The low ranges of friction are obtained with effective lubricants.

The effect of changing the coefficient of friction on the optimum results has also been studied. The coefficient of friction has been varied from $\mu = 0.05$ to $\mu = 0.125$,

with an increment of 0.025. Steel has been taken as the material of the sheet to be rolled, with the initial thickness $1.6X10^{-3}$ m. Different percentage reductions up to 40 percent have been considered in each case. The computer time taken for solving one optimization problem is approximately 6 minutes. The variation of the optimum values of roll deflections, roll radius and the front and back tensions with a variation in the percentage reductions have been shown in Figures 4.9 to 4.12. The optimum values of the objective function and the design parameters are given in Tables 4.6 to 4.9.

The optimization results in this case indicate that

1. The roll deflections increase with increasing reductions. However the magnitude of deflections is highest for $\mu = 0.125$ and the lowest for $\mu = 0.05$.

2. The roll radius decreases with increasing reductions in thickness.

3. The front and back tensions decrease with increasing reductions in thickness.

These trends can be explained from the fact that, the roll force is directly proportional to the coefficient of friction. Any increase in the coefficient of friction results in an increase in the roll force, which in turn increases the roll deflections (see Figure 4.9). The corresponding values of the roll radius and the front and back tensions decrease as heavy reductions are taken.

In the case of varying roll radius, the trends in Figure 4.13 show that the optimum values of deflections of the rolls increases with increasing reduction. However, the

magnitude of deflection of the rolls is decreasing with increasing roll radius. This is explained from the fact that the deflections of the rolls is inversely proportional to the roll radius as evident from Equation 4.11. The effect of changing the back tensions and front tensions is also observed in the Figures 4.14 and 4.15 respectively. The deflections of the rolls decrease with increasing tensions. This is because, as the tensions increase, the force on the rolls tends to decrease which ion turn decreases the deflections in the rolls.

Hot Rolling with Constant Coefficient of Friction

The hot rolling optimization problem has been studied for three different materials, namely, steel, copper and aluminum, for an input thickness of $25X10^{-3}$ m. Different percentage reductions in the range of 20 to 80 percent have been considered in each case. The variation of the optimum values of roll deflections, roll radius and the front and back tensions with a variation in the percentage reductions have been shown in Figures 4.16 to 4.19. The optimum values of the objective function and the design parameters are given in Tables 4.11 to 4.13. In this case, the flow stress of the material is a function of strain rate and temperature. For comparison purposes, the temperature considered in our study is about 0.7 times the melting temperature of the above materials.

The observations made in this case are very much similar to that in the case of cold rolling, except that the magnitudes of the roll deflections have been found to be

much lesser. This is because, in hot rolling, the metal is heated to a temperature of about 0.7 times its melting temperature, making the metal softer and ductile. This reduces the forces on the rolls while rolling which in turn causes less deflections of the rolls.

Effect of Changing the Coefficient of Friction during Hot Rolling

In hot rolling, the coefficient of friction ranges from about 0.2, with effective lubrication, to as high as 0.5, indicating sticking, which usually occurs with steels and high-temperature alloys. The effect of changing the coefficient of friction on the optimum results for hot rolling has also been studied. The coefficient of friction has been varied from $\mu = 0.2$ to $\mu = 0.35$, with an increment of 0.05. Steel has been taken as the material of the sheet to be rolled, with the initial thickness $25X10^{-3}$ m. Different percentage reductions in the range of 20 to 80 percent have been considered in each case. The computer time taken for solving one optimization problem is approximately 6 minutes. The variation of the optimum values of roll deflections, roll radius and the front and back tensions with a variation in the percentage reductions have been shown in Figures 4.20 to 4.23. The optimum values of the objective function and the design parameters are given in Tables 4.14 to 4.17.

The optimization results indicate that:

1. The roll deflections increase with increasing reductions. However, the magnitude of deflections are highest for $\mu = 0.35$.

2. The roll radius decreases with increasing reductions in thickness.

3. The front and back tensions decrease with increasing percentage reductions.

In this case the magnitude of the deflections of the rolls and the other rolling parameters is much less than that observed in the case of the cold rolling process. This is because, as the metal is heated to an elevated temperature, it tends to become soft and more ductile, which reduces the forces on the rolls. Thus the trends are explained.

Practical Significance of the Problem

Any deflections in the rolls while rolling a metallic sheet will effect the final quality of the product and also the roll life. For this purpose the deflections in the rolls have to be kept to a minimum possible value. This can be achieved by designing the roll mill, with specific values of roll radius and the front and back tensions, so that the deflections in the rolls will be minimum.

In our study, efforts have been made to minimize the roll deflections. Using this technique, roll mills can be designed specifying the values for the various rolling parameters, for any input thickness and for any material to be rolled. Considering an example, of a steel sheet of input thickness $1.6X10^{-3}m$ to be reduced in thickness by 20 percent. The designer should specify the values of the roll radius and the front and back tensions to be maintained for this particular reduction, corresponding to the values given in Table 4.3, if the deflections in the rolls have to be minimum.

This not only helps in improving the quality of the product as well as life of the rolls but also helps in reducing the maintenance costs of the rolls.

4.4 CASE 2: Minimization of the Energy Consumption

Several single pass mills in series constitute a tandem mill. In multipass rolling, as shown in the Figure 4.24, a sheet of initial thickness h_0 is reduced to its final thickness h_f in several passes. The model objective function is the sum of the objective functions of the passes, and the constraints which apply depend on the pass being rolled. The optimization of multipass rolling is considered in this section.

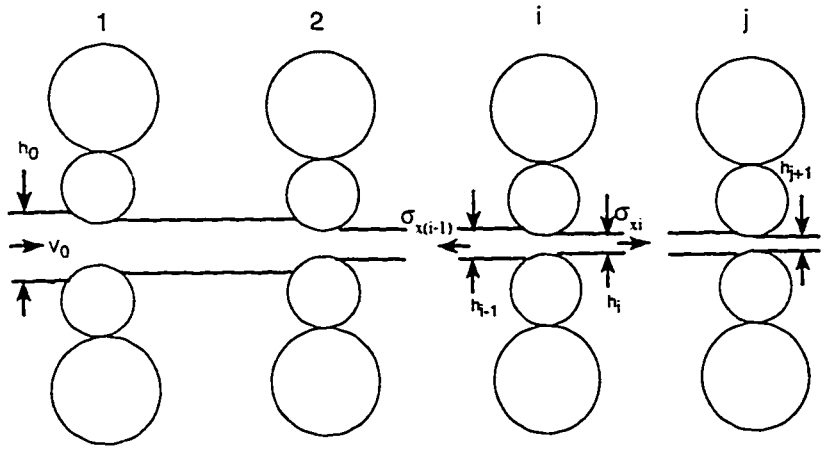

Figure 4.24: Schematic diagram of the multipass rolling

The objective function considered in the case of multipass rolling process is, to find the optimum number of passes for a particular reduction such that the total energy consumed by the tandem mill is minimum.

Finding the optimum conditions of rolling for a particular reduction, reduces the energy consumed by the tandem mill which in turn reduces the cost of power

and reduces the roll and maintenance costs. This will help in reducing the overall production cost. Hence, the above objective function of minimizing the total energy consumed is considered in this section.

4.4.1 Governing equations

The objective function is taken as the algebraic sum of the energy consumed at each station as

$$f(\overline{X}) = \sum_{i=1}^{j}(e_i) \tag{4.35}$$

where, e_i represents the energy consumption of the ith mill, and j indicates the total number of rolling mills in series. The design vector is taken as

$$\overline{X} = \begin{Bmatrix} R_i \\ \vdots \\ R_j \\ \sigma_1 \\ \vdots \\ \sigma_{j+1} \\ h_i \\ \vdots \\ h_j \end{Bmatrix}$$

where R_i is the radius of the rolls in the ith mill, σ_1 is the back tension in the first mill, σ_{j+1} is the front tension of the last (j_{th}) mill, σ_i is the tension between $i-1st$

and i_{th} mills ($i = 1, 2, 3, ...j$), h_i is the thickness of the strip between the $(i-1)_{th}$ and i_{th} mills ($i = 1, 2, 3, ...j$), h_0 is the input thickness and h_{j+1} is the output thickness of the strip. In the case of multipass rolling, the constraints stated in the case of a single pass rolling mill need to be satisfied along with an upper bound on the reduction ratio at each mill of the tandem. Thus the objective function and the constraints can be expressed mathematically as follows:

$$\sum_{i=1}^{j}(e_i) = \sum_{i=1}^{j} 2\pi \left[2G_i + P_i\mu_i d_i + R_i(\sigma_i + \sigma_{i+1})\left[1 + 2\frac{R_i}{h_{i+1}}(1 - cos\phi_{N_i})\right]\right] \quad (4.36)$$

$$R_i \geq 0 \qquad i = 1, 2, ...j \quad (4.37)$$

$$\sigma_i \geq 0 \qquad i = 1, 2, ...j+1 \quad (4.38)$$

$$0 \leq \phi_{N_i} \leq \alpha_i \qquad i = 1, 2, ...j \quad (4.39)$$

$$0 \leq \alpha_i \leq 2tan^{-1}(\mu_i) \qquad i = 1, 2, ...j \quad (4.40)$$

$$\sigma_{c_i} \leq \sigma_{max_i} \qquad i = 1, 2, ...j \quad (4.41)$$

$$\frac{P_i Z_i^2}{6E_i D_i^2}(5Z_i + 24a_i) + \frac{4P_i Z_i}{3\pi E_i D_i^2} \leq \delta_{max_i} \qquad i = 1, 2, ...j \quad (4.42)$$

$$\frac{h_i - h_{i+1}}{h_i} \leq r_{max_i} \qquad i = 1, 2, ...j \quad (4.43)$$

and an another constraint to be satisfied in the case of multipass rolling is that the sum of the true strains at each station must be equal to the total true strain for a

reduction from h_0 to h_f.

$$\sum_{i=1}^{j} \bar{\epsilon}_i = \bar{\epsilon}_T \tag{4.44}$$

The other constraint that has to be satisfied is that the true strain induced in the material to be rolled at each station should not exceed the true strain at fracture for that particular material.

$$ln(h_i/h_{i+1}) < \bar{\epsilon}_f \qquad i = 1, 2, ...j \tag{4.45}$$

In the above equations, ϕ_{n_i} and α_i are the neutral and bite angles, respectively, in the *ith* mill, μ_i is the friction coefficient between the material and the rolls in the *ith* mill, σ_{c_i} and σ_{max_i} are the induced and the permissible stresses in the rolls of the *ith* mill, δ_{max_i} is the maximum deflection of the rolls allowed at the *ith* stage, r_{max_i} is the maximum permissible reduction at the *ith* stage, P_i and G_i are the load and torque at each stage, respectively. Z_i is as shown in Figure 4.2 and a_i is given by Eqn.4.10.

4.4.2 Algorithm for multipass rolling model

The algorithm for the multipass rolling model used here is more akin to that used by Shuaib et al. [39], for the minimization of the cost in a multipass machining process.

Step 1: The number of mills (j), is set to one, i.e., $j = 1$, and the optimal solution $c(j)$, for the resulting non-linear problem is determined.

Step 2: The number of mills is set to $j = j + 1$, and the optimal solution $e(j)$, for the resulting model is determined.

Step 3: If $e(j) \leq e(j-1)$, go to step 2; otherwise stop.

The flow chart of the above algorithm is as shown in Figure 4.25.

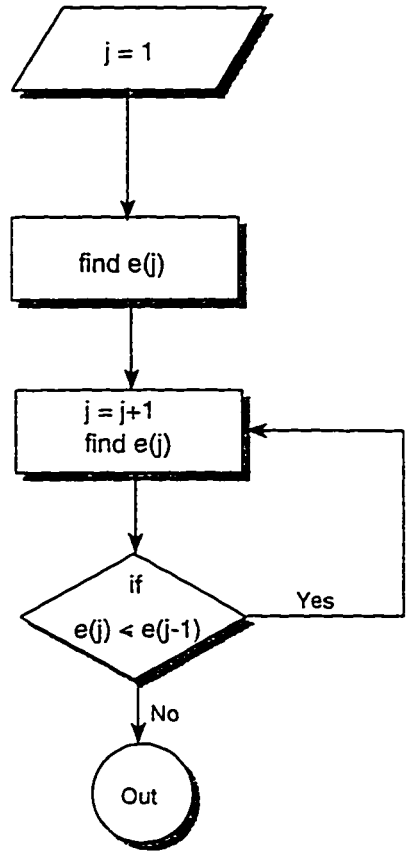

Figure 4.25: Flow chart describing the algorithm for multipass rolling

4.4.3 Results

Results for both the cold and hot rolling processes are presented here:

Results for Cold Rolling Process

In the present work, cast steel is taken as the roll material. as it is the most commonly used material in the industry for the manufacturing of the rolls. The other data assumed for the numerical computations are as follows [1, 22], which are determined from the practical considerations of the rolling process:

- Maximum permissible stress in the rolls = $15X10^8 N/m^2$
- Modulus of elasticity of the roll material = $1758.00X10^8 N/m^2$
- Coefficient of friction at each station = 0.055
- Poison's ratio for the material to be rolled = 0.3
- Upper bound on the deflection of the rolls at each station = $12.7X10^{-6}m$
- Initial thickness of the material = $3.2X10^{-3}m$
- The total reduction required = 40%
- The maximum allowable reduction at each station = 30%

For comparison purposes, the calculations have been carried out for a total reduction of 40% for three materials, namely, annealed steel, copper and aluminum.

whose material behavior is governed by the equation 4.33. The values of K and n for these materials are as same as before. The values of the strain at fracture and the maximum permissible reduction in area that could be undertaken for the three materials used is given in the Table 4.2, [1].

The optimum values of the design variables obtained for different values of j, i.e., for the different number of mills, are given in the Tables from 4.18 to 4.27

Table 4.18: Optimum values of the design variables and the objective function during cold rolling of steel for j=1.

Name of the Design Variable	Optimum Values obtained	Value of the Objective Function (J/rev)
	j = 1	
Radius (m)	0.2732	$6.852X10^5$
Back Tension ($10^7 N/m^2$)	3.587	
Front Tension ($10^7 N/m^2$)	2.165	
Final Thickness ($10^{-3}m$)	1.92	
Reduction ($i\%$)	40	

Table 4.19: Optimum values of the design variables and the objective function during cold rolling of steel for j=2.

Name of the Design Variable	Optimum Values obtained		Value of the Objective Function (J/rev)
	j = 1	j=2	
Radius (m)	0.2092	0.1817	$1.693X10^5$
Back Tension ($10^7 N/m^2$)	5.147	4.828	
Front Tension ($10^7 N/m^2$)	4.828	5.893	
Final Thickness ($10^{-3}m$)	2.31	1.92	
Reduction (%)	27.81	16.88	

Table 4.20: Optimum values of the design variables and the objective function during cold rolling of steel for j=3.

Name of the Design Variable	Optimum Values obtained			Value of the Objective Function (J/rev)
	j = 1	j=2	j=3	
Radius (m)	0.186	0.179	0.171	$0.6514X10^5$
Back Tension ($10^7 N/m^2$)	6.965	6.101	7.208	
Front Tension ($10^7 N/m^2$)	6.101	7.208	6.847	
Final Thickness ($10^{-3}m$)	2.41	2.15	1.92	
Reduction (%)	24.65	10.5	11.02	

Table 4.21: Optimum values of the design variables and the objective function during cold rolling of steel for j=4.

Name of the Design Variable	Optimum Values obtained				Value of the Objective Function (J/rev)
	j = 1	j=2	j=3	j=4	
Radius (m)	0.197	0.191	0.186	0.184	$1.3627X10^5$
Back Tension ($10^7 N/m^2$)	4.205	3.841	4.415	4.958	
Front Tension ($10^7 N/m^2$)	3.841	4.415	4.958	4.672	
Final Thickness ($10^{-3}m$)	2.76	2.45	2.20	1.92	
Reduction (%)	13.48	11.27	10.26	12.88	

Table 4.22: Optimum values of the design variables and the objective function during cold rolling of copper for j=1.

Name of the Design Variable	Optimum Values obtained	Value of the Objective Function (J/rev)
	j = 1	
Radius (m)	0.1989	$0.7939X10^5$
Back Tension ($10^7 N/m^2$)	0.2012	
Front Tension ($10^7 N/m^2$)	0.1972	
Final Thickness ($10^{-3}m$)	1.92	
Reduction (%)	40	

Table 4.23: Optimum values of the design variables and the objective function during cold rolling of copper for j=2.

Name of the Design Variable	Optimum Values obtained		Value of the Objective Function (J/rev)
	j = 1	j=2	
Radius (m)	0.1806	0.1797	$0.2012X10^5$
Back Tension $(10^7 N/m^2)$	0.2663	0.2279	
Front Tension $(10^7 N/m^2)$	0.2279	0.2128	
Final Thickness $(10^{-3}m)$	2.504	1.92	
Reduction (%)	21.74	23.32	

Table 4.24: Optimum values of the design variables and the objective function during cold rolling of copper for j=3.

Name of the Design Variable	Optimum Values obtained			Value of the Objective Function (J/rev)
	j = 1	j=2	j=3	
Radius (m)	0.1875	0.1823	0.1782	$0.5208X10^5$
Back Tension $(10^7 N/m^2)$	0.1503	0.1957	0.2438	
Front Tension $(10^7 N/m^2)$	0.1957	0.2438	0.1847	
Final Thickness $(10^{-3}m)$	2.66	2.24	1.92	
Reduction (%)	16.84	15.52	14.59	

Table 4.25: Optimum values of the design variables and the objective function during cold rolling of aluminum for j=1.

Name of the Design Variable	Optimum Values obtained	Value of the Objective Function (J/rev)
	j = 1	
Radius (m)	0.1619	$0.3209X10^5$
Back Tension $(10^7 N/m^2)$	0.1178	
Front Tension $(10^7 N/m^2)$	0.1643	
Final Thickness $(10^{-3}m)$	1.92	
Reduction (%)	40	

Table 4.26: Optimum values of the design variables and the objective function during cold rolling of aluminum for j=2.

Name of the Design Variable	Optimum Values obtained		Value of the Objective Function (J/rev)
	j = 1	j=2	
Radius (m)	0.1472	0.1391	$0.1052X10^5$
Back Tension ($10^7 N/m^2$)	0.1968	0.2183	
Front Tension ($10^7 N/m^2$)	0.2183	0.1874	
Final Thickness ($10^{-3}m$)	2.33	1.92	
Reduction (%)	27.04	17.76	

Table 4.27: Optimum values of the design variables and the objective function during cold rolling of aluminum for j=3.

Name of the Design Variable	Optimum Values obtained			Value of the Objective Function (J/rev)
	j = 1	j=2	j=3	
Radius (m)	0.1528	0.1502	0.1489	$0.2971X10^5$
Back Tension ($10^7 N/m^2$)	0.1009	0.1138	0.1092	
Front Tension ($10^7 N/m^2$)	0.1138	0.1092	0.1275	
Final Thickness ($10^{-3}m$)	2.606	2.228	1.92	
Reduction (%)	18.56	14.47	13.82	

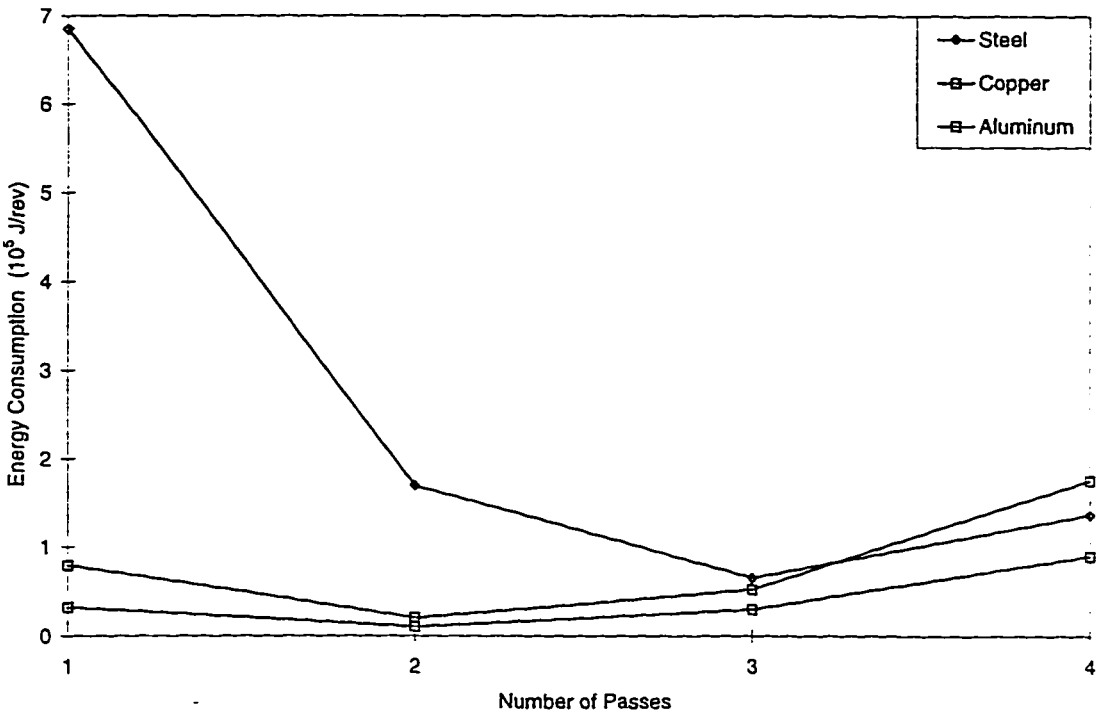

Figure 4.26: Variation of the energy consumption with the number of passes for cold rolling

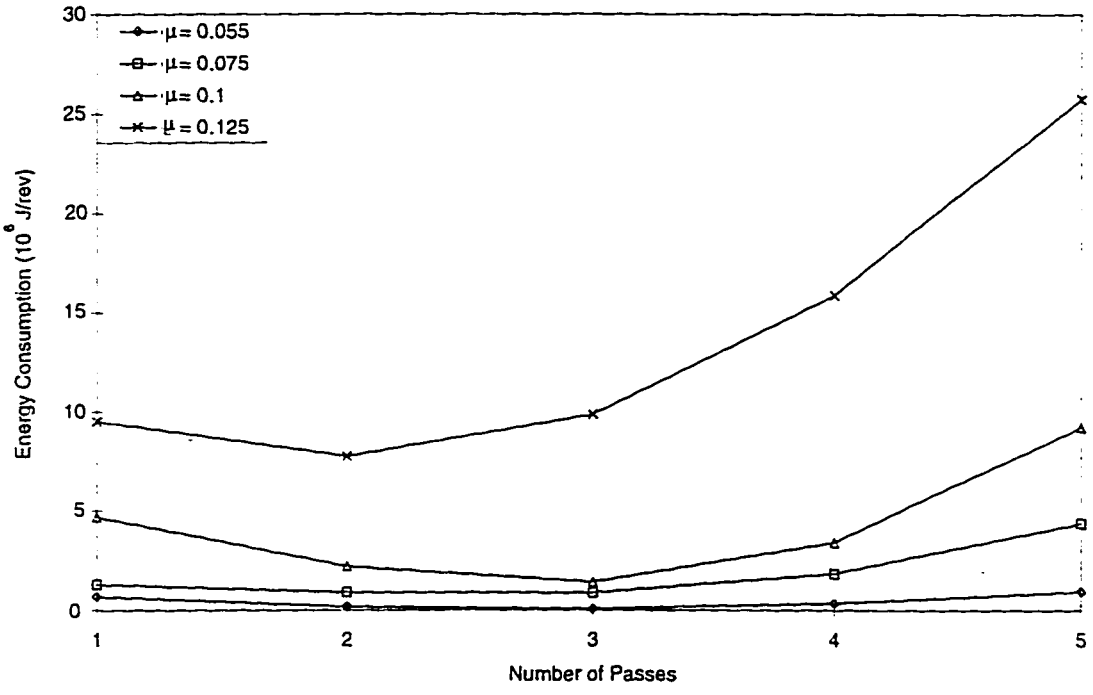

Figure 4.27: Variation of the energy consumption with the number of passes for cold rolling of steel as a function of coefficient of friction.

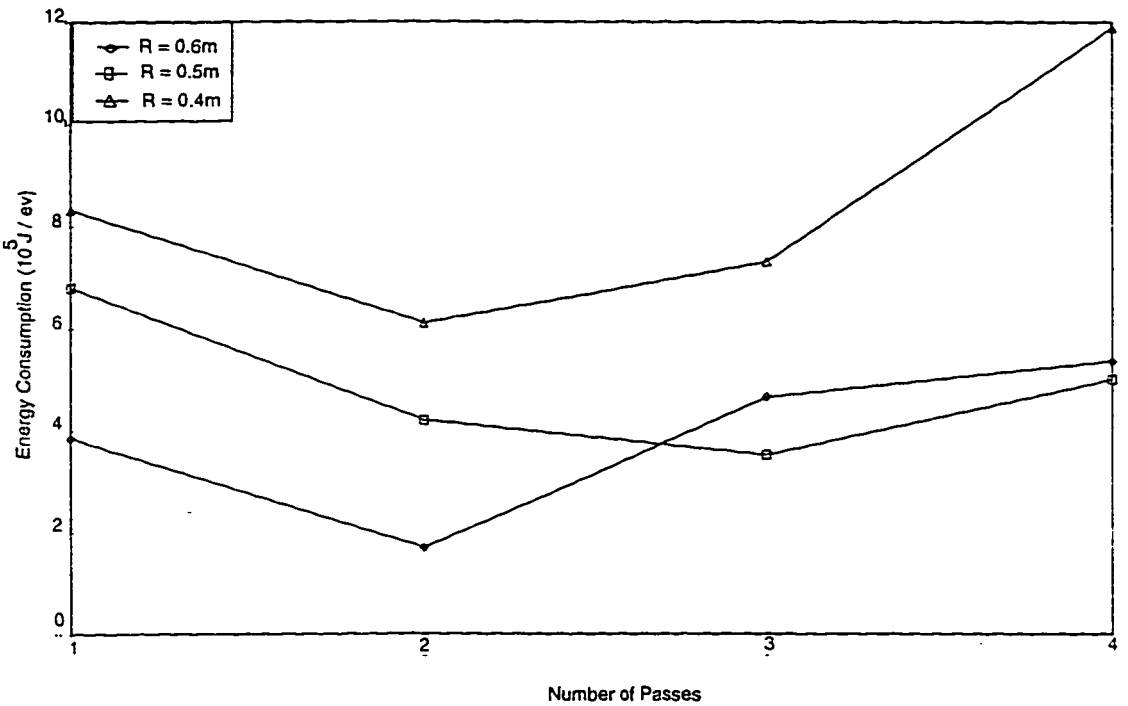

Figure 4.28: Variation of the energy consumption with the number of passes for cold rolling of steel as a function of roll radius.

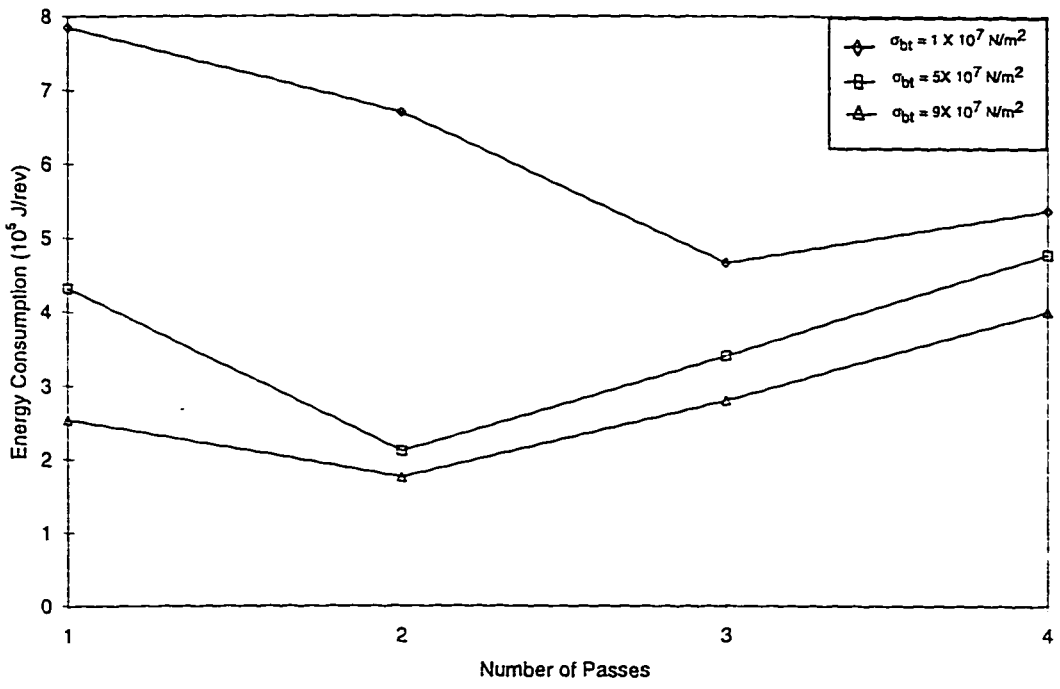

Figure 4.29: Variation of the energy consumption with the number of passes for cold rolling of steel as a function of back tension.

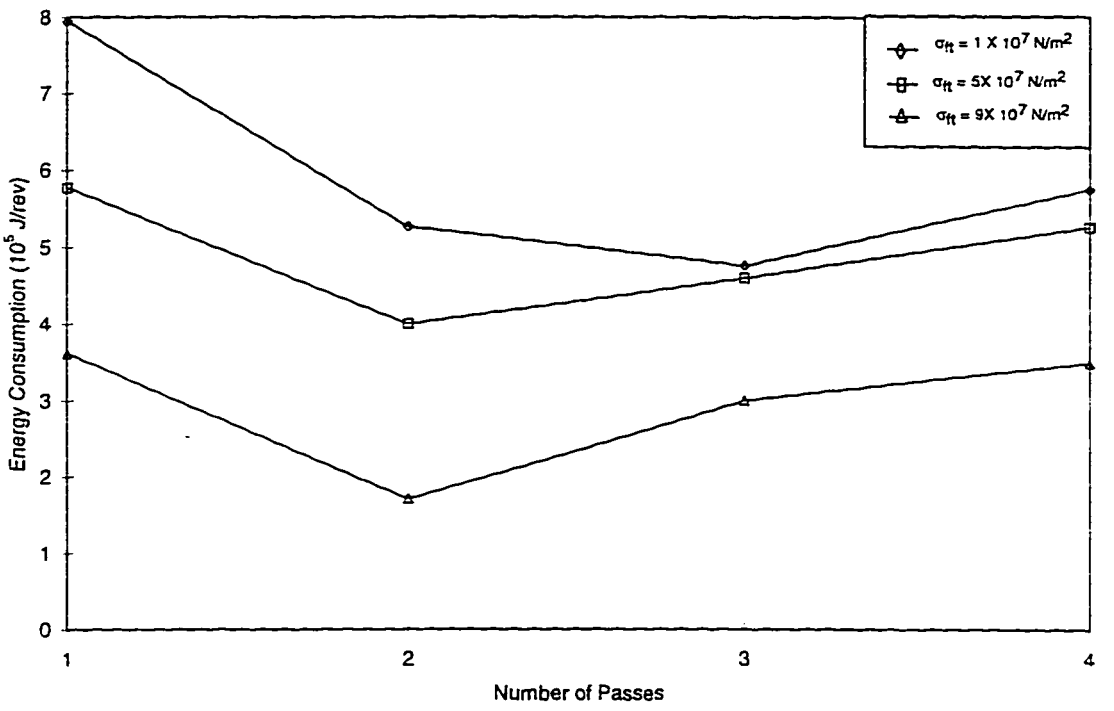

Figure 4.30: Variation of the energy consumption with the number of passes for cold rolling of steel as a function of front tension.

Results for Hot Rolling Process

In the present work, cast steel is taken as the roll material, as it is the most commonly used material in the industry for the manufacturing of the rolls. The other data assumed for the numerical computations are as follows [1, 38], which are determined from the practical considerations of the rolling process:

- Modulus of elasticity of the roll material = $1758.00X10^8 N/m^2$
- Coefficient of friction at each station = 0.2
- Poison's ratio for the material to be rolled = 0.3
- Upper bound on the deflection of the rolls at each station = $12.7X10^{-7}m$
- Initial thickness of the material = $31.75X10^{-3}m$
- The total reduction required = 80%
- the maximum allowable reduction at each station = 70%

The calculations were carried out for three materials, namely, annealed steel, copper and aluminum whose material behavior at elevated temperatures is governed by the Equation 4.34 and the temperature considered is about 0.7 times the melting temperature of the materials. The values of c and m for these materials are as same as before. The optimum values of the design variables obtained for different values of j, i.e., for the different number of mills, are given in the Tables from 4.28 to 4.38

Table 4.28: Optimum values of the design variables and the objective function during hot rolling of steel for j=1.

Name of the Design Variable	Optimum Values obtained	Value of the Objective Function (J/rev)
	j = 1	
Radius (m)	0.2092	$5.087X10^4$
Back Tension ($10^6N/m^2$)	4.308	
Front Tension ($10^6N/m^2$)	4.748	
Final Thickness ($10^{-3}m$)	6.35	
Reduction (%)	80	

Table 4.29: Optimum values of the design variables and the objective function during hot rolling of steel for j=2.

Name of the Design Variable	Optimum Values obtained		Value of the Objective Function (J/rev)
	j = 1	j=2	
Radius (m)	0.192	0.205	$4.287X10^4$
Back Tension ($10^6N/m^2$)	5.748	5.032	
Front Tension ($10^6N/m^2$)	5.032	5.693	
Final Thickness ($10^{-3}m$)	11.35	6.35	
Reduction (%)	64.25	44.05	

Table 4.30: Optimum values of the design variables and the objective function during hot rolling of steel for j=3.

Name of the Design Variable	Optimum Values obtained			Value of the Objective Function (J/rev)
	j = 1	j=2	j=3	
Radius (m)	0.183	0.179	0.178	$1.897X10^4$
Back Tension ($10^6N/m^2$)	6.652	6.165	6.847	
Front Tension ($10^6N/m^2$)	6.165	6.847	5.728	
Final Thickness ($10^{-3}m$)	12.50	8.07	6.35	
Reduction (%)	60.62	35.42	21.31	

Table 4.31: Optimum values of the design variables and the objective function during hot rolling of steel for j=4.

Name of the Design Variable	Optimum Values obtained				Value of the Objective Function (J/rev)
	j = 1	j=2	j=3	j=4	
Radius (m)	0.169	0.163	0.156	0.155	$0.905X10^4$
Back Tension ($10^6 N/m^2$)	8.205	8.415	7.958	8.172	
Front Tension ($10^6 N/m^2$)	8.415	7.958	8.172	8.308	
Final Thickness ($10^{-3}m$)	14.39	10.86	8.98	6.35	
Reduction (%)	54.65	24.53	17.23	29.28	

Table 4.32: Optimum values of the design variables and the objective function during hot rolling of steel for j=5.

Name of the Design Variable	Optimum Values obtained					Objective Function (J/rev)
	j = 1	j=2	j=3	j=4	j=5	
Radius (m)	0.178	0.172	0.168	0.162	0.157	$2.643X10^4$
Back Tension ($10^6 N/m^2$)	7.318	7.109	6.829	7.001	6.926	
Front Tension ($10^6 N/m^2$)	7.109	6.829	7.001	6.926	7.279	
Final Thickness ($10^{-3}m$)	20.24	13.90	11.05	8.20	6.35	
Reduction (%)	36.25	31.28	20.45	25.75	22.56	

Table 4.33: Optimum values of the design variables and the objective function during hot rolling of copper for j=1.

Name of the Design Variable	Optimum Values obtained	Value of the Objective Function (J/rev)
	j = 1	
Radius (m)	0.1304	$3.038X10^3$
Back Tension ($10^6 N/m^2$)	6.179	
Front Tension ($10^6 N/m^2$)	6.204	
Final Thickness ($10^{-3}m$)	6.35	
Reduction (%)	80	

Table 4.34: Optimum values of the design variables and the objective function during hot rolling of copper for j=2.

Name of the Design Variable	Optimum Values obtained		Value of the Objective Function (J/rev)
	j = 1	j=2	
Radius (m)	0.1173	0.1105	$1.237X10^3$
Back Tension ($10^5 N/m^2$)	8.207	8.413	
Front Tension ($10^5 N/m^2$)	8.413	8.362	
Final Thickness ($10^{-3}m$)	10.91	6.35	
Reduction (%)	65.62	41.79	

Table 4.35: Optimum values of the design variables and the objective function during hot rolling of copper for j=3.

Name of the Design Variable	Optimum Values obtained			Value of the Objective Function (J/rev)
	j = 1	j=2	j=3	
Radius (m)	0.1291	0.1202	0.1180	$2.417X10^3$
Back Tension ($10^5 N/m^2$)	5.298	5.763	6.009	
Front Tension ($10^5 N/m^2$)	5.763	6.009	5.902	
Final Thickness ($10^{-3}m$)	13.25	8.88	6.35	
Reduction (%)	58.25	32.95	28.49	

Table 4.36: Optimum values of the design variables and the objective function during hot rolling of aluminum for j=1.

Name of the Design Variable	Optimum Values obtained	Value of the Objective Function (J/rev)
	j = 1	
Radius (m)	0.1174	$1.167X10^3$
Back Tension ($10^5 N/m^2$)	1.109	
Front Tension ($10^5 N/m^2$)	2.003	
Final Thickness ($10^{-3}m$)	6.35	
Reduction (%)	80	

Table 4.37: Optimum values of the design variables and the objective function during hot rolling of aluminum for j=2.

Name of the Design Variable	Optimum Values obtained		Value of the Objective Function (J/rev)
	j = 1	j=2	
Radius (m)	0.1106	0.1002	$0.9942X10^3$
Back Tension ($10^5 N/m^2$)	1.207	1.113	
Front Tension ($10^5 N/m^2$)	1.113	1.005	
Final Thickness ($10^{-3}m$)	10.08	6.35	
Reduction (%)	68.25	37.00	

Table 4.38: Optimum values of the design variables and the objective function during hot rolling of aluminum for j=3.

Name of the Design Variable	Optimum Values obtained			Value of the Objective Function (J/rev)
	j = 1	j=2	j=3	
Radius (m)	0.1207	0.1195	0.1151	$1.683X10^3$
Back Tension ($10^5 N/m^2$)	1.041	1.149	1.231	
Front Tension ($10^5 N/m^2$)	1.149	1.231	1.079	
Final Thickness ($10^{-3}m$)	14.90	9.57	6.35	
Reduction (%)	53.05	35.75	33.64	

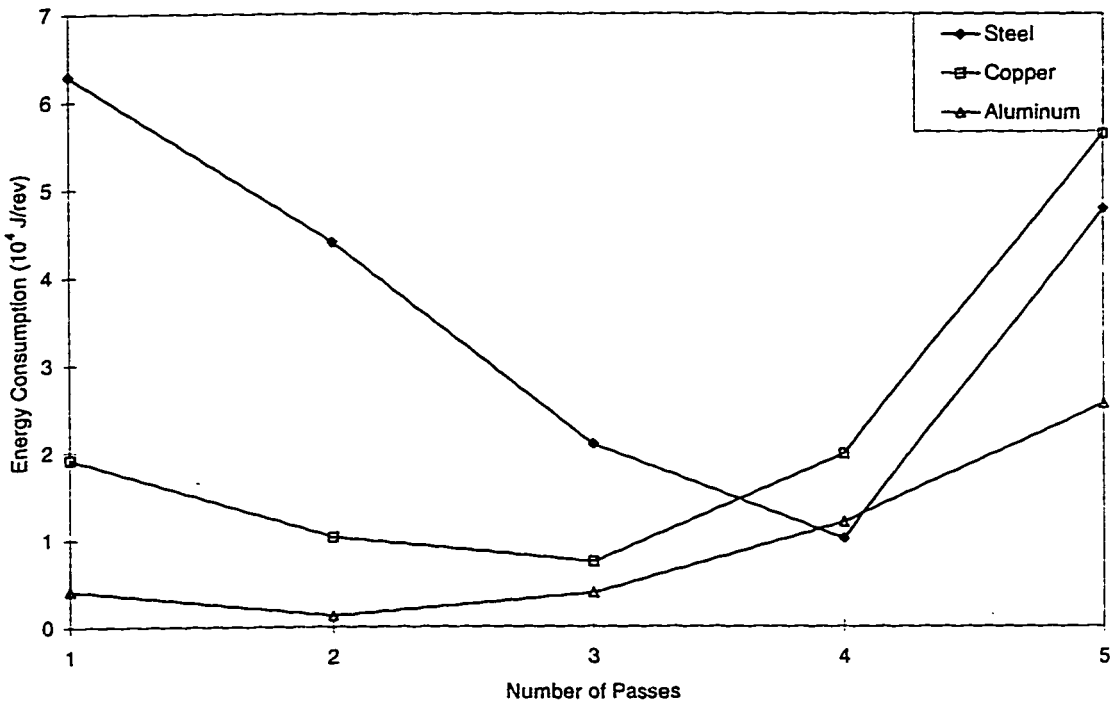

Figure 4.31: Variation of the energy consumption with the number of passes for hot rolling

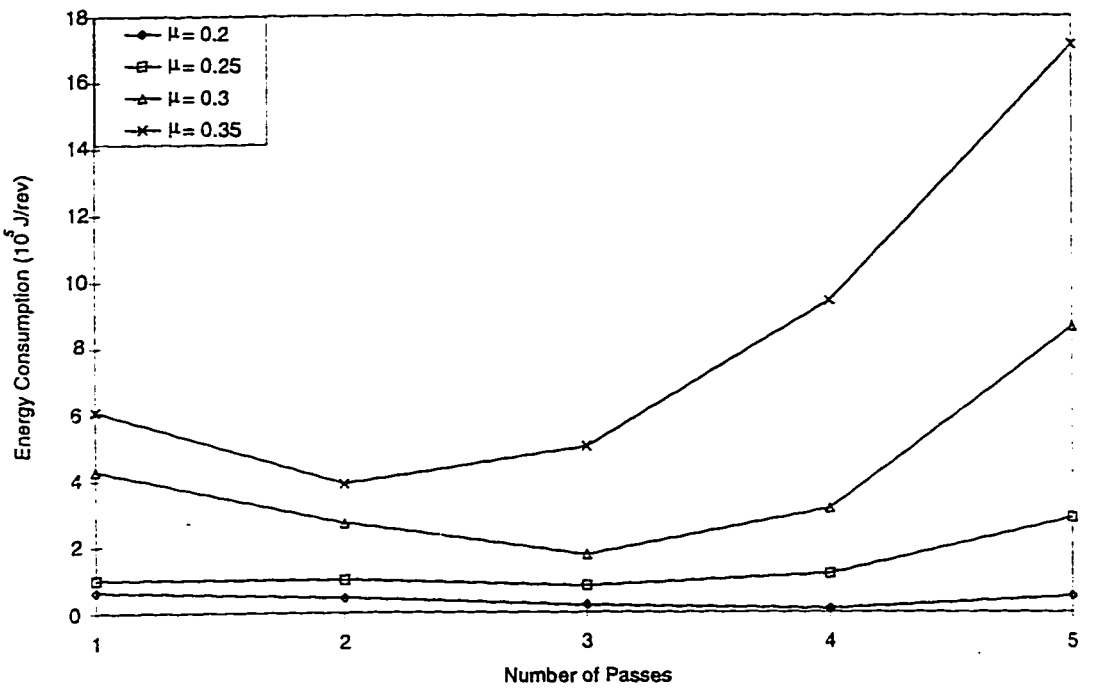

Figure 4.32: Variation of the energy consumption with the number of passes for hot rolling of steel as a function of coefficient of friction.

Table 4.39: Summary of the results of rolling with constant coefficient of friction

Name of the Material	Optimum Number of Passes		Objective Function ($10^5 J/rev$)	
	Cold Rolling	Hot Rolling	Cold Rolling	Hot Rolling
Steel	3	4	0.6514	0.0905
Copper	2	3	0.2012	0.0123
Aluminum	2	2	0.1052	0.0099

Table 4.40: Summary of the results of rolling with different values of coefficient of friction for steel

Coefficient of Friction(μ)		Optimum Number of Passes		Objective Function ($10^5 J/rev$)	
Cold Rolling	Hot Rolling	Cold Rolling	Hot Rolling	Cold Rolling	Hot Rolling
0.055	0.2	3	4	0.6514	0.1005
0.075	0.25	3	3	8.759	0.793
0.1	0.3	3	3	14.093	1.735
0.125	0.35	2	2	37.51	3.892

4.4.4 Discussions

The problem of determining the optimum operational conditions for minimum energy and the process parameters of multipass rolling process has been considered. The process has been formulated and solved as a constrained nonlinear programming problem, considering the roll radius, and the front and back tensions as design variables. The minimization of the total energy consumption by the tandem mill has been considered as the objective function. Constraints have been placed on the induced stresses, neutral angle and the angle of bite at each station. An upper bound has also been placed on the deflections of the rolls at each station. Constraints have also been placed on the maximum allowable reduction on each station and that the sum of the true strains at each station must be equal to the total true strain fro a reduction from h_0 to h_f.

Cold Rolling with Constant Coefficient of friction

The multipass rolling problem has been studied for an initial thickness of $3.2X10^{-3}m$ for cold rolling. taking steel, copper and aluminum as the test materials. The summary of the results obtained for the three materials are as shown in the Table 4.39 and the comparison of the variation of the objective function, i.e., the total algebraic sum of the energy consumed at each station with the number of passes is shown in Figure 4.26. It has been observed from the figures that, the total energy consumed, initially decreases with the number of passes and then shows an increasing

trend, giving the optimal number of passes to be $j = 3$ in the case of cold rolling of steel. Similarly the optimal number of passes obtained for aluminum and copper are $j = 2$ and $j = 2$ respectively. The variation in the number of passes, i.e., three for steel and two for copper and aluminum respectively could be because of the high strength constant (K) of steel when compared to that of copper and aluminum.

Considering the single pass, we observe that the total reduction of 40% is taken at the first station due to which there are high roll forces and higher roll deflections. But as the number of passes is increased to $j = 2$, the total reduction of 40%, is divided among the two available stations. On observation, it can be noticed that, a higher percentage of reduction which is less than the percentage reduction taken in the single pass, is undertaken at the first station. The remaining lower amount of reduction is done at the second station. This reduces the roll radii at both the stations, which in turn reduces the forces and torques and the energy consumed, as shown in the Table 4.19. Thus, the algebraic sum of the energies consumed at both the stations is less than the energy consumed in the single pass process. A similar trend is followed in the case of the three passes, where again, a higher percentage of reduction is undertaken at the first station and the remaining percentage reduction is divided among the remaining two stations. Thus, decreasing the total energy consumption of the tandem mill. But, as the number of passes is increased from 3 to 4, the total energy consumed by the tandem mill is increasing and this can be explained because of the reductions almost being equally divided among all the

stations. Due to this, all the stations are active, i.e., energy is consumed at all the stations, and since the objective function is the algebraic sum of the energy consumed at all the mills, the energy consumed by the tandem mill increases and the roll radii, in this case is more than what it was in the case of three stations to accommodate for these reductions. Thus the roll forces are more which in turn increases the total energy consumption of the tandem mill (see Figure 4.26)

Effect of Changing the various rolling parameters

The effect of changing the coefficient of friction on the optimum results has also been studied. The coefficient of friction has been varied from $\mu = 0.05$ to $\mu = 0.125$, with an increment of 0.025. Steel has been taken as the material of the sheet to be rolled, with the initial thickness $3.2X10^{-3}$ m. The variation of the total energy consumed with the number of passes have been shown in the Figure 4.27. Table 4.40 summarizes the optimum values of the energy consumed in each case.

The optimization results in this case indicate that the energy consumption increases with an increase in the coefficient of friction. This is because, as the coefficient of friction increases there is an increase in the roll force and roll torque which in turn increases the energy consumption. The optimum number of passes were also found for the energy consumption to be minimum in each case. They were found to be $j = 3$ for $\mu = 0.055, 0.075 and 0.1$. However, for $\mu = 0.125$ the optimum number of passes reduced to two. This could be explained from the fact that, as the

friction increases the energy consumption of the tandem mill also increases. Thus to keep the energy consumption minimum by satisfying all the other constraints, the number of passes has been reduced to two in this case.

The effect of changing the rolling parameters namely, the roll radius, back and front tensions on the optimum energy consumed has been studied. The results are as shown in the Figures 4.28 to 4.30. It has ben observed that as the roll radius increases, the energy consumption increases. This is because, as the roll radius increases the force and the torque on the rolls increases which in turn increases the energy consumption. In the case of varying the back and front tensions, it has been observed that as the tensions are increased, the energy consumption decreases. This is because, an increase in the tension tends to reduce the force on the rolls which reduces the energy consumption. Thus the trends are explained.

Hot Rolling with Constant Coefficient of friction

The multi pass hot rolling problem has been studied for three different materials, namely steel, copper and aluminum. The input thickness of the sheet is taken as $31.75X10^{(}-3)m$. The problem has been studied for a total reduction of 80%. The results obtained for the three materials are summarized in the Table 4.39. The comparison of the variation of the total algebraic sum of the energy consumed at each station with the number of passes is shown in Figure 4.31.

The observations made in this case are that the optimum values of the energy

consumption decreases from steel to copper and then to aluminum. Moreover, the magnitude of the values of the energy consumption are much lesser when compared to that obtained in the cold rolling process. This is because in hot rolling the material is heated to about 0.7 times the melting temperature of that material which makes the material soft and ductile thus reducing the forces on the rolls. This reduces the energy consumption. The energy consumption for steel is higher when compared to that obtained for copper and aluminum because the strength coefficient of steel is much higher and steel is harder when compared to copper and aluminum. The optimal number of passes have also been found o be $j = 4$ for steel, $j = 2$ for copper and $j = 2$ for aluminum. It can be observed that the optimal number of passes for steel is higher than that for copper and aluminum. This is because of the higher strength of steel when compared to the other two materials.

Effect of Changing the Coefficient of Friction during Cold Rolling

In hot rolling, the coefficient of friction ranges from about 0.2, with effective lubrication, to as high as 0.5, indicating sticking, which usually occurs with steels and high-temperature alloys. The effect of changing the coefficient of friction on the optimum results for hot rolling has also been studied. The coefficient of friction has been varied from $\mu = 0.2$ to $\mu = 0.35$, with an increment of 0.05. The problem has been studied for a total reduction of 80%. Steel has been taken as the material of the sheet to be rolled, with the initial thickness $31.75X10^{-3}$ m. The results are

summarized in the Table 4.40 and the variation of the energy consumption is as shown in the Figure 4.32.

The optimal results indicate that the energy consumption increases with an increase in the coefficient of friction. This is because as the coefficient of friction increases there is an increase in the roll force and roll torque which in turn increases the energy consumption. However, the magnitude of the values obtained for the energy consumption in this case are much lesser when compared to that obtained in cold rolling, since, in hot rolling the material is heated to about 0.7 times the melting temperature of that material which makes the material soft and ductile thus reducing the forces on the rolls. This reduces the energy consumption. The optimal number of passes have also been found o be $j = 4$ for $\mu = 0.2$, $j = 3$ for $\mu = 0.25$ and $\mu = 0.3$ and $j = 2$ for $\mu = 0.35$. It can be observed that, as the coefficient of friction increases the optimal number of passes is decreasing. This could be explained from the fact that, as the friction increases the energy consumption of the tandem mill also increases. Thus to keep the energy consumption minimum by satisfying all the other constraints, the number of passes has been reduced successively.

Cost effectiveness: Considering the case of the steel strip of initial thickness $3.2X10^{-3}m$, to be reduced by 40%, it can be observed that the desired reduction can be achieved in one pass or more. But the optimum number of passes found in this case is three, which implies that if the above strip is reduced in three passes, then there is a saving in the amount of energy consumed. This is one of the factors

effecting the cost of production. The cost of the three rolls can be justified by the fact that, if rolling is done with the optimum conditions, then there will be less forces acting on the rolls decreasing the wear and tear of the rolls which in turn increases the roll life reducing the maintenance and replacement costs. Thus, rolling the sheet in three passes, with the optimum amount of reduction at each station reduces the overall cost of production.

Chapter 5

Conclusions and Recommendations

5.1 Conclusions

This work has been motivated by the realization that the recent trend towards high-speed rolling of thin strips has demonstrated the increasing need of the design of rolling mills for controlling interstand tensions, thickness and shape of the final product. Although the procedures for the design of cold rolling mills are well established not much has been studied in the direction of finding optimal conditions and parameters for the rolling process. With the advent of fast computers and the development of new mathematical programming techniques have opened up a new phase in the field of optimization.

In this research attention has been focussed on determining the optimal design parameters of single pass and multipass strip rolling using the new mathematical programming techniques. In order to optimize the process effectively the existing process model has also been enhanced especially near the neutral point. The friction model developed by Wanheim and Bay [9], has also been incorporated. Later, optimization of the rolling process has been carried out by using the above mentioned enhanced process model.

The first part of the study presents the modifications made to the existing process model. It has been enhanced by incorporating the modifications in the frictional model suggested by Christensen et al. [6] and Wanheim [9] wherein the frictional stress is a function of pressure and friction factor. The concept of the neutral zone has also been incorporated in the model, wherein the frictional stress changes its sign over a zone rather than at a point. This seems to offer a more realistic pressure distribution over the rolls, and compares favorably with the experimental observation of Christensen et al. [6].

The later part of the study presents the various steps of optimization of the rolling process, using the above mentioned enhanced process model. The rolling problem is formulated and solved as a constrained nonlinear programming problem by considering the radius of the rolls, and the front and back tensions as design variables. Two objective functions, namely:

1. The minimization of the deflection of the rolls, in the case of single pass rolling

process: In the rolling process, the quality of the final product and the roll life depends on the deflections in the rolls making them undesirable. Thus, they have to be kept down to the minimum possible value. This aim has been achieved by taking the minimization of the deflections of the rolls as the objective function.

2. The minimization of the total energy consumed by the tandem mill, in the case of multipass rolling process: The scarcity of the power available calls for the conservation of the energy in every field. Large amounts of energy is being consumed everyday by the rolling industry, which has to be conserved. Efforts have been made to achieve this objective by the optimization of the rolling process.

Constraints have been placed on the induced stresses in the rolls, neutral angle and the angle of bite and the material properties. The problem has been solved for both cold and hot rolling processes. Three materials namely, Steel, Copper and Aluminum have been selected to study the variation of the optimal conditions. The effect of changing the various rolling parameters like the coefficient of friction, roll radius, back and front tensions on the optimal conditions has also been studied.

CASE 1: Minimization of the deflection of the rolls

It has been observed that, in both cold as well as hot rolling process, the deflections of the rolls increase with an increase in the percent reduction in thickness. As

expected, the deflections were greater for steel than for copper and aluminum. The optimum values of the radius of the rolls, back tension and front tensions also showed a decreasing trend with an increase in the percent reduction. The coefficient of friction has also been varied, and it has been observed that, the deflections increased with an increase in the friction. As the roll radius increased the deflections in the rolls decreased and in the case of increasing back and front tensions the deflections in the rolls decreased.

Using this optimization technique, roll mills can be designed specifying the values for the various rolling parameters, for any input thickness and for any material to be rolled. Considering an example, of a steel sheet of input thickness $1.6X10^{-3}m$ to be reduced in thickness by 20 percent. The designer should specify the values of the roll radius and the front and back tensions to be maintained for this particular reduction, corresponding to the values given in Table 4.3, if the deflections in the rolls have to be minimum. This not only helps in improving the quality of the product as well as life of the rolls but also helps in reducing the maintenance costs.

CASE 2: Minimization of the energy consumption

The multipass rolling process has been studied, to estimate the optimum number of passes to obtain a particular reduction, so that the total energy consumed by the tandem mill is minimum. It has been found, in the case of steel as the material to be rolled, that the optimum number of passes to obtain a reduction of 40%, from

an initial thickness of $3.2X10^{-3}m$ is three. Similarly, optimum number of passes have been obtained by varying coefficients of friction, roll radius and back and front tensions. The results obtained for all the cases have been found to be within the general trends usually encountered in strip rolling.

Using the above optimization technique we can conserve a lot of energy and reduce the total production costs. For example, considering the case of the steel strip of initial thickness $3.2X10^{-3}m$, to be reduced by 40%, it can be observed that the desired reduction can be achieved in one pass or more. But the optimum number of passes found in this case is three, which implies that if the above strip is reduced in three passes then there is a saving in the amount of energy consumed. This is one of the factors effecting the cost of production. The cost of the three rolls can be justified by the fact that, if rolling is done with the optimum conditions, then there will be less forces acting on the rolls decreasing the wear and tear of the rolls which in turn increases the roll life reducing the maintenance and replacement costs. Thus, rolling the sheet in three passes, with the optimum amount of reduction at each station reduces the overall cost of production.

5.2 Recommendations

A review of the results of this work has indicated some areas of the present study which may be extended and developed. An extension of the present work could be.

to consider the minimization of the cost of production as the objective function. This can be done if a suitable equation for the cost of production can be derived in terms of the various design variables such as, the cost incurred for a roll replacement, roll material and various maintenance costs. Another possible extension could be to incorporate the surface finish to be obtained as one of the constraints. This can be done if a suitable equation can be developed for measuring the surface roughness of the sheet. If the existing friction model can be enhanced by incorporating the ideas presented by Byong et al. [40], wherein the friction is varying along the contact length, then the process model could be more realistic. Rao and Lee [41] presented a finite element solution of strip rolling, taking the material behavior in the form of a stress-strain curve obtained from a plane-strain compression test and measured interfacial velocities as prescribed boundary conditions as the input data. This concept could also be incorporated in the process model which could be a give more realistic one. One of the other possible extensions could be of maximizing the production rate by considering the upper bound model as presented by Aviitzur [28]. This problem could be worthwhile pursuing since the maximization of production rate is a very practical objective function from the point of view of the industry.

References

[1] Serope Kalpakjian. *Manufacturing Processes for Engineering Materials.* Addison - Wesley, 1978.

[2] Orowan, E. "The Calculation of Roll Pressure in Hot and Cold Rolling". *Proc. Inst. Mech. Eng.*, 150, 1943.

[3] Ford, H., Ellis, F. and Bland, D. R. "Cold Rolling with Strip Tension, Part I - A New Approximate Method of Calculation and a Comparison with Other Methods". *J. Iron and Steel Inst.*, 168, 1951.

[4] Bland, D. R. and Sims, R. B. "A Note on the Theory of Rolling with Tension". *Proc. Inst. Mech. Eng.*, 167, 1953.

[5] Hugh Ford, Alexander, J. M. "Simplified Hot-Rolling Calculations". *Journal of Institute of Metals*, 92, 1963.

[6] Christensen, P., Everfelt, H., Bay, N. "Pressure Distribution in Plate Rolling". *Annals of the CIRP*, 35, 1986.

[7] Alexander, J. M., Gunasekara, J. S. "Analysis of Rolling". *Annals of the CIRP*, 36(1):203–206, 1987.

[8] Jaronokov, V. A., Chaturvedi, R. C. *Rolling of Metals.* Yantrik, Lucknow. 1981.

[9] Wanheim, T., Bay, N., Petersen, A. S. "A Theoretically determined Model For Friction In Metal Working Processes". *Wear*, 28, 1974.

[10] Chen, C. C., Kobayashi, S. "Rigid Plastic Finite Element Analysis of Ring Compression". *AMD*, 28, 1974.

[11] Von Karman, T. "On the Theory of Rolling". *Z. Angew. Math. Mech*, 5, 1925.

[12] Sienel, E. and Fangmeier, E. "Research on the Specific Resistance to Deformation When Rolling Soft Carbon Steels at Temperatures Between 700^0C and 1200^0C" . *Mitt. K. W. Inst. Eisenf.*, 12, 1930.

[13] Trinks, W. "Pressures and Roll Flattening in Cold Rolling". *Blast Furnace and Steel Plant.* 25, 1937.

[14] Tselikov, A. I. "Effect of External Friction and Tension on the Pressure of the Metal on the Rolls in Rolling". *Metallurg.* (6):61–76, 1939.

[15] Bland, D. R. and Ford, H. "An Approximate Treatment of the Elastic Compression of the Strip in Cold Rolling". *J. Iron and Steel Inst.*, 171, 1952.

[16] Bland, D. R. and Ford, H. "The Calculation of Roll Force and Torque in Hot and Cold Rolling". *Proc. Inst. Mech. Eng.*, 159, 1948.

[17] Sims, R. B. "Calculation of Roll Force and Torque in Cold Rolling by Graphical and Experimental Methods". *J. Iron and Steel Inst.*, 1954.

[18] Sims, R. B. "Calculation of Roll Force and Torque in Hot Rolling Process". *Proc. Inst. Mech. Eng.*, 1954.

[19] Ford, H., Ellis, F. and Bland, D. R. "Cold Rolling with Strip Tension, Part II-Comparison of Calculated and Experimental Results". *J. Iron and Steel Inst.*. 171, 1952.

[20] Underwood, L. R. *The Rolling of Metals- Theory and Experiment*, volume 1. Chapman-and Hall, 1950.

[21] Tarnovskii, I. Y., Pozdeyev, A. A. and Lyashkov, V. b. *Deformation of Metals During Rolling.* Pergamon Press, 1965.

[22] William L. Roberts. *Cold Rolling of Steel.* Dekker, 1978.

[23] Murthy, A. and Lenard, J. G. "Statistical Evaluation of Some Hot Rolling Theories". *J. Eng. Matl. Tech., Trans ASME*, 104, 1982.

[24] Alexander, J. M. "On the Theory of Rolling". *Proc. R. Soc. London.* A326. 1972.

[25] Venter, R. D. and Abd-Rabbo, A. A. "Modelling of the Rolling Process". *Int. J. Mech. Sci.*, 22, 1980.

[26] Crane, F. A. A., Alexander, J. M. . "Slip-Line Fields and Deformation in Hot Rolling of Strip". *Journal of the Institute of Metals*, 96, 1968.

[27] Wanheim, T. "Friction at High Normal Pressures". *Wear*, 25, 1973.

[28] Avitzur, B. "Pass Reduction Schedule for Optimum Production of a Hot Strip Mill". *Iron and Steel Eng.*, 1962.

[29] Devendra Rusia. "Review and Evaluation of Different Methods for Force and Torque Calculations in the Strip Rolling Process". *J. of Materials Shaping Technology*, 9, 1991.

[30] Shivpuri, R. and Shin, W . "A Methodology for Roll Pass Optimization for Multipass Shape Rolling". *International Journal of Machine Tools Manufacture*, 32(5):671-683, 1992.

[31] John W. Turley . "Selection of Optimum Work Roll SIze for Cold Rolling Applications". *Iron and Steel Engineer*, 1985.

[32] Rao, S. S. and Kumar, A. "Optimization of Cold Rolling by Nonlinear Programming". *J. of Eng. for Ind.*, 100, 1978.

[33] Bay, N. "Friction Stress and Normal Stress in Bulk Metal Forming Processes". *Journal of Mechanical Working Technology*, 14, 1987.

[34] Wusatowski, Z. *Fundamentals of Rolling.* Pergamon Press, 1969.

[35] Andrew Grace. *Optimization Toolbox, MATLAB. User's Guide.* The Math Works Inc., 1992.

[36] Philip E. Gill, Walter Murray and Margret H. Wright. *Practical Optimization.* Academic Press, 1981.

[37] Rao S. S. *Optimization Theory and Applications.* Wiley Eastern Limited, second edition, 1978.

[38] William L. Roberts. *Hot Rolling of Steel.* Dekker, 1978.

[39] Shuaib, A. N. and Duffuaa, S. O. "A Methodology For Multipass Machining Optimization". *The Arabian Journal for Science and Engineering*, 15(4). 1990.

[40] Byong Bai Yoon. *Experimental & Computational Procedures for investigating Frictional behavior in Sheet Stretching.* PhD thesis, University of Michigan, 1989.

[41] Rao, R. S. and Lee, H. Y. "A Finite Element Solution of Strip Rolling". *J. of Mech. Working Tech.*, 20, 1989.

Appendix A

Development of the Basic Equations

Wanheim et al. have outlined the develpoment of the slip-line field , with increasing downwards load. Assuming a constant true friction stress τ at the tool/workpiece asperity contact, all slip-lines of the β family meet the tool/workpiece interface at angle θ given by

$$f = \tau/k = cos2\theta \tag{A.1}$$

where f is the friction factor. Figure (A.1) shows the deformation of the asperity when the slip-line field has just reached the bottom of the valley. The original asperity ACD, which is triangular in cross-section, has been deformed into the quadrangle BCDE, which causes the right-hand angle of the valley to increase from γ_0 to γ_R whereas the left hand angle remains constant, $\gamma_L = \gamma_0$. The relationship between γ_0, γ_R and the friction factor can be derived as follows:

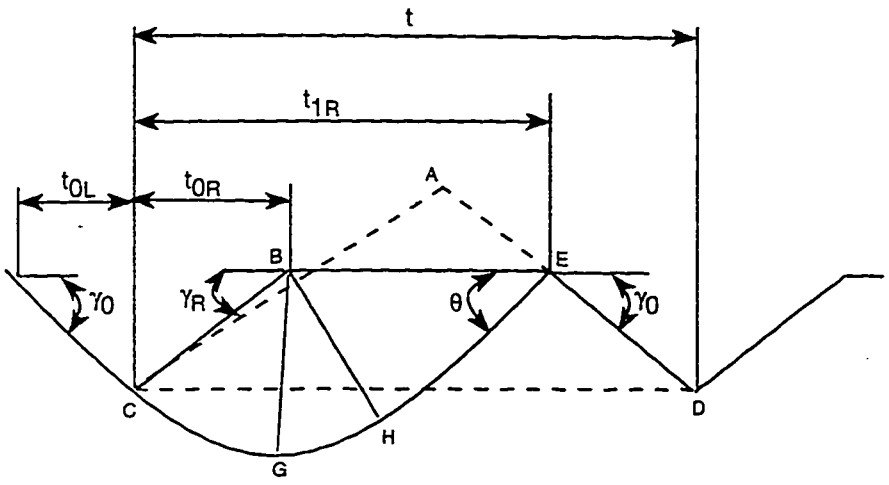

Figure A.1: Slip-line field corresponding to the limit of propotionality

The realtionship between γ_0, γ_R and f is determined from the volume constancy in the plastic deformation of the asperity, Figure (A.1). Thus, the area of triangle ACD equals the area of the quadrangle BCDE.

$$A_{ACD} = A_{BCDE} \tag{A.2}$$

$$A_{ACD} = t_0^2 tan\gamma_0 \tag{A.3}$$

$$A_{BCDE} = \frac{1}{2} t_R tan\gamma_R \left(\frac{t_R}{\sqrt{2} cos\gamma_R sin\theta} + 2t_0 \right) \tag{A.4}$$

Inserting into Equation (A.2) gives:

$$tan^2\gamma_0 \left(1 + \frac{\sqrt{2}}{cos\gamma_R sin\theta} + \frac{1}{2cos^2\gamma_R sin^2\theta} \right) - tan\gamma_0 \frac{\sqrt{2} tan\gamma_R}{cos\gamma_R sin\theta} - tan^2\gamma_R = 0 \tag{A.5}$$

Equation (A.1) gives:

$$cos2\theta = f \tag{A.6}$$

$$sin\theta = \sqrt{\frac{1-f}{2}} \tag{A.7}$$

$$sin2\theta = \sqrt{1-f^2} \tag{A.8}$$

$$cos\theta = \sqrt{\frac{1+f}{2}} \tag{A.9}$$

Equations (A.5) and (A.7) lead directly to Equation (A.10), which is as follows:

$$tan^2\gamma_0 \left(1 + \frac{2}{cos\gamma_R \sqrt{1-f}} + \frac{1}{cos^2\gamma_R (1-f)} \right) - 2tan\gamma_0 \frac{\sqrt{2} tan\gamma_R}{cos\gamma_R sin\theta} - tan^2\gamma_R = 0 \tag{A.10}$$

Geometrical consideration from Figure (A.1) give the limit of propotionality in the real contact area ratio:

$$\alpha' = \frac{t_{1R} - t_{0R}}{t_{1R} + t_{0L}} = \frac{\frac{t_{1R}}{t_{0R}} - 1}{\frac{t_{1R}}{t_{0R}} + \frac{t_{0L}}{t_{0R}}} \tag{A.11}$$

$$sin\theta = \frac{t_{0R}}{\sqrt{2} cos\gamma_R (t_{1R} - t_{0R})} \tag{A.12}$$

$$\frac{t_{1R}}{t_{0R}} = \frac{1 + \sqrt{2} cos\gamma_R sin\theta}{\sqrt{2} cos\gamma_R sin\theta} \tag{A.13}$$

$$\frac{t_{0L}}{t_{0R}} = tan\gamma_R cot\gamma_0 \tag{A.14}$$

Inserting into Equation (A.11), Equation (A.12) to Equation (A.13) gives:

$$\alpha' = \frac{1}{1 + \sqrt{2} sin\theta (cos\gamma_R + sin\gamma_R cot\gamma_0)} \tag{A.15}$$

Inserting Equation (A.7) into Equation (A.11) gives:

$$\alpha' = \frac{1}{1 + \sqrt{1-f}(cos\gamma_R + sin\gamma_R cot\gamma_0)} \tag{A.16}$$

From the tatic equilibrium of the slip line field, the limit of propotuonality in pressure q' is obtained as follows:

$$q'(t_{1R} + t_{0L}) = p_{1R}(t_{1R} - t_{0R}) \tag{A.17}$$

$$q' = \alpha' p_{1R} \tag{A.18}$$

where

$$\frac{p_{IR}}{\sigma_0} = \frac{1}{\sqrt{3}}\left(1 + \frac{\pi}{2} + 2\theta - 2\gamma_R + sin2\theta\right) + \frac{4}{\sqrt{3}}(I-1)\,\Delta\phi \tag{A.19}$$

and $\Delta\phi = 5^0$; $I = 1, 2, 3, ..., 14$;
Using Equations (A.18), (A.19) along with the Equations (A.6) to (A.8), we get:

$$\frac{q'}{\sigma_0} = \frac{1 + \frac{\pi}{2} + Arccosf - 2\gamma_R + \sqrt{1-f^2}}{\sqrt{3}[1 + \sqrt{1-f}(cos\gamma_R + sin\gamma_R cot\gamma_0)]} \tag{A.20}$$

In the case of $\gamma \approx 0^0$ Equation (A.20) reduces to

$$\frac{q'}{\sigma_0} = \frac{1 + \frac{\pi}{2} + Arccosf + \sqrt{1-f^2}}{\sqrt{3}[1 + \sqrt{1-f}]} \tag{A.21}$$

Appendix B

Code for CONSTR Function

```
function [x, OPTIONS,lambda, HESS]=constr1(FUN,x,OPTIONS,VLB,VUB,GRADFUN,P1,
P2,P3,P4,P5,P6,P7,P8,P9,P10,P11,P12,P13,P14,P15)
%CONSTR Finds the constrained minimum of a function of several variables.
%
%       X=CONSTR('FUN',X0) starts at X0 and finds a constrained minimum to
%       the function which is described in FUN (usually an M-file: FUN.M).
%       The function 'FUN' should return two arguments: a scalar value of the
%       function to be minimized, F, and a matrix of constraints, G:
%       [F,G]=FUN(X). F is minimized such that G < zeros(G).
%
%       X=CONSTR('FUN',X,OPTIONS) allows a vector of optional parameters to
%       be defined. For more information type HELP FOPTIONS.
%
%       X=CONSTR('FUN',X,OPTIONS,VLB,VUB) defines a set of lower and upper
%       bounds on the design variables, X, so that the solution is always in
%       the range VLB < X < VUB.
%
%       X=CONSTR('FUN',X,OPTIONS,VLB,VUB,'GRADFUN') allows a function
%       'GRADFUN' to be entered which returns the partial derivatives of the
%       function and the  constraints at X:  [gf,GC] = GRADFUN(X).

%       Copyright (c) 1990 by the MathWorks, Inc.
%       Andy Grace 7-9-90.

%
%       X=CONSTR('FUN',X,OPTIONS,VLB,VUB,GRADFUN,P1,P2,..) allows
%       coefficients, P1, P2, ... to be passed directly to FUN:
%       [F,G]=FUN(X,P1,P2,...). Empty arguments ([]) are ignored.


global OPT_STOP OPT_STEP;
OPT_STEP = 0;
OPT_STOP = 0;

% Set up parameters.
XOUT(:)=x;

if ~any(FUN<48) % Check alphanumeric
```

```
        etype = 1;
        evalstr = [FUN,];
        evalstr=[evalstr, '(x'];
        for i=1:nargin - 6
                etype = 2;
                evalstr = [evalstr,',P',int2str(i)];
        end
        evalstr = [evalstr, ')'];
else
        etype = 3;
        evalstr=[FUN,'; g=g(:);'];
end

if nargin < 3, OPTIONS=[]; end
if nargin < 4, VLB=[]; end
if nargin < 5, VUB=[]; end
if nargin < 6, GRADFUN=[]; end

VLB=VLB(:); lenvlb=length(VLB);
VUB=VUB(:); lenvub=length(VUB);
bestf = Inf;

nvars = length(XOUT);

CHG = 1e-7*abs(XOUT)+1e-7*ones(nvars,1);
if lenvlb*lenvlb>0
      if any(VLB(1:lenvub)>VUB), error('Bounds Infeasible'), end
end
for i=1:lenvlb
       if lenvlb>0,if XOUT(i)<VLB(i),XOUT(i)=VLB(i)+1e-4; end,end
end
for i=1:lenvub
       if lenvub>0,if XOUT(i)>VUB(i),XOUT(i)=VUB(i);CHG(i)=-CHG(i);end,
end
end

% Used for semi-infinite optimization:
s = nan; POINT =[]; NEWLAMBDA =[]; LAMBDA = []; NPOINT =[]; FLAG = 2;

x(:) = XOUT;
```

```
if etype == 1,
        [f, g(:)] = feval(FUN,x);
elseif etype == 2
        [f, g(:)] = eval(evalstr);
else
        eval(evalstr);
end

ncstr = length(g);
if ncstr == 0
        g = -1;
        ncstr = 1;
        if etype ~= 3
                evalstr = ['[f,g] =', evalstr, ';'];
                etype = 3;
        end
        evalstr = [evalstr,'g=-1; '];
end


if length(GRADFUN)
        if ~any(GRADFUN<48) % Check alphanumeric
                gtype = 1;
                evalstr2 = [GRADFUN,'(x'];
                for i=1:nargin - 6
                        gtype = 2;
                        evalstr2 = [evalstr2,',P',int2str(i)];
                end
                evalstr2 = [evalstr2, ')'];
        else
                gtype = 3;
                evalstr2=[GRADFUN,';'];
        end
end

OLDX=XOUT;
OLDG=g;
OLDgf=zeros(nvars,1);
gf=zeros(nvars,1);
OLDAN=zeros(ncstr,nvars);
```

```
LAMBDA=zeros(ncstr,1);
sizep = length(OPTIONS);
OPTIONS = foptions(OPTIONS);
if lenvlb*lenvlb>0
      if any(VLB(1:lenvub)>VUB), error('Bounds Infeasible'), end
end
for i=1:lenvlb
       if lenvlb>0,if XOUT(i)<VLB(i),XOUT(i)=VLB(i)+eps; end,end
end
OPTIONS(18)=1;
if OPTIONS(1)>0
        disp('')
        disp('f-COUNT   FUNCTION       MAX{g}         STEP  Procedures');
end
HESS=eye(nvars,nvars);
if sizep<1 |OPTIONS(14)==0, OPTIONS(14)=nvars*100;end
OPTIONS(10)=1;
OPTIONS(11)=1;
GNEW=1e8*CHG;



%---------------------------------Main Loop-----------------------------
status = 0;
while status ~= 1

%----------------GRADIENTS---------------

        if ~length(GRADFUN) | OPTIONS(9)
% Finite Difference gradients
                POINT = NPOINT;
                oldf = f;
                oldg = g;
                ncstr = length(g);
                FLAG = 0; % For semi-infinite
                gg = zeros(nvars, ncstr);  % For semi-infinite
% Try to make the finite differences equal to 1e-8.
                CHG = -1e-8./(GNEW+eps);
                CHG = sign(CHG+eps).*min(max(abs(CHG),OPTIONS(16)),
                             OPTIONS(17));
                OPT_STEP = 1;
```

```
                for gcnt=1:nvars
                        if gcnt == nvars, FLAG = -1; end
                        temp = XOUT(gcnt);
                        XOUT(gcnt)= temp + CHG(gcnt);
                        x(:) =XOUT;
                        if etype == 1,
                        [f, g(:)] = feval(FUN,x);
                        elseif etype == 2
                                [f, g(:)] = eval(evalstr);
                        else
                                eval(evalstr);
                        end
                        OPT_STEP = 0;
% Next line used for problems with varying number of constraints
                         if ncstr~=length(g), diff=length(g); g=v2sort(oldg,g);
                         end
                         gf(gcnt,1) = (f-oldf)/CHG(gcnt);
                         gg(gcnt,:) = (g - oldg)'/CHG(gcnt);
                         XOUT(gcnt) = temp;
                end
% Gradient check
                if OPTIONS(9) == 1
                        gfFD = gf;
                        ggFD = gg;
                        x(:)=XOUT;
                        if gtype == 1
                                [gf(:), gg] = feval(GRADFUN, x);
                        elseif gtype == 2
                                [gf(:), gg] = eval(evalstr2);
                        else
                                eval(evalstr2);
                        end
                        disp('Function derivative')
                        graderr(gfFD, gf, evalstr2);
                        disp('Constraint derivative')
                        graderr(ggFD, gg, evalstr2);
                        OPTIONS(9) = 0;
                end
                FLAG = 1; % For semi-infinite
                OPTIONS(10) = OPTIONS(10) + nvars;
                f=oldf;
```

```
                g=oldg;
        else
% User-supplied gradients
                if gtype == 1
                        [gf(:), gg] = feval(GRADFUN, x);
                elseif gtype == 2
                        [gf(:), gg] = eval(evalstr2);
                else
                        eval(evalstr2);
                end
        end
        AN=gg';
        how='';

%-------------SEARCH DIRECTION---------------

        for i=1:OPTIONS(13)
                schg=AN(i,:)*gf;
                if schg>0
                        AN(i,:)=-AN(i,:);
                        g(i)=-g(i);
                end
        end

        if OPTIONS(11)>1  % Check for first call
% For equality constraints make gradient face in
% opposite direction to function gradient.
                if OPTIONS(7)~=5,
                        NEWLAMBDA=LAMBDA;
                end
                [ma,na] = size(AN);
                GNEW=gf+AN'*NEWLAMBDA;
                GOLD=OLDgf+OLDAN'*LAMBDA;
                YL=GNEW-GOLD;
                sdiff=XOUT-OLDX;
% Make sure Hessian is positive definite in update.
                if YL'*sdiff<OPTIONS(18)^2*1e-3
                        while YL'*sdiff<-1e-5
                                [YMAX,YIND]=min(YL.*sdiff);
                                YL(YIND)=YL(YIND)/2;
                        end
```

```
                        if YL'*sdiff < (eps*norm(HESS,'fro'));
                                how=' mod Hess(2)';
                                FACTOR=AN'*g - OLDAN'*OLDG;
                                FACTOR=FACTOR.*(sdiff.*FACTOR>0).
                                *(YL.*sdiff<=eps);
                                WT=1e-2;
                                if max(abs(FACTOR))==0; FACTOR=1e-5*sign(sdiff);
                                end
                                while YL'*sdiff < (eps*norm(HESS,'fro'))
                                  & WT < 1/eps
                                        YL=YL+WT*FACTOR;
                                        WT=WT*2;
                                end
                         else
                                how=' mod Hess';
                        end
                end

%----------Perform BFGS Update If YL'S Is Positive---------
                if YL'*sdiff>eps
                        HESS=HESS+(YL*YL')/(YL'*sdiff)-(HESS*sdiff*sdiff'*HESS')
                                  /(sdiff'*HESS*sdiff);
% BFGS Update using Cholesky factorization  of Gill, Murray and Wright.
% In practice this was less robust than above method and slower.
%       R=chol(HESS);
%       s2=R*S; y=R'\YL;
%       W=eye(nvars,nvars)-(s2'*s2)\(s2*s2') + (y'*s2)\(y*y');
%       HESS=R'*W*R;
                else
                        how=[how,' (no update)'];
                end

        else % First call
                  OLDLAMBDA=(eps+gf'*gf)*ones(ncstr,1)./(sum(AN'.*AN')'+eps) ;
        end % if OPTIONS(11)>1
        OPTIONS(11)=OPTIONS(11)+1;

        LOLD=LAMBDA;
        OLDAN=AN;
        OLDgf=gf;
        OLDG=g;
```

```
        OLDF=f;
        OLDX=XOUT;
        XN=zeros(nvars,1);
        if (OPTIONS(7)>0&OPTIONS(7)<5)
        % Minimax and attgoal problems have special Hessian:
                HESS(nvars,1:nvars)=zeros(1,nvars);
                HESS(1:nvars,nvars)=zeros(nvars,1);
                HESS(nvars,nvars)=1e-8*norm(HESS,'inf');
                XN(nvars)=max(g); % Make a feasible solution for qp
        end
        if lenvlb>0,
                AN=[AN;-eye(lenvlb,nvars)];
                GT=[g;-XOUT(1:lenvlb)+VLB];
        else
                GT=g;
        end
        if lenvub>0
                AN=[AN;eye(lenvub,nvars)];
                GT=[GT;XOUT(1:lenvub)-VUB];
        end
        [SD,lambda,howqp]=qp(HESS,gf,AN,-GT, [], [], XN,OPTIONS(13),-1);
        lambda(1:OPTIONS(13)) = abs(lambda(1:OPTIONS(13)));
        ga=[abs(g(1:OPTIONS(13)));g(OPTIONS(13)+1:ncstr)];
        mg=max(ga);
        if OPTIONS(1)>0
                if howqp(1) == 'o'; howqp = ' '; end
                disp([sprintf('%5.0f %12.6g %12.6g ',OPTIONS(10),f,mg),
                 sprintf('%12.3g  ',OPTIONS(18)),how, ' ',howqp]);
        end
        LAMBDA=lambda(1:ncstr);
        OLDLAMBDA=max([LAMBDA';0.5*(LAMBDA+OLDLAMBDA)'])' ;

%---------------LINESEARCH--------------------
        MATX=XOUT;
        MATL = f+sum(OLDLAMBDA.*(ga>0).*ga) + 1e-30;
        infeas = (howqp(1) == 'i');
        if OPTIONS(7)==0 | OPTIONS(7) == 5
% This merit function looks for improvement in either the constraint
% or the objective function unless the sub-problem is infeasible in which
% case only a reduction in the maximum constraint is tolerated.
% This less "stringent" merit function has produced faster convergence in
```

```
% a large number of problems.
                if mg > 0
                        MATL2 = mg;
                elseif f >=0
                        MATL2 = -1/(f+1);
                else
                        MATL2 = 0;
                end
                if ~infeas & f < 0
                        MATL2 = MATL2 + f - 1;
                end
        else
% Merit function used for MINIMAX or ATTGOAL problems.
                MATL2=mg+f;
        end
        if mg < eps & f < bestf
                bestf = f;
                bestx = XOUT;
        end
        MERIT = MATL + 1;
        MERIT2 = MATL2 + 1;
        OPTIONS(18)=2;
        while (MERIT2 > MATL2) & (MERIT > MATL)
                    & OPTIONS(10) < OPTIONS(14)
                OPTIONS(18)=OPTIONS(18)/2;
                if OPTIONS(18) < 1e-4,
                        OPTIONS(18) = -OPTIONS(18);

                % Semi-infinite may have changing sampling interval
                % so avoid too stringent check for improvement
                        if OPTIONS(7) == 5,
                                OPTIONS(18) = -OPTIONS(18);
                                MATL2 = MATL2 + 10;
                        end
                end
                XOUT = MATX + OPTIONS(18)*SD;
                x(:)=XOUT;
                if etype == 1,
                        [f, g(:)] = feval(FUN,x);
                elseif etype == 2
                        [f, g(:)] = eval(evalstr);
```

```
                else
                        eval(evalstr);
                end
                OPTIONS(10) = OPTIONS(10) + 1;
                ga=[abs(g(1:OPTIONS(13)));g(OPTIONS(13)+1:length(g))];
                mg=max(ga);
                MERIT = f+sum(OLDLAMBDA.*(ga>0).*ga);
                if OPTIONS(7)==0 | OPTIONS(7) == 5
                        if mg > 0
                                MERIT2 = mg;
                        elseif f >=0
                                MERIT2 = -1/(f+1);
                        else
                                MERIT2 = 0;
                        end
                        if ~infeas & f < 0
                                MERIT2 = MERIT2 + f - 1;
                        end
                else
                        MERIT2=mg+f;
                end
        end
%------------Finished Line Search-------------

        if OPTIONS(7)~=5
                mf=abs(OPTIONS(18));
                LAMBDA=mf*LAMBDA+(1-mf)*LOLD;
        end
        if max(abs(SD))<2*OPTIONS(2) & abs(gf'*SD)<
                        2*OPTIONS(3) & (mg<OPTIONS(4) |
                        (howqp(1) == 'i' & mg > 0 ) )
                if OPTIONS(1)>0
                        disp([sprintf('%5.0f %12.6g %12.6g ',OPTIONS(10),f,mg)
                              sprintf('%12.3g  ',OPTIONS(18)),how, ' ',howqp]
                        if howqp(1) ~= 'i'
                                disp('Optimization Terminated Successfully')
                                disp('Active Constraints:'),
                                find(LAMBDA>0)
                        end
                end
                if (howqp(1) == 'i' & mg > 0)
```

```
                        disp('Warning: No feasible solution found.')
                end
                status=1;

        else
        %       NEED=[LAMBDA>0]|G>0
                if OPTIONS(10) >= OPTIONS(14) | OPT_STOP
                        XOUT = MATX;
                        f = OLDF;
                        if ~OPT_STOP
                       disp('Maximum number of iterations exceeded')
                       disp('increase OPTIONS(14)')
                       else
                      disp('Optimization terminated prematurely by user')
                      end
                      status=1;
                end
        end
end

% If a better unconstrained solution was found earlier, use it:
if f > bestf
        XOUT = bestx;
        f = bestf;
end
OPTIONS(8)=f;
x(:) = XOUT;
```

Vita

- MOHAMMED ABDUL SAMAD
- Born in India.
- Permanent Address :
  H.No. 12-2-823/A/50,
  Santosh Nagar Colony, Mehdipatnam
  Hyderabad 500028, A. P., INDIA, Ph.0091-40-3514317.
- Received Bachelor of Engineering (**B.E.**) degree in Mechanical Engineering from Osmania University, Hyderabad, India in July 1993.
- Joined KFUPM in September 1994. Received Master of Science (**M.S.**) degree in Mechanical Engineering with specialization in Materials and Manufacturing from KFUPM, in May 1997.